

NUMERICAL INVESTIGATION OF FAILURE MECHANISMS OF CAST IRON

WATER MAINS

by

© Hordiyamulla Liyanage Kasuni Tharuka

A Thesis submitted to the

School of Graduate Studies

in partial fulfilment of the requirements for the degree of

Master of Engineering

Faculty of Engineering and Applied Science

Memorial University of Newfoundland

October 2016

St. John's

Newfoundland

Abstract

Cast Iron water mains used in potable water transportation systems are facing a rapidly growing rate of failure. The most common failure mode of cast iron water main is circumferential cracking that occurs due to high longitudinal stresses in the pipe wall, when the longitudinal stress exceeds the strength of the pipe material. However, the circumferential failure mechanism of the pipe is not well understood. Conventional methods of pipe analysis predict higher circumferential stresses, which would cause longitudinal cracking in the pipe. The higher longitudinal stress is attributed to a number of factors such as corrosion pits on pipe wall, lack of bedding support due to erosion of bedding soil, and localized concentrated supports (or forces) due to lumps of soil or rock pieces. The failure mechanisms of buried cast iron water mains subjected to three factors such as non-uniform bedding support, pitting corrosion and localized concentrated supports are investigated in this thesis. A detailed numerical investigation is carried out based on three-dimensional finite element analyses using ANSYS software. The non-uniform bedding is found to create high longitudinal stresses for larger void at the pipe invert. Although pitting corrosion alone results in high circumferential stresses, when it occurs simultaneously with a non-uniform bedding condition, the peak stresses result in the longitudinal direction. Longitudinal stress is generally higher than the circumferential stress for the pipes with higher relative stiffness with respect to soil. The presence of localized supports is found to be a critical factor, which leads the stresses to exceed the strength of the cast iron material. This study contributes to the development of a better understanding of the mechanism of cast iron water mains failure.

Acknowledgements

First and foremost I am very grateful to my supervisor Dr. Ashutosh Dhar, for the continuous support, guidance and encouragement and also for the financial support provided. Also, I greatly acknowledge the funding received by Research and Development Corporation (RDC) of Newfoundland and Labrador and the School of Graduate Studies, Memorial University of Newfoundland.

Furthermore, I highly appreciate the support given by the research and administration staff of the Faculty of Engineering and Applied Science, Memorial University, especially Dr. Leonard Lye, Moya Crocker, Coleen Mahoney and everyone who helped me in different ways. My sincere gratitude goes to the Canadian Geotechnical Society (CGS), especially Sylvia Dooley, Chair of Newfoundland CGS Chapter, for awarding me with the travel grant for presenting a paper at 68th Canadian Geotechnical Engineering Conference, which was a splendid encouragement for me on those days.

Finally, I would like to thank my friends, my loving and supportive husband, Dinesh Herath, my parents, my sister and brother for all the love and support. Thank you!

Table of Contents

Abstract.....	ii
Acknowledgements.....	iii
Table of Contents.....	iv
List of Tables.....	ix
List of Figures.....	x
List of Symbols, Nomenclature or Abbreviations.....	xv
Chapter 1. Introduction and Overview.....	1
1.1 Identification of the Problem.....	2
1.2 Objectives.....	4
1.3 Framework of Thesis.....	5
1.4 References.....	7
Co-authorship Statement.....	8
Chapter 2. Literature Review.....	10
2.1 Introduction.....	10
2.2 Material Behaviour.....	10
2.3 Structural Behaviour.....	13
2.4 Forces acting on Water Pipelines.....	15

2.4.1	Internal Water Pressure.....	15
2.4.2	Bending Forces	15
2.4.3	External Forces	15
2.4.4	Soil Movement Induced Tensile Stresses	16
2.4.5	Temperature Induced Forces.....	16
2.5	Failure Mechanisms of Cast Iron Pipelines.....	17
2.5.1	Circumferential Cracking.....	17
2.5.2	Longitudinal Cracking	18
2.5.3	Corrosion Pits.....	19
2.5.4	Bell Shearing.....	19
2.5.5	Spiral Cracking	20
2.6	Causes of Failure.....	21
2.6.1	Corrosion.....	21
2.6.2	Pitting Corrosion.....	23
2.6.3	Loss of Bedding Supports.....	24
2.6.4	Concentrated Localized Supports	27
2.6.5	Manufacturing Defects.....	28
2.6.6	Human Error	30
2.7	Finite Element Modelling.....	30

2.7.1	Element Types	31
2.7.2	Nonlinearities	32
2.7.2.1	Material Nonlinearity	33
2.7.2.2	Geometrical Nonlinearity	34
2.7.2.3	Boundary Condition Nonlinearity	34
2.8	Summary	36
2.9	References	36
Chapter 3. Three Dimensional Finite Element Analyses of Partially Supported Water Mains		42
3.1	Introduction	43
3.2	Problem Statement	44
3.3	Outline of the Structural Model	48
3.4	Numerical Modeling	52
3.4.1	Model Description	52
3.4.2	Materials	54
3.4.3	Boundary Conditions	54
3.4.4	Model Validation	55
3.5	Results	56
3.5.1	Effect of Void Geometry without Point Supports.....	57

3.5.2	Effect of Void Geometry with Point Supports.....	62
3.6	Conclusions	65
3.7	References	66
Chapter 4. Stresses in Cast Iron Water Mains Subjected to Non-Uniform Bedding and		
Localized Concentrated Forces.....		
4.1	Introduction	70
4.2	FE Modelling.....	75
4.3	Model Description.....	76
4.4	Material Parameters.....	78
4.5	Analytical Solution (Rajani and Tasfamariam 2004).....	80
4.6	Comparison of Models	82
4.7	Effect of Voids	88
4.8	Effects of Localized Supports	96
4.9	Conclusions	99
4.10	References	101
Chapter 5. Numerical Modelling of Buried Cast Iron Water Mains Subjected to Pitting		
Corrosion		
5.1	Introduction	106
5.2	FE Model.....	109

5.3	Material Parameters.....	113
5.4	Effects of Bedding Support	114
5.5	Effect of Material Stiffness	123
5.6	Effect of Localized Point Forces	129
5.7	Comparison of Pipe with and without Pit	132
5.8	Conclusions	134
5.9	References	136
Chapter 6.	Summary	139
6.1	Introduction	139
6.2	Conclusions	140
6.2.1	Erosion Voids with Rigid Localized Support	140
6.2.2	Partially Supported Bedding with Flexible Localized Supports.....	140
6.2.3	Effect of a Corrosion Pit	141
6.3	Recommendations for Future Study.....	141

List of Tables

Table 2-1: Typical mechanical properties of grey cast iron. (After ASM International, 1990)	11
Table 2-2: Different elastic modulus values used in different studies	13
Table 3-1: Parametric study	52
Table 4-1: Material Parameters	79
Table 4-2: Maximum stresses in pipe wall at mid-span of the unsupported zone	90
Table 5-1: Properties of materials and other parameters	114
Table 5-2: Factor of safety in longitudinal and circumferential directions of the pipe for different conditions	125
Table 5-3: Maximum pipe stresses for varying pit sizes and relative stiffness	126
Table 5-4: Maximum stresses for voids with localized supports	130
Table 5-5: Factor of safety in longitudinal and circumferential directions of the pipe with localized supports for different conditions	132

List of Figures

Figure 1-1: Failure rate of each failure mode for different materials. (After Folkman, 2012)	2
Figure 1-2: Sketch of cast iron pipeline subjected to an erosion void	3
Figure 1-3: Sketch of cast iron pipeline subjected to an erosion void and localized concentrated support (not to scale)	4
Figure 2-1: Stress-strain relationship of different classes of grey cast iron material. (After ASM International, 1990)	12
Figure 2-2: "Bath-tub" curve of the life cycle of a buried cast iron pipeline. (After Rajani and Tesfamariam, 2004)	14
Figure 2-3: Circumferential crack in an 8 inch diameter cast iron pipeline. (after Vipulanandan et al., 2011)	17
Figure 2-4: Longitudinal crack in a 24" diameter cast iron pipeline. (after Rajani and Abdel- Akher, 2012)	18
Figure 2-5: Corrosion pit in a cast iron water main extracted from Memorial University premises	19
Figure 2-6: Illustration of bell shearing failure. (After Makar et al., 2001)	20
Figure 2-7: Spiral crack of a medium diameter ductile iron pipeline. (After Makar et al., 2001)	20
Figure 2-8: Types of corrosion (After CorrView International, 2012).....	22
Figure 2-9: Schematic model of pipe-soil interaction of Rajani and Tesfamariam (2004)	25

Figure 2-10: Sequence of stages leading to failure as interpreted by Farshad (2006)	28
Figure 2-11: Porosity of a pit cast pipe extracted in Toronto (After Makar et al., 2001). 29	
Figure 2-12: Geometry of SOLID186 element (ANSYS, 2013)	32
Figure 2-13: Geometry of CONTA174 element	35
Figure 2-14: Different contact algorithms. (After Dezfooli et al., 2015)	36
Figure 3-1: A corrosion in a water main	45
Figure 3-2: A segment of water main exhumed from Memorial University Campus	46
Figure 3-3: Water leaking through a circumferential crack at the City of Mount Pearl (Arsenault, 2015)	46
Figure 3-4: Longitudinal section of the pipe system (all dimensions are in mm)	48
Figure 3-5: Cross sectional schematic of symmetric and un-symmetric void angles of (a) 90° (b) 45° and (c) 22.5° at the invert, and (d) 90° (e) 45° and (f) 22.5° at the springline	51
Figure 3-6: Typical finite element mesh used to model the pipe-soil structure	53
Figure 3-7: Comparison of results from analytical model and finite element analysis	56
Figure 3-8: Variation in longitudinal stresses around the pipe circumference at mid-length of the void (a) for the symmetric case, (b) for the unsymmetric case and (c) Maximum longitudinal stresses, for voids at the invert.....	58
Figure 3-9: Variation in longitudinal stresses around the pipe circumference (a) for the symmetric case, (b) for the unsymmetric case and (c) Maximum longitudinal stresses, for voids at the springline	59
Figure 3-10: Variation in hoop stresses around the pipe circumference (a) symmetric voids, (b) unsymmetric voids and (c) Maximum hoop stresses, for voids at the invert.....	61

Figure 3-11: Variation in hoop stresses around the pipe circumference (a) symmetric voids, (b) unsymmetric voids & (c) Maximum longitudinal stresses, for voids at the springline	62
Figure 3-12: Variation in longitudinal stresses around the pipe circumference (a) for symmetric, (b) for unsymmetric, voids at invert.....	64
Figure 3-13: Variation in hoop stresses around the pipe circumference (a) for symmetric, (b) for unsymmetric, voids at invert	64
Figure 4-1: Schematic of a longitudinal section of the pipe-soil system.....	75
Figure 4-2: Typical finite element mesh used to model the pipe-soil structure	77
Figure 4-3: Winkler pipe-soil model (After Rajani and Tesfamariam, 2004)	80
Figure 4-4: Comparison of flexural stresses from analytical model and 2D FE analysis.	84
Figure 4-5: Cross-section of pipe-soil system with 180° void at the invert.....	85
Figure 4-6: Comparison of flexural stresses for a void thickness of 200 mm	86
Figure 4-7: Comparison of flexural stresses for a void thickness of 50 mm	86
Figure 4-8: Flexural stresses with elastic and elastio-plastic soil models	88
Figure 4-9: Void sizes and locations.....	89
Figure 4-10: Stress distribution along the circumference of thick wall pipes (void thickness = 50 mm, pipe modulus = 138 GPa).....	91
Figure 4-11: A circumferential crack near the pipe invert in the City of Mount Pearl, adapted from Liyanage and Dhar, (2015).....	92
Figure 4-12: Stress distribution around thin wall pipes (void thickness=50 mm, void angle=180°, Ep=138 MPa).....	93

Figure 4-13: Pipe stresses for a void thickness of 200 mm ($E_p = 138$ MPa, void angle = 180°).....	95
Figure 4-14: Pipe stresses for the void between the invert and springline	96
Figure 4-15: Pipe backfill containing rock pieces	97
Figure 4-16: Modeling point support.....	97
Figure 4-17: Stresses on a partially supported pipe with localized soil reactions	98
Figure 5-1: Schematic of a longitudinal section of buried pipe.....	110
Figure 5-2: Idealization of pipe with concentrated support near the void	111
Figure 5-3: A typical FE model	112
Figure 5-4: Longitudinal stresses for the pipe in uniform bedding	116
Figure 5-5: Circumferential stresses for the pipe in uniform bedding.....	117
Figure 5-6: Stresses in the pipe wall for 1 m long void in the soil bedding (void extends 90°).....	119
Figure 5-7: Stresses around pipe circumference.....	121
Figure 5-8: Stresses at pipe mid-length in a thick-wall pipe with a void depth of 50mm	122
Figure 5-9: Stresses in a thick pipe for a void angle of 180°	123
Figure 5-10: Pipe stresses for a void angle and thickness of 180° and 50mm, respectively (Pipe modulus = 138GPa).....	124
Figure 5-11: Maximum longitudinal and circumferential stresses with relative stiffness	127

Figure 5-12: Maximum stresses in longitudinal and circumferential directions as a function of relative stiffness between pipe and soil for different pit sizes..... 128

Figure 5-13: Stresses on a partially supported pipe with localized soil reactions 129

Figure 5-14: Comparison of stresses for the pipe with and without pit..... 133

Figure 5-15: Comparison of stresses for the pipe with and without pit with localized support..... 134

List of Symbols, Nomenclature or Abbreviations

D = pipe outer diameter

E_p = Young's modulus of pipe

E_s = Young's modulus of soil

F_z = maximum spring load

I_{zz} = moment of inertia

k'_s = elastic foundation modulus

M_{xx} = bending moment

q = line load

R = pipe radius

v = vertical deflection

v_b = vertical deflection in unsupported zone

v_c = vertical deflection in plastic zone

v_e = vertical deflection in the elastic zone

α = factor used to replace 0.65 in elastic foundation modulus

λ = reciprocal of the flexural characteristic length

ν_s = Poisson's ratio

σ_x = flexural stress

ϕ' = Effective angle of internal friction

ψ = dilation angle

Chapter 1. Introduction and Overview

Buried pipelines are essential infrastructure in water transportation systems as they serve an essential commodity, water, to many communities and industries. In the early days, ancient civilizations used clay, lead, bronze and wood to manufacture water pipelines that functioned as aqueducts and tunnels. However, with the invention of cast iron material, water distribution networks grew rapidly in USA in 1890s (Koelble and Hogan, 1967).

As reported by American Water Works Association (2011), during the time period of 1870 to 1920 in almost all the regions across North America, the estimated distribution of watermains by cast iron was 100%. This statistic clearly reflects that those watermains have aged about 96 to 146 years at present. It is evident from statistical records reported by American Water Works Association (2011) that the average estimated service life of cast iron pipelines is about 105 to 135 years. Given the above facts, it is without a doubt that the cast iron pipelines are in the “dawn of the replacement era” as stated by American Water Works Association.

In addition, about 240,000 water main breaks are occurring every year in the United States. As a result, the estimated water loss from water distribution systems is about 1.7 trillion gallons per year with a financial cost of \$2.6 billion per year (Murray, 2007). Consequently, the 2013 report card for America’s infrastructure issued by American Society of Civil Engineers granted a “D” grade symbolizing a poor status for drinking water infrastructure.

1.1 Identification of the Problem

Failure of Cast Iron water main occurs frequently due to various reasons. Aging of pipelines, aggressive environmental conditions and undesirable soil conditions contribute to this problem. Since potable water transportation systems serve a major commodity to many communities, the importance of minimising the number of failures is highly recognized. In order to do so, one should understand the problem thoroughly. It is also essential to understand the problem specifications. Moreover, if the problem is complex, it could be divided into sub-problems and each sub-problem analysed to understand its requirements.

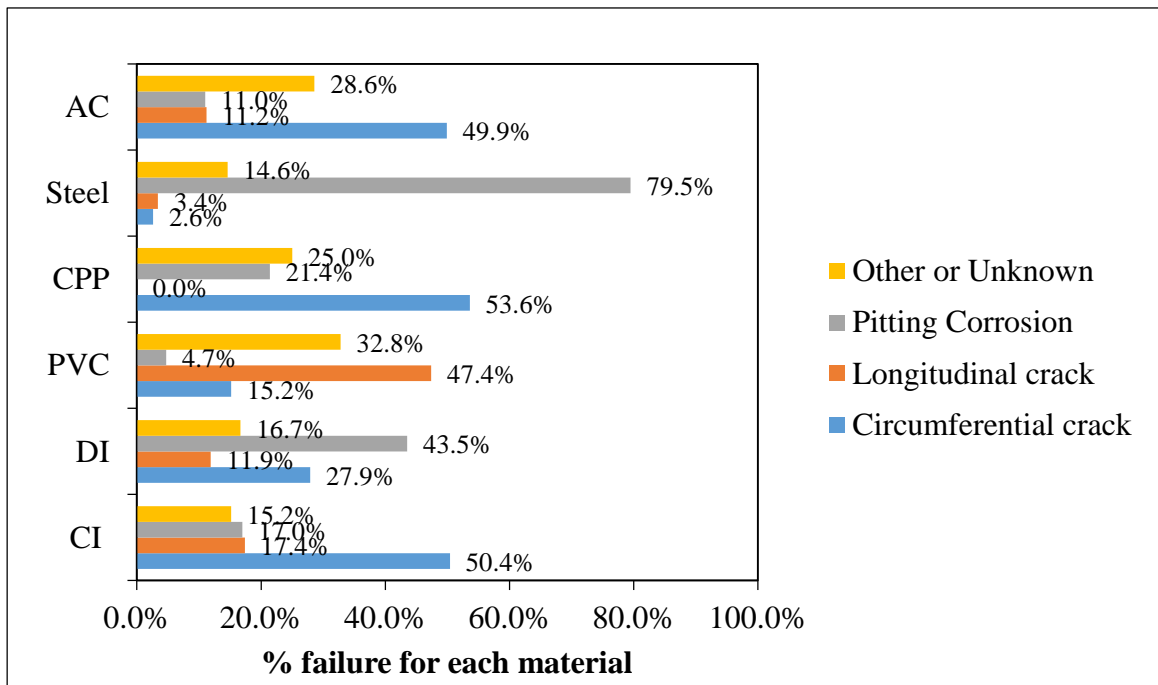


Figure 1-1: Failure rate of each failure mode for different materials. (After Folkman, 2012)

The most common failure mode of cast iron pipelines in the field is the circumferential cracking due to the maximum stresses in the longitudinal direction. As the statistics from the past literature show, about 50% of failure in cast iron pipelines are caused by circumferential cracking, while the second highest failure rate is only 17% which is caused by longitudinal cracking (as shown in Figure 1-1).

Circumferential cracking in the pipes can be caused mainly due to high bending moments. When cast iron pipes age and deteriorate, corrosion pits may emerge in the pipe wall. Through these holes unexpected water leakages may develop, eroding the bedding soil surrounding the pipeline. As a consequence, this phenomenon may weaken the bedding support in the pipeline, eventually giving rise to unwanted erosion voids in the bedding around the pipeline. When a pipeline is subjected to these erosion voids, the pipeline may bend towards the void due to soil, traffic and frost loads and self weight, exerting flexural stresses in longitudinal direction of the pipe wall. A much exaggerated form of such a situation is illustrated in Figure 1-2.

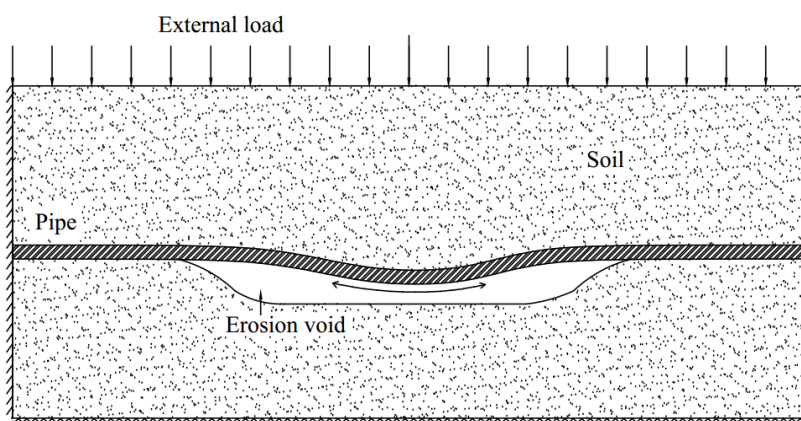


Figure 1-2: Sketch of cast iron pipeline subjected to an erosion void

Furthermore, when the surrounding bedding erodes away, initially the light weight fine soil particles disintegrate and wear away. At the next stage the remaining bulky coarse soil particles attempt to erode away, however due to their coarseness and size they may conglomerate locally and develop a localized concentrated support to the pipeline. This scenario is sketched in Figure 1-3.

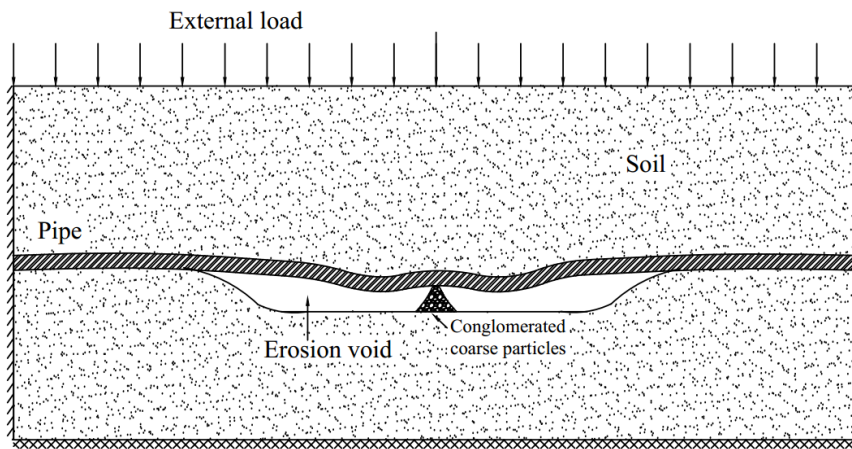


Figure 1-3: Sketch of cast iron pipeline subjected to an erosion void and localized concentrated support (not to scale)

1.2 Objectives

The objectives of this research are:

1. To study the stresses in cast iron water mains subjected to partially supported bedding condition using three dimensional finite element analyses.
2. To examine the stresses in cast iron water mains subjected to non-uniform bedding and localized concentrated forces.

3. To investigate the effect of pitting corrosion on the failure mechanism of buried cast iron water mains.

1.3 Framework of Thesis

This thesis is written in the manuscript format and it is organized in six chapters that include Introduction and Overview (Chapter 1), Literature review (Chapter 2), three major research publications (Chapter 3,4 and 5) and Summary (Chapter 6). A brief synopsis of each chapter is outlined as follows.

In Chapter 2, a comprehensive literature review on structural capacity of cast iron water mains and finite element modelling is presented. This section discusses material and structural behaviour of cast iron water mains. A much elaborated review on the failure mechanisms of cast iron water mains, including illustrated examples, is also presented here. Furthermore, previous literature on finite element modelling of pipe-soil systems and nonlinearity considerations associated with simulating actual field conditions are also reviewed and discussed in Chapter 2.

In Chapter 3, a study of a three dimensional analysis of a partially supported cast iron water main subjected to soil load, vehicle surcharge and internal water pressure is presented. The paper discusses the pipe wall stresses in circumferential and longitudinal directions when the pipeline is exposed to erosion voids with different sizes and symmetric and unsymmetric shapes, and located at springline and invert of the pipeline. Moreover, it introduces the importance of studying the effect of localized concentrated supports on pipe wall stresses that lead to ultimate failure by analysing the same system subjected to a rigid

point support. This paper was published in the 68th Canadian Geotechnical Conference (GeoQuebec2015) in Quebec City.

In Chapter 4, a study of stresses in cast iron water mains subjected to non-uniform bedding and localized concentrated forces is presented. This paper evaluates an existing analytical solution for calculating pipe wall stresses by using the finite element method. Also the parametric study deployed in this paper is more focused on pipe wall thickness, the relative stiffness between pipe and soil, erosion void depth, angle and location. In addition, it provides a unique approach that investigates the effect of flexible localized concentrated supports on pipe walls and emphasises a failure mechanism of cast iron water main. This paper is submitted to the Soils and Foundations journal.

In Chapter 5, an investigation on the effect of pitting corrosion of buried cast iron water mains using numerical modelling is presented. This paper discusses on the possible circumferential cracking of buried cast iron water mains subjected to pitting corrosion, non-uniform bedding condition and localized concentrated supports. It also studies the effect of the relative stiffness of the pipe with respect to soil on the development of higher longitudinal stresses.

Chapter 6 is the summary of the thesis and it includes the overall conclusion, recommendations and suggestions for future work.

1.4 References

- American Water Works Association. (2011). "Buried No Longer: Confronting America's Water Infrastructure Challenge." American Water Works Association. <http://www.awwa.org/Portals/0/files/legreg/documents/BuriedNoLonger.pdf>.
- Koelble, F. T., and Hogan, W. T. (1967). Cast Iron Soil Pipe and Fittings Handbook. Tennessee: Cast Iron Soil Pipe Institute.
- Murray, D. J. (2007). "Aging Water Infrastructure Research Program: Addressing the Challenge through Innovation." Brochure EPA/600/F-07/015. Washington, DC: U.S. Environmental Protection Agency.
- Folkman, S. (2012). "Water Main Break Rates in the USA and Canada: A Comprehensive Study." Utah State University Buried Structures Laboratory.

Co-authorship Statement

In all the papers presented in the following chapters, myself, Hordiyamulla Liyanage Kasuni Tharuka, is the principle author. My supervisor Dr. Ashutosh Dhar co-authored each manuscript providing guidance and support. The dedication from each authors for each manuscript is detailed as follows.

Liyanage, K., and Dhar, A. S. (2015). “Three Dimensional Finite Element Analyses of Partially Supported Water Mains.” Presented in 68th Canadian Geotechnical Conference, Quebec City, QC, Canada and is published in the conference proceedings.

I am the primary author and carried out all analysis. I prepared the first draft of the manuscripts and subsequently revised the manuscripts based on the co-authors’ feedback and the peer review process. As a co-author, Dr. Ashutosh Dhar provided support in developing the idea, provided guidance on finite element modelling and reviewed the manuscript.

Liyanage, K., and Dhar, A. S. (2016). “Stresses in Cast Iron Water Mains Subjected to Non-Uniform Bedding and Localized Concentrated Forces”. Soils and Foundations Journal (under review).

Within the capacity of the primary author, I created the framework of the study, developed finite element models and drafted the initial manuscript. Dr. Ashutosh Dhar co-authored the manuscript who supported on developing the idea, provided guidance during finite element modelling and reviewed the manuscript.

Liyanage, K., and Dhar, A. S. (2016). “Numerical Modelling of Buried Cast Iron Water Mains Subjected to Pitting Corrosion”. Engineering Failure Analysis Journal (under review).

I am the primary author and I developed the idea and the methodology of the study. I carried out finite element analysis and prepared the initial draft of the manuscript. As the co-author, Dr. Ashutosh Dhar supported in developing the idea, helped during finite element analysis and reviewed the manuscript.

Chapter 2. Literature Review

2.1 Introduction

Cast iron is one of the oldest pipe materials used for municipal water transportation systems. However, understanding the structural behaviour and failure mechanisms of cast iron pipes was not a subject of research attention until the water main failure became a concern for the municipalities. Over the last few decades, researchers are focusing on developing a better understanding of the material behaviours and the structural behaviour of the pipes under various installation and loading conditions. This chapter presents a review of literature pertaining to address cast iron water main problems.

2.2 Material Behaviour

According to ASTM specification, grey cast iron (i.e., grade A 48 cast iron) is categorized in terms of tensile strength in an ascending manner starting from class 20, having a minimum tensile strength of 140 MPa, to class 60, having a minimum tensile strength of 410 MPa. Typical mechanical properties of grey cast iron are summarized in Table 2-1. It is important to realize that the compressive strength is about three to four times higher than the tensile strength for cast iron.

Table 2-1: Typical mechanical properties of grey cast iron. (After ASM International, 1990)

ASTM A 48 class	Tensile strength (MPa)	Compressive strength (MPa)	Elastic modulus (GPa)
20	152	572	66-97
25	179	669	79-102
30	214	752	90-113
35	252	855	100-119
40	293	965	110-138
50	362	1130	130-157
60	431	1293	141-162

Typical stress strain relationships of class 40 and class 20 grey cast iron materials under tension and compression are shown in Figure 2-1. As observed in the past literature, the behaviour of grey cast iron is usually not compatible with Hooke's law over the full range of stress-strain relationship (ASM International, 1990). However, it shows a quasi-linear behaviour. The stress-strain curve consists of a linear segment at the initial stress values, and when the stress increases, the curve traverses into the plastic zone with a mild excursion. Therefore, there are several ways of determining the modulus of elasticity using the stress-strain graph. It is best practice to use the slope of the line connecting the origin and the point corresponding to one-fourth of the tensile strength of the stress-strain curve

(ASM International, 1990). However, the slope near the origin of the stress-strain graph can also be considered for small deformations.

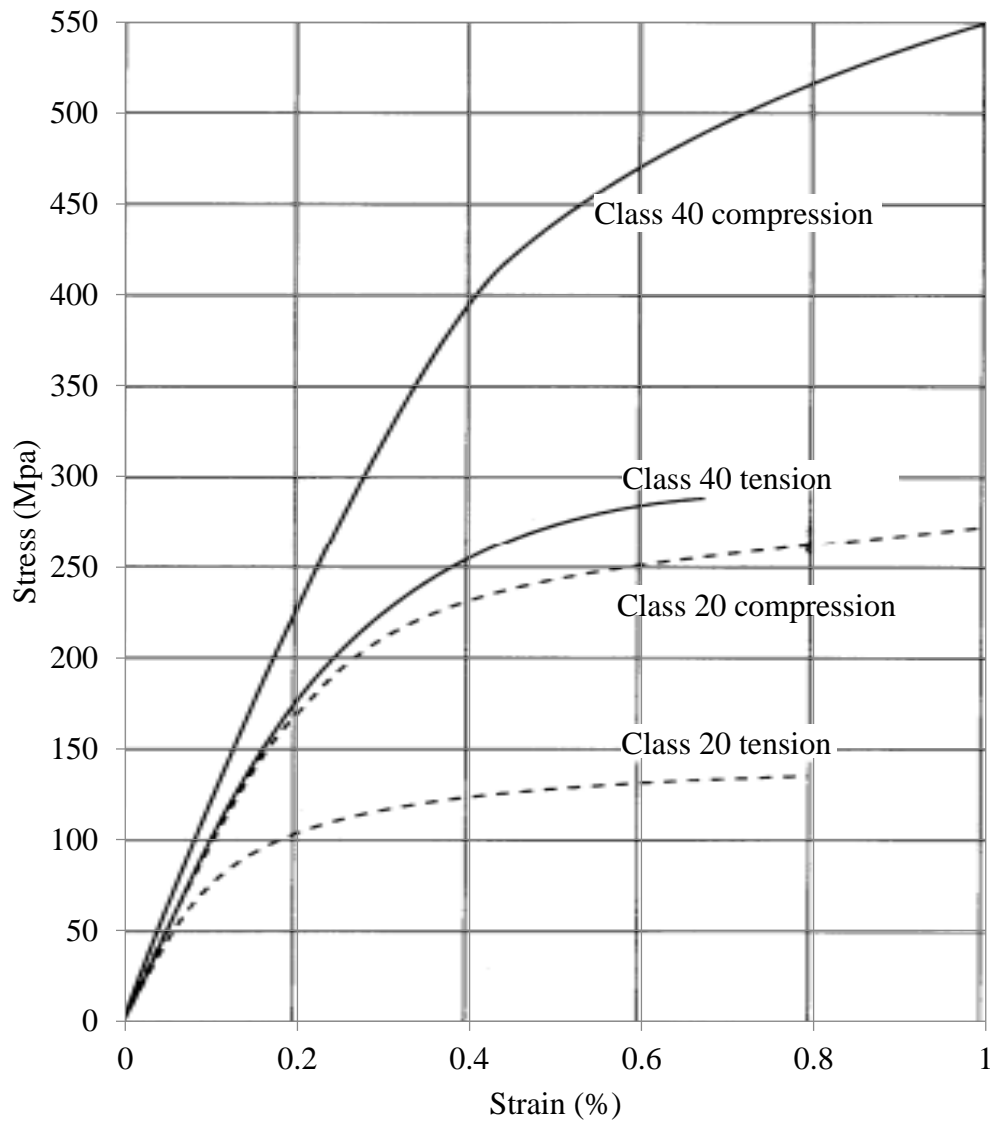


Figure 2-1: Stress-strain relationship of different classes of grey cast iron material. (After ASM International, 1990)

According to ASTM specification A 48, the Young's modulus of grey cast iron can vary between 66 GPa to 162 GPa. However, many researchers use different values for Young's modulus of grey cast iron which are summarized in Table 2-2.

Table 2-2: Different elastic modulus values used in different studies

Reference	Young's Modulus (GPa)
Balkaya et al. (2012)	70
Rajani and Abdel-Akher (2012)	120-157
Shao and Zhang (2008)	206
Makar et al. (2005)	216.5
Seica and Packer (2004)	23-150
Rajani and Tesfamariam (2004)	206
Rajani et al. (2000)	38-168
Rajani et al. (1995)	207

2.3 Structural Behaviour

Structural behaviour of pipes varies during the lifetime over different phases. The life cycle of a buried pipeline can be categorized into three main phases, namely: 'burn-in phase', 'in-use phase' and 'wear-out phase', all of which can be presented in a bath-tub curve as shown in Figure 2-2 (Rajani and Tesfamariam, 2004).

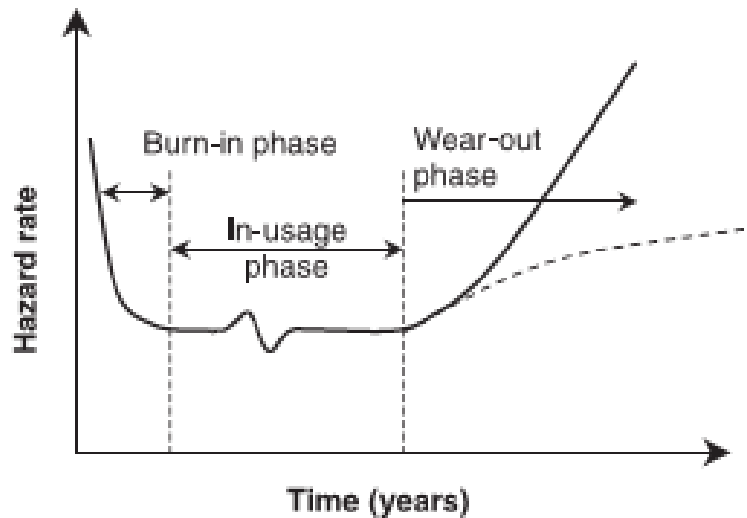


Figure 2-2: "Bath-tub" curve of the life cycle of a buried cast iron pipeline. (After Rajani and Tesfamariam, 2004)

The 'burn-in phase', which represents the period just after installation, has a declining frequency of hazards. The risks associated with this phase are vastly due to faulty installation or faulty pipes. Secondly, the pipeline enters the 'in-usage phase' in which the hazard rate is low and steady, as the pipeline operates according to the design. Usually an uninterrupted performance of the pipeline is expected in this period unless any unusual heavy loads or third-party interferences occur. Finally, the 'wear-out phase' exhibits the period when the pipe is subjected to aging and deterioration. As can be seen from Figure 2-2, the incline in the hazard rate is variable, which depends on the pipe properties and environmental conditions. Rajani and Tesfamariam (2004) illustrated that factor of safety of the pipe is low at 'wear-out phase' and it may reach its failure or breakage point.

2.4 Forces acting on Water Pipelines

In general, five categories of forces are identified on cast iron water pipes. These include the forces due to internal water pressure, bending forces, external forces, soil movement induced forces and temperature induced forces.

2.4.1 Internal Water Pressure

Internal water pressure is the major design load considered for water main design. The internal water pressure in its nominal level is not capable of causing pipe failure, since the pipeline is usually designed for that load. However, it could become a critical force if the water freezes or large surge pressures occur (Rajani et al., 1996). The resulting large hoop stresses may lead to failure of the pipeline.

2.4.2 Bending Forces

Bending forces may be exerted due to inadequate bedding support underneath the pipe, which in turn may create additional longitudinal stresses. Even though the longitudinal stresses due to bending forces alone may not cause pipe failure, when these are combined with other effects, the pipe may fail by circumferential cracking. This scenario is not well investigated in the past.

2.4.3 External Forces

External forces to the pipe may occur as a result of soil weight or vehicle load above the pipeline. In addition, frost loading and expansive clays may also impose additional loads (Makar et al., 2001). Failure due to the external forces is generally not encountered

particularly up to the 'in-usage phase' of the pipeline service life, because additional provisions are taken in the design with high safety margins to provide sufficient ring stiffness and to control ring deflection. However, at the 'wear-out phase', when the factor of safety of the pipe is reduced, the external forces may cause pipeline failure.

2.4.4 Soil Movement Induced Tensile Stresses

Soil movement induces additional tensile and/or bending stresses in several ways. Bending due to non-uniform bedding support, longitudinal friction between the soil and the pipe surface, as well as conglomerated soil particles creating a concentrated point-like force on the pipe wall, often add to the tensile stresses.

2.4.5 Temperature Induced Forces

Published literature indicates that water main failure rate in winter is at least twice as high as in summer (Ciottoni, 1985; Morris, 1967), demonstrating that temperature significantly contribute to the stress development on the pipe wall. Rajani and Tesfamariam (2004) reported that forces induced by temperature differences are highly unaccounted for in axial, flexural and circumferential response analyses in structural design of water mains. Aging pipelines that are subjected to temperature differentials between water in the pipe (1°C - 2°C) and the adjacent soil (10°C -12°C), showed a high rate of failure (Rajani and Tesfamariam, 2004).

2.5 Failure Mechanisms of Cast Iron Pipelines

Makar et al. (2001) performed an extensive study on failure mechanisms in grey cast iron pipes by investigating real cases of failures that occurred in the Ontario region. They indicated the major failure modes of cast iron pipelines as blowout holes, circumferential cracking, bell splitting, longitudinal cracking, bell shearing and spiral cracking.

2.5.1 Circumferential Cracking

Circumferential cracking in pipe wall may be caused due to excessive longitudinal stresses resulting from bending of the pipe as well as contraction due to shrinkage. Different failure modes are expected due to excessive longitudinal stresses.



Figure 2-3: Circumferential crack in an 8 inch diameter cast iron pipeline. (after Vipulanandan et al., 2011)

Figure 2-3 demonstrates a circumferential break in a 8 inch diameter cast iron pipeline buried 4 ft beneath the ground in a clayey soil (Vipulanandan et al., 2011). It is to be noted

that, although small diameter pipes have lower water pressure, they consist of a smaller moment of inertia, which makes them more vulnerable to failure through circumferential cracking.

2.5.2 Longitudinal Cracking

Makar et al. (2001) revealed that large diameter pipelines are prone to longitudinal cracking (as illustrated in Figure 2-4) and shearing at the bell due to higher water pressure. High water pressure induces excessive circumferential tension in the pipe wall. External load also causes circumferential bending (ovalling) that induces additional circumferential stresses. The circumferential stress, if exceeds the strength of the material, causes longitudinal cracking.



Figure 2-4: Longitudinal crack in a 24" diameter cast iron pipeline. (after Rajani and Abdel-Akher, 2012)

2.5.3 Corrosion Pits

Corrosion may cause blowout holes when pipe wall thickness is reduced, followed by internal pressure blowing out the remaining wall thickness, creating a very small hole (as shown in Figure 2-5). This type of holes may result in redistribution of pipe wall stresses leading to a mechanism of pipeline failure.



Figure 2-5: Corrosion pit in a cast iron water main extracted from Memorial University premises

2.5.4 Bell Shearing

Bell and spigot connections are usually used to join watermains. At the design stage, these connections allow axial movement and slight rotation of about 3° - 4° in order to facilitate any unexpected, but limited, bending of the pipe (Rajani and Tesfamariam, 2004). However, Rajani and Tesfamariam (2004) indicated that these allowances will be restrained as a result of aging of cast iron pipelines. As a result, the compressive forces due to bending pushes the spigot of a pipe into the bell of the adjacent pipe, eventually creating

a shear crack propagating from the bell (Makar et al., 2001). Figure 2-6 represents a schematic diagram of a typical failure pattern by bell shearing mechanism.

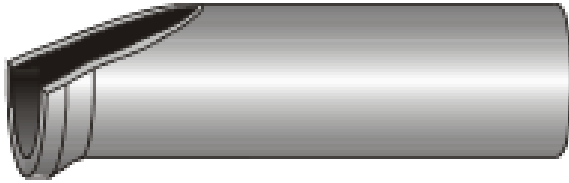


Figure 2-6: Illustration of bell shearing failure. (After Makar et al., 2001)

2.5.5 Spiral Cracking

The spiral cracking is a failure mode in between circumferential cracking and longitudinal cracking. It occurs mostly in medium diameter (380mm-500mm) pipes (Makar et al., 2001) due to a combination of bending forces and internal pressure resulting in high pressure surges. Initially, the crack starts in circumferential direction while propagating in longitudinal direction. A similar crack pattern of this type of failure of a ductile iron pipeline is shown in Figure 2-7.

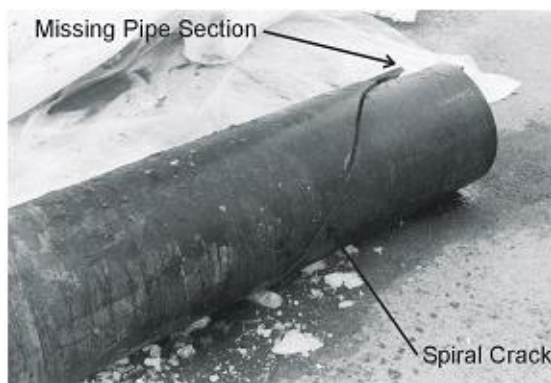


Figure 2-7: Spiral crack of a medium diameter ductile iron pipeline. (After Makar et al., 2001)

2.6 Causes of Failure

Different failure modes may occur due to various causes such as corrosion, loss of bedding support, concentrated localized forces, manufacturing flaws, and human errors. Failure of a water main can be caused by a single cause or multiple causes occurring simultaneously. Over the past several years, effort has been devoted to the study of failure mechanisms on cast iron pipelines. The current research focuses on three major causes of failure, namely, loss of bedding supports, concentrated localized supports and pitting corrosion that are briefly outlined below.

2.6.1 Corrosion

Corrosion is a major cause of cast iron pipeline failure, as it represents the most serious threat and major monetary loss to water distribution systems. According to Koch et al. (2002), the estimated total annual cost of corrosion was \$276 billion in the year 2001 in USA. Folkman (2012) reports that one in four water main breaks are caused by corrosion, which is ranked as the second highest cause of water pipeline failure.

There are several types of corrosion identified in water mains, such as uniform corrosion, pitting corrosion, tuberculation, galvanic corrosion and crevice corrosion. Each type of corrosion is illustrated with actual field observations as shown in Figure 2-8.



(a) Uniform corrosion



(b) Pitting corrosion



(c) Tuberculation



(d) Galvanic corrosion



(c) Crevice corrosion

Figure 2-8: Types of corrosion (After CorrView International, 2012)

2.6.2 Pitting Corrosion

Pitting corrosion can be diagnosed as cavities or holes restrained to a point or small localized area of the pipeline wall. This is one of the most dangerous forms of corrosion due to difficulty in detecting, predicting and designing against.

Makar et al. (2005) investigated the effects of pitting corrosion experimentally and numerically using artificial holes on the pipe wall. They reported on typical sizes of corrosion pits that contribute to circumferential failure. Makar et al. (2005) conducted a parametric study and considered pit diameters of 10mm, 20mm, 40mm, 60mm and 80mm under different effects of loading conditions such as water pressure, frost load, temperature changes, loss of support, soil properties and wall thickness. It was evident from the parametric study that the corrosion pits influenced the localized strain distribution and produced significant stress concentrations. They concluded that spun cast pipes with pit sizes larger than 40mm in diameter are vulnerable to circumferential failure, whereas pit cast pipes with pit sizes larger than 20mm in diameter are vulnerable to circumferential failure. Makar et al. (2005) reported that water pressure only with corrosion pits may not lead to pipe failure. Nevertheless, if the pipe is subjected to higher stresses due to other environmental conditions, then the effect of water pressure could be significant. The study demonstrated that the effect of pitting corrosion in pit cast pipes and thin wall (9mm thick) spun cast pipes exhibits more vulnerability to circumferential failure than thick wall (12mm thick) spun cast pipes. The loss of bedding support in combination with corrosion pits was found to lead significantly high bending stress in the pipe. Depending on the boundary

conditions, the pit cast pipes having an unsupported length of 3m could exceed failure strains with pit sizes greater than 40mm to 60mm (Makar et al., 2005).

2.6.3 Loss of Bedding Supports

Loss of bedding support due to erosion of the soil has been recognized as a cause for stress development on the pipe wall. Rajani and Tesfamariam (2004) developed an analytical approach to quantify the contributions of different stress drivers such as pipe material type and size, bedding conditions, under the impact of the unsupported length of the pipeline. The soil was modelled using elastic and elastoplastic Winkler springs.

Rajani and Tesfamariam (2004) assumed that the cast iron pipe deformations are very small and within the elastic zone during loading, while soil may undergo plastic deformation near the unsupported region. Hence two distinct soil regions were classified as elastoplastic and elastic. Accordingly, they idealized the system as a beam on an elastoplastic foundation (as shown in Figure 2-9).

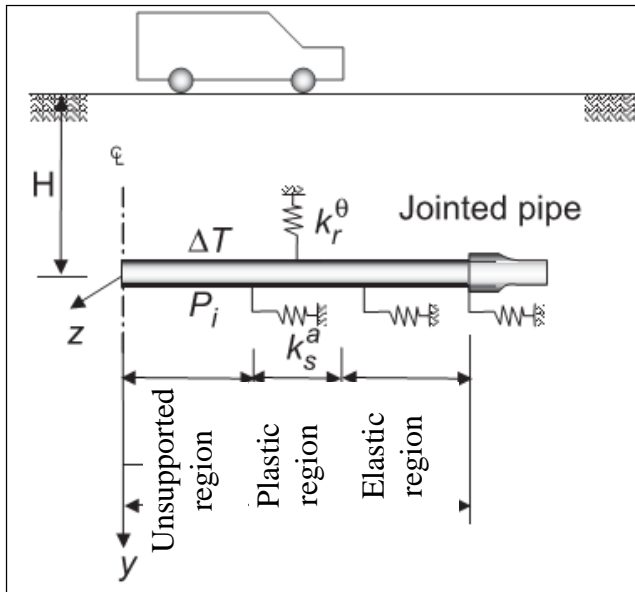


Figure 2-9: Schematic model of pipe-soil interaction of Rajani and Tesfamariam (2004)

After performing the sensitivity analysis, they observed that pipe size/diameter has a great influence on the flexural stress, which is the most significant out of the axial and circumferential responses. Larger diameter water mains produced higher stresses. Furthermore, they indicated that as the extent of the unsupported length increases, the flexural stress also increased. In this Winkler-type model, the most dominant parameter for the flexural response is the lateral foundation modulus (k'_s) of the soil. Rajani and Tesfamariam (2004) concluded that the pipe behaves like a simply supported beam when k'_s is very small, the flexural stress drastically varies when k'_s is less than 50MPa, and finally flexural response stabilizes when k'_s exceeds 50MPa. In addition, they revealed that the elastoplastic behaviour of soil slightly increases the flexural stresses above that of analysis carried out with entirely elastic soil.

Shao and Zhang (2008) reviewed the model of Rajani and Tesfamariam (2004) and proposed a method to evaluate the extent of elastic and plastic regions in soil. However, when comparing the effect of elastoplasticity in the soil, the results reported by Shao and Zhang (2008) were contradictory to the results reported by Rajani and Tesfamariam (2004). Shao and Zhang (2008) argued that when the soil began to yield, the elastic soil could offer more axial resistance than elastoplastic soil, because elastic soil is stiffer than elastoplastic soil.

Finite element analyses were also used to investigate partially supported buried pipelines. Balkaya et al. (2012) demonstrated the behaviour of three dimensional stresses under the variations in erosion voids and parameters of soil and pipe using a finite element analysis. One of the significant findings of the study was that finite element analyses indicated low stresses in radial and longitudinal directions when compared with the stresses in circumferential direction. The peak tension was always found in the circumferential direction. Nonetheless, it should be noted that they used a linear elastic material model for cast iron pipe with elastic modulus of 70GPa and a Mohr-Coulomb elastoplastic material model with friction angle of 35° for medium dense sandy soil with elastic modulus of 40MPa. After performing a parametric study, Balkaya et al. (2012) observed that the stresses in the pipe increased in either case, as the erosion void length, angle or depth increases, or as the pipe thickness decreases.

Kamel and Meguid (2013) investigated experimentally and numerically the effect of contact loss between a buried sewer steel pipeline and surrounding sandy soil on the changes in earth pressure distribution and changes in pipe stresses. A two-dimensional

numerical simulation was performed using ABAQUS software in order to compare the results of experimental analysis. They concluded that the void size and location are the most predominant parameters that affect the earth pressure distribution around the pipe wall. The changes in the earth pressure can cause rapid change in the pipe wall stresses within a limited area. Bending moments in the pipe wall were found to be higher when the void size was larger. As well, when the location of the void is at the invert, the maximum change in moment was found at the vicinity of the void.

A similar study, incorporating an elastoplastic three dimensional finite element analyses was presented in Meguid and Kamel (2014) for buried rigid concrete pipeline. The voids were assumed as simplified circular geometry and defined semi-cylindrical zones at locations next to pipe invert and springline in order to simulate the presence of erosion voids. The study was concluded by finding that the highest change in pipe wall stresses were always in the vicinity of the voids. As well, circumferential stresses experienced a maximum increment of 36% when the void was at springline and a maximum reduction of 65% when the void was at invert. Progressive increment in void size led the longitudinal stresses to experience a maximum increment of 80% when the void was at springline, and a maximum increment of 225% when the void was at invert.

2.6.4 Concentrated Localized Supports

Farshad (2006) demonstrated a step-by-step failure case study of a buried GFRP (glass fiber reinforced polyester) pipe subjected to localized concentrated supports by coarse bedding particles as shown in Figure 2-10.

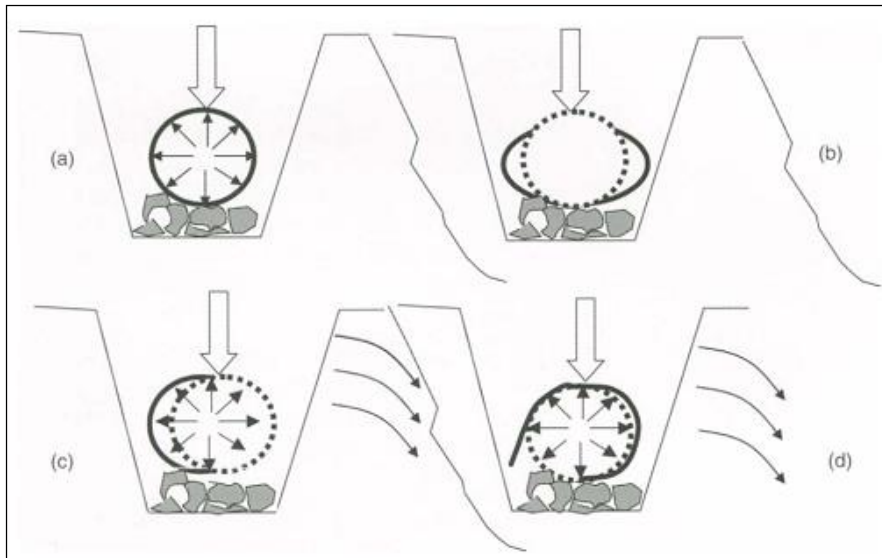


Figure 2-10: Sequence of stages leading to failure as interpreted by Farshad (2006)

As reported by Farshad (2006), the stages leading to the complete failure of the GFRP pipeline include, firstly, concentrated point loading on the pipe on coarse bedding due to large pieces of underlying stones. Secondly, the pipe became deformed by exceeding the elastic limit. Meanwhile, lateral displacement of surrounding adjacent soil could produce an unbalanced stress distribution in the pipe. Eventually, the pipe ruptured at the bottom zone due to combined action of vertical soil load, point load from underlying coarse bedding particles and frictional forces due to lateral displacement of surrounding soil. However, the effect of localized support on a buried cast iron water main has not been investigated to date.

2.6.5 Manufacturing Defects

There are several methods of manufacturing cast iron pipelines. Pit casting and spun casting are the most recognized among them. The process of pit casting or vertically casting

includes a vertical sand mould being poured with molten cast iron (Rajani et al., 2000). Eventually the moulds are removed when the metal is solidified after cooling. On the other hand, spun casting, horizontally casting or centrifugally casting involves a rotating sand mould being poured horizontally with molten cast iron using a ladle located at the center of the mould (Rajani et al., 2000). Depending upon the type of manufacturing method, a variety of defects could be identified in cast iron pipelines. Such manufacturing defects include porosity, inclusion of unintentional objects and changes in pipe wall thickness.

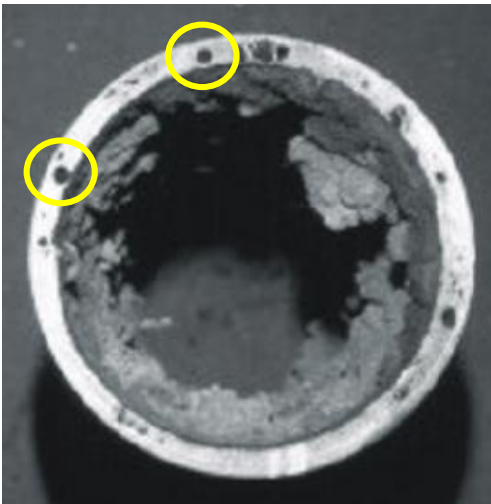


Figure 2-11: Porosity of a pit cast pipe extracted in Toronto (After Makar et al., 2001)

Pit cast pipes show greater contingency to porosity than spun cast pipes because air bubbles have to travel from the bottom of the pipe to the top to escape in the pit casting process, where as in spun cast pipes the escape path of air bubbles is much shorter since they only have to reach the inner wall of the pipe (Makar et al., 2001). As illustrated by Makar et al. (2001), pit cast pipes contained pores as large as 8mm to 9mm (Figure 2-11) and spun cast pipes contained pores as small as 2mm.

Inclusion of unintentional objects can cause formation of unexpected cracks, reduction in total cross section of the pipe, as well as stress concentrations. Moreover, changes in pipe wall thickness are another detrimental effect of ill-manufacturing procedure. As observed by Makar et al. (2001), pit cast pipes contained variations in pipe wall thickness up to 8mm at one side of the pipe and 14mm at the other. They also emphasized that even though the spun casting process produces precise uniform thickness around the circumference of the pipe, spun cast pipe was observed with change in pipe wall thickness from 18mm to 15mm spanning over a length of 2m.

2.6.6 Human Error

Human error is another important aspect to explore when considering failure on cast iron water pipelines. Improper design, poor installation, third party damage from excavation and repairing of adjacent properties, malpractice in transportation and negligence in maintenance are some of the factors under this category contributing to failure. Makar et al. (2001) report that several cast iron pipes were failed due to corrosion pits, and these pits were formed at the places where the black coating of the pipe was scratched during installation. Also they reported that subsequent failures have occurred after repairing one pipe section subjected to severe corrosion using stainless steel clamps, and suspected that the subsequent failures were caused by the third party damage due to repairing procedure.

2.7 Finite Element Modelling

The finite element method is a widely recognized numerical procedure that can provide approximate solutions to large scale problems using computer literacy within minimum

time consumption. A number of different approaches are used to model soil-pipe interaction problems, depending upon the capability of the software. Modelling capability of ANSYS (finite element software used in the current research) is briefly discussed below with application to soil-pipe interaction problems.

2.7.1 Element Types

ANSYS finite element software provides a wide variety of element types including BEAM, SOLID, PIPE, COMBIN, CONTAC, TARGE and so on. Researchers employed these elements for modelling of different soil-pipe interaction problems. A study conducted on elasto-plastic stress-strain analysis of buried steel pipeline using ANSYS software utilized PIPE288 element and COMBIN39 element for pipe and soil respectively (Trifonov and Cherniy, 2012). PIPE288 element, based on Timoshenko beam theory, is a three-dimensional two-node linear, quadratic or cubic element. It has six degrees of freedom and is most appropriate for linear and nonlinear applications. Furthermore, it includes added mass, hydrodynamic added mass and loading, and buoyant loading.

Riagusoff et al. (2010) deployed SOLID186 elements to model a pipe to study the cold bending operation used for in-situ pipeline route adjustments during on-shore pipeline construction. SOLID186 is a three dimensional 20-node higher order solid element consisting of three degrees of freedom per each node (as shown in Figure 2-12). It displays quadratic displacement behaviour and supports the mixed formulation capability for simulating deformations of nearly incompressible elastoplastic materials and fully incompressible hyper elastic materials.

pipe and/or the soil, the effect of interaction at the interface between pipe and soil and material behaviour. Notably, the following nonlinearities are expected in the finite element analysis in order to simulate the actual behaviour of the problem.

2.7.2.1 Material Nonlinearity

Typically, the material behaviour becomes nonlinear when the stress and/or strain exceed the elastic limits. In this study, the cast iron pipeline is expected to behave as a linear elastic material. However, soil is expected to behave as an elastoplastic material. Several failure criteria depending on the material behaviour have been available in the literature such as Tresca, Von Mises, Mohr-Coulomb and Drucker Prager. Tresca and Von Mises yield criteria are mostly suitable for isotropic metallic materials, whereas Mohr-Coulomb and Drucker Prager yield criteria are most applicable for materials that are strongly dependent on hydrostatic pressure such as soil, rock and concrete.

In fact, Tresca and Mohr-Coulomb yield surfaces produce a hexagonal cylinder and a hexagonal cone, respectively, while Von Mises and Drucker Prager yield surfaces produce a circular cylinder and a circular cone, respectively. Hence, yield and strength of the material is dependent on the intermediate principle stress in the Von Mises and the Drucker Prager failure criterion.

Previous studies indicate several methods to simulate this elastoplastic behaviour of soil. For instance, the Mohr-Coulomb model was used for the soil material when simulation was performed by ABAQUS finite element package (Balkaya et al., 2012; Meguid and Kamel, 2014). Also, in previous research, nonlinear spring elements were used to model the elastic-

perfectly plastic behaviour of soil material through ANSYS finite element software (Trifonov and Cherniy, 2012). The Drucker-Prager constitutive model in ANSYS software was used to adapt the plastic failure criterion of elastoplastic soil material behaviour (Yang, 2012).

2.7.2.2 Geometrical Nonlinearity

Geometrical nonlinearity is particularly important when a structure undergoes large deformations, large rotations and linearized pre-buckling. In general, equilibrium equations are formulated in the undeformed state considering geometric linearity. However, when geometric nonlinearity concept is incorporated, the equilibrium equations along with the stiffness matrix change to adopt the variations in deformed mesh configuration after each load increment (Watkins and Anderson, 1999).

2.7.2.3 Boundary Condition Nonlinearity

Nonlinear boundary conditions can be related to the behaviour of the contact between pipe and soil, as well as the behaviour of the applied external loading sequence. The literature on boundary condition nonlinearity shows a variety of approaches.

A study on elastic-plastic finite element analysis for buried steel pipelines simulated the pipe-soil interaction using a nonlinear surface-to-surface contact model, in which the target surface and the contact surface were modelled by TARGE170 elements and CONTA174 elements respectively (Wu et al., 2016). CONTA174 is a three dimensional 8-node higher order element with a quadrilateral shape which can be laid on the three dimensional solid elements surfaces with mid nodes as shown in Figure 2-13. CONTA174 elements paired

with TARGE170 elements via a shared real constant set to provide contact and sliding within rigid-to-flexible bodies and flexible-to-flexible bodies. Pipe-soil contact can be recognized as a rigid-to-flexible contact, in which the rigid surface (i.e.: pipe external wall) can be laid with TARGE170 elements, whereas the flexible surface (i.e.: soil layer adjacent to pipe external wall) can be laid with CONTA174 elements.

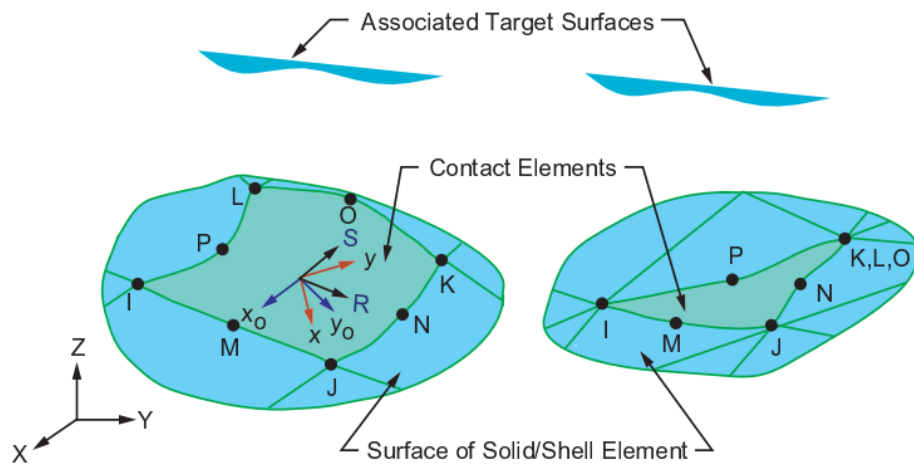


Figure 2-13: Geometry of CONTA174 element (ANSYS, 2013)

Dezfooli et al. (2015) simulated the interface between pipe and soil and the interface between different soil layers using contact algorithms. They used node-to-surface contacts, where each contact involves a single slave node and a group of nearby master nodes, and surface-to-surface contacts, where an average group of slave nodes are coupled with a group of nearby master nodes (Figure 2-14).

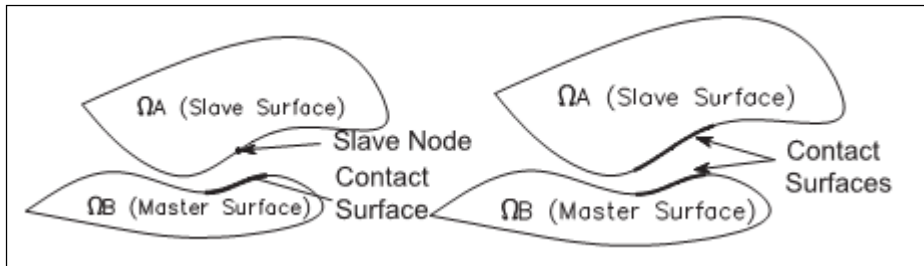


Figure 2-14: Different contact algorithms. (After Dezfooli et al., 2015)

2.8 Summary

An overview of cast iron material, failure modes observed in cast iron water mains, and different approaches of analysing pipe-soil interaction is presented in this chapter. The circumferential cracking, caused by excessive longitudinal stresses, was identified as the major failure mode for cast iron water main. However, high longitudinal stresses were not generally calculated in the analysis of pipe available in published literature, indicating that the mechanics of the circumferential cracking is not well-understood. Current literature does not include studies on pipe with lack of bedding support considering the effect of high relative stiffness of the pipe with respect to the surrounding soil as well as on the effects of pitting corrosion and localized concentrated forces on longitudinal stress development in the pipe wall, which are the focus of the present research.

2.9 References

ANSYS (2015). ANSYS® Academic Research, Release 16.2. ANSYS, Inc.

- ASM International. (1990). Properties and Selection: Irons, Steels, and High-Performance Alloys. ASM International. http://www.asminternational.org/online-catalog/handbooks/-/journal_content/56/10192/06181G/PUBLICATION.
- AWWA. (1967). USA Standard for Thickness Design of Cast-Iron Pipe. American Water Works Association. Vol. C101–67.
- Balkaya, M., Moore, I. D., and Sađlamer, A. (2012). “Study of Nonuniform Bedding Support Because of Erosion under Cast Iron Water Distribution Pipes.” *Journal of Geotechnical and Geoenvironmental Engineering* 138 (10): 1247–56. doi:10.1061/(ASCE)GT.1943-5606.0000689.
- Ciottoni, A.S. (1985). “Updating the New York City Water System.” In *Proceeding of the Speciality Conference on Infrastructure for Urban Growth*, 69–77. New York.
- CorrView International (2012) “Forms of Corrosion”. <http://www.corrview.com/>, accessed on January 15, 2016.
- Dezfooli, M. S., Abolmaali, A., and Razavi, M. (2015). “Coupled Nonlinear Finite-Element Analysis of Soil–Steel Pipe Structure Interaction.” *International Journal of Geomechanics* 15 (1): 04014032. doi:10.1061/(ASCE)GM.1943-5622.0000387.
- Farshad, M. (2006). “3 - Fracture of Plastic Pipes.” In *Plastic Pipe Systems*, edited by Mehdi Farshad, 53–100. Oxford: Elsevier Science. <http://www.sciencedirect.com/science/article/pii/B9781856174961500045>.

- Kamel, S., and Meguid, M. A. (2013). "Investigating the Effects of Local Contact Loss on the Earth Pressure Distribution on Rigid Pipes." *Geotechnical and Geological Engineering* 31 (1): 199–212. doi:10.1007/s10706-012-9580-8.
- Koch, G. H., Brongers, M. P. H., Thompson, N. G., Virmani, Y. P., and Payer, J. H. (2002). "Corrosion Cost and Preventive Strategies in the United States." FHWA-RD-01-156. National Technical Information Service. <https://trid.trb.org/view.aspx?id=707382>.
- Makar, J. M., Desnoyers, R., and McDonald, S. E. (2001). "Failure Modes and Mechanisms in Gray Cast Iron Pipe." In *Underground Infrastructure Research Conference*, 1–10. Kitchener, Ontario.
- Makar, J. M., Rogge, R., McDonald, S., and Tesfamariam, S. (2005). "The Effect of Corrosion Pitting on Circumferential Failures in Grey Iron Pipes." Denver: American Water Works Association.
- Meguid, M. A., and Kamel, S. (2014). "A Three-Dimensional Analysis of the Effects of Erosion Voids on Rigid Pipes." *Tunnelling and Underground Space Technology* 43 (July): 276–89. doi:10.1016/j.tust.2014.05.019.
- Morris, R. E. (1967). "Principal Causes and Remedies of Water Main Breaks." *Journal (American Water Works Association)* 59 (7): 782–98.

- Rajani, B., and Abdel-Akher, A. (2012). "Re-Assessment of Resistance of Cast Iron Pipes Subjected to Vertical Loads and Internal Pressure." *Engineering Structures* 45 (December): 192–212. doi:10.1016/j.engstruct.2012.06.019.
- Rajani, B., Makar, J., McDonald, S., Zhan, C., Kuraoka, S., Jen, C., and Viens, M. (2000). "Investigation of Grey Cast Iron Water Mains to Develop a Methodology for Estimating Service Life." Denver: Awwa Research Foundation.
- Rajani, B., and Tesfamariam, S. (2004). "Uncoupled Axial, Flexural, and Circumferential Pipe–soil Interaction Analyses of Partially Supported Jointed Water Mains." *Canadian Geotechnical Journal* 41 (6): 997–1010. doi:10.1139/t04-048.
- Rajani, B.B., Robertson, P. K., and Morgenstern, N. R. (1995). "Simplified Design Methods for Pipelines Subject to Transverse and Longitudinal Soil Movements." *Canadian Geotechnical Journal* 32 (2): 309–23. doi:10.1139/t95-032.
- Rajani, B., Zhan, C., and Kuraoka, S. (1996). "Pipe Soil Interaction Analysis of Jointed Water Mains." *Canadian Geotechnical Journal* 33 (3): 393–404. doi:10.1139/t96-061.
- Ravishankar, P., and Satyam, D. N. (2013). "Finite Element Modeling to Study Soil Structure Interaction Parameters for Tall Structures." In 18th International Conference on Soil-Mechanics and Geotechnical Engineering, 225–30. Paris. <http://www.tc207ssi.org/conferences/2013/index.html>.

- Riagusoff, I. I. T., Kenedi, P. P., Souza, L. F. G. D., and Pacheco, P. M. C. L. (2010). "Modeling of Pipe Cold Bending: A Finite Element Approach." In VI National Congress of Mechanical Engineering - CONEM 2010. Brazil. <https://www.researchgate.net/>.
- Seica, M. V., and Packer, J. A. (2004). "Mechanical Properties and Strength of Aged Cast Iron Water Pipes." *Journal of Materials in Civil Engineering* 16 (1): 69–77. doi:10.1061/(ASCE)0899-1561(2004)16:1(69).
- Shao, Y., and Zhang, T. (2008). "Elastoplastic Pipe-Soil Interaction Analyses of Partially-Supported Jointed Water Mains." *Journal of Zhejiang University SCIENCE A* 9 (11): 1497–1506. doi:10.1631/jzus.A071327.
- Folkman, S. (2012). "Water Main Break Rates in the USA and Canada: A Comprehensive Study." Utah State University Buried Structures Laboratory.
- Trickey, S. A., and Moore, I. D. (2005). "Numerical Study of Frost-Induced Ring Fractures in Cast Iron Water Pipes." In Canadian Geotechnical Conference. Saskatoon.
- Trifonov, O. V., and Cherniy, V. P. (2012). "Elastoplastic Stress–strain Analysis of Buried Steel Pipelines Subjected to Fault Displacements with Account for Service Loads." *Soil Dynamics and Earthquake Engineering* 33 (1): 54–62. doi:10.1016/j.soildyn.2011.10.001.
- Vipulanandan, C., Qiao, W., and Hovsepian, H. (2011). "Case Studies on Water Pipeline Failures in the Active Zone." In Geo-Frontiers Congress 2011, 2474–83. Dallas,

Texas, United States: American Society of Civil Engineers.
<http://ascelibrary.org/doi/abs/10.1061/41165%28397%29253>.

Watkins, R. K., and Anderson, L. R. (1999). *Structural Mechanics of Buried Pipes*. CRC Press.

Wu, G., Zhang, P., Li, Z., Ke, Z., Li, G., and Jiang, A.. (2016). “Elastic-Plastic Finite Element Analysis for Zhongwei--Guiyang Natural Gas Pipeline Endangered by Collapse.” *International Journal of Science* 3 (2): 70–75.

Yang, Z. (2012). “Pipe-Soil Interaction Effect on Construction of Curve Pipe-Jacking.” ICPTT 2012, November, 1880–89.

Chapter 3. Three Dimensional Finite Element Analyses of Partially Supported Water Mains

Kasuni H. Liyanage, Ashutosh Sutra Dhar

Department of Civil Engineering, Faculty of Engineering and Applied Science, Memorial

University of Newfoundland, St. John's, NL, Canada

Abstract

Buried water mains used in water distribution systems are subjected to aggressive environmental conditions and undesirable soil conditions, causing deterioration of the pipelines. As a result, a number of water main breaks occur every year in many municipalities. Circumferential cracking is a predominant failure mode for water mains which results from excessive longitudinal stresses. The longitudinal stress in the pipe wall may be due to non-uniform soil support condition caused through erosion of surrounding soil by water from any leakages. Localized concentrated supports are also expected on the pipe wall within the erosion voids due to the presence of large rock pieces when the fine soil particles are eroded away. In the current research, three dimensional finite element analyses are used to investigate the effects of erosion voids and localized supports on pipe wall stresses. A cast iron water main buried in elastoplastic soil, subjected to soil load and surcharge, is considered. FE results are compared with analytical solutions available in the literature for evaluation. A parametric study is followed up in order to investigate the influence of the void size, location and geometry around the pipe circumference on the stress development in the pipe wall.

3.1 Introduction

Buried water mains are important infrastructure carrying potable water to communities. The aged pipelines, which were constructed several decades ago, are vulnerable for accelerated deterioration. Due to structural deterioration along with several other factors, a number of water mains fail every year in the municipalities. According to the Watermain Break Clock (2015), approximately 850 water main failures occur in North America every day. It has thus become a growing demand to maintain the structural integrity of water main infrastructure.

To demonstrate the life cycle of a buried pipeline, Rajani and Tesfamariam (2004) described three main phases in the life cycle of the pipeline, namely; burn-in phase, in-use phase and wear-out phase. A significant part of water main infrastructure is currently in its wear-out phase. The infrastructure is thus most susceptible to failure due to deterioration and ageing. Unexpected loading may also contribute to the breakage of the pipelines.

Pipe wall thinning due to corrosion is generally considered as the primary cause of the failures. However, researchers have recognized that mechanisms of pipe failures have more complexity than the wall thinning only. Pipe failure modes observed in the field are often different from those predicted based on conventional analysis. The conventional analysis predicts wall cracking in longitudinal direction resulting from excessive circumferential stresses (Balkaya et al. 2012). However, the majority of the pipe failures in the field show circumferential cracking that would have resulted from excessive longitudinal stresses (Arsenault, 2015).

Limited research information is currently available in the literature on the longitudinal stresses on buried water mains. Some recent studies on the effects of erosion voids on pipe wall stresses (Rajani and Tesfamariam, 2004; Balkaya et al., 2012; Meguid and Kamel, 2014) are available. Balkaya et al. (2012) investigated cast iron water mains and showed that peak tensions are always in the hoop direction for the erosion voids. The hoop tension is likely to cause longitudinal fracture. In this paper, the longitudinal stresses on partially supported water mains, investigated using three-dimensional finite element analysis, are presented.

3.2 Problem Statement

Corrosion is considered as the major cause of municipal metal pipes (such as cast iron, ductile iron, steel etc.) failure (McDonald et al., 2001; Rajeev et al., 2013). Corrosion may cause leakage of water that erodes the surrounding bedding gradually. Figure 3-1 shows a corrosion hole on a water main exhumed from the campus of Memorial University of Newfoundland.

However, other factors may also contribute significantly to the failure of water mains. Figure 3-2 shows a water main segment exhumed from the campus of Memorial University of Newfoundland that failed with no sign of corrosion.



Figure 3-1: A corrosion in a water main

Figure 3-3 shows water leaking through a circumferential crack of a water main in service at the City of Mount Pearl in Newfoundland. The water main did not show any sign of corrosion. The pipe was repaired using a repair clamp and is now in service.

Apart from corrosion, other factors contributing to pipeline failure could be:

- manufacturing flaws such as porosity in the material, inclusion of unintentional objects and/or changes in pipe wall thickness;
- excessive stresses due to localized concentrated forces, unsupported pipe spans, change in direction of pipe route, creep effects etc.;
- poor installation; and
- additional load due to excavations on or near pipelines or repair procedures.



Figure 3-2: A segment of water main exhumed from Memorial University Campus



Figure 3-3: Water leaking through a circumferential crack at the City of Mount Pearl
(Arsenault, 2015)

Most of the previous studies investigating the failure mechanism of deteriorated water mains focused on the study of the pipe wall stresses due to the lack of soil support caused

by erosion voids (Rajani and Tesfamariam, 2004; Shao and Zhang, 2008; Meguid and Kamel, 2014; Balkaya et al., 2012). Rajani and Tesfamariam (2004) developed a Winkler pipe-soil interaction model and derived an analytical solution for stresses in the pipe wall, which was further reviewed by Shao and Zhang (2008). Meguid and Kamel (2014) performed an elasto-plastic finite element analyses to investigate the effect on earth pressure distribution as well as pipe wall stresses in concrete pipes. They revealed that the development of erosion voids under the invert of rigid pipes is the most critical condition. The study based on finite element modelling of cast-iron water mains showed that the hoop stresses are higher than the radial and longitudinal stresses, and that the peak tension is always in the hoop direction which leads to the cause of longitudinal fracture (Balkaya et al. 2012). Balkaya et al. (2012) investigated 300 mm diameter pipelines with 12 mm and 4 mm wall thicknesses and voids symmetrical with the springline and the invert of the pipes. The Young's modulus of cast iron pipe material and soil were 70 GPa and 40 MPa, respectively.. However, the Young's modulus in cast iron can vary and can be as high as 200 GPa. Soil modulus can also vary along the length of the pipeline and can be as low as 10 MPa. The relatively higher pipe stiffness with respect to the soil may mobilize higher bending stresses to the pipe, resulting in higher longitudinal stresses.

Longitudinal stress may also be caused by localized concentrated support at the corrosion voids around the pipeline. Water through leaks may wash away fine to medium soil particles leaving relatively coarse particles at void spaces that may exert concentrated load on the pipe. To the author's knowledge, the effects of the localized stress concentrations on pipe wall stresses have not been investigated to date.

In the present research, partially supported buried water mains are investigated considering erosion voids of symmetric and un-symmetric shapes about the springline and invert of the pipelines. The effects of stress concentrations due to localized soil support are also investigated. A parametric study is undertaken to identify the parameter contributing the longitudinal stresses in the pipe wall.

3.3 Outline of the Structural Model

In this analysis, a cast iron (CI) pipeline buried in an elastoplastic soil, subjected to soil load, vehicle surcharge, internal water pressure and localized lack of ground support is considered (Figure 3-4).

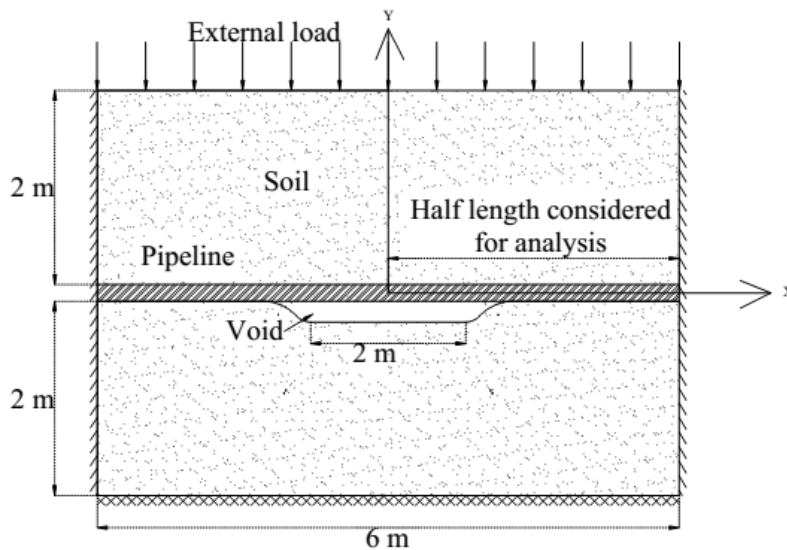
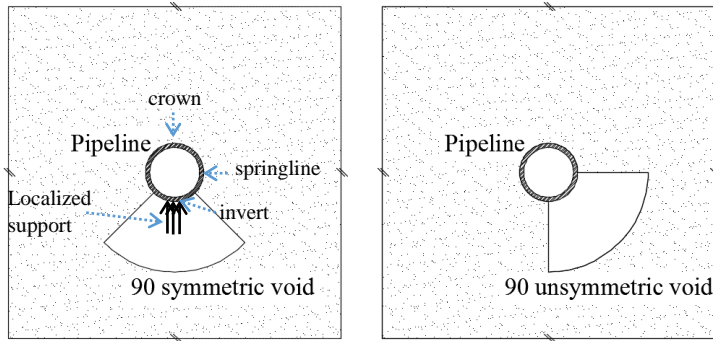


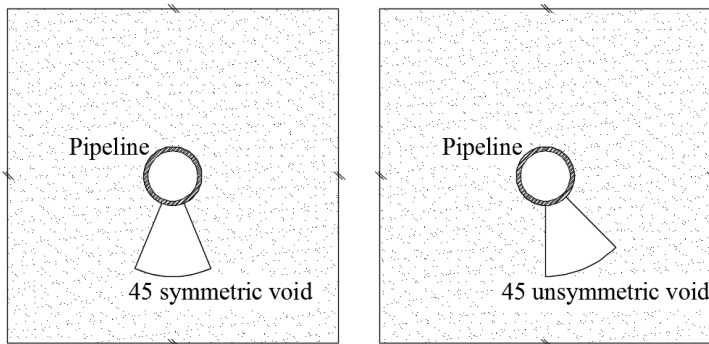
Figure 3-4: Longitudinal section of the pipe system (all dimensions are in mm)

In the finite element analysis, only half of the soil, pipe and unsupported length are modeled, assuming symmetry of the system about a plane at the mid-length of the pipeline. A pipeline of 6 m in length is considered. Therefore, only a 3m long pipe segment, along

with surrounding soil, is modeled. A 150mm (6 inches) diameter CI pipe with a thickness of 12.6 mm is selected for the analysis. A non-uniform bedding condition is modelled in terms of an unsupported pipe length (void in the adjacent soil) of 2000 mm length.

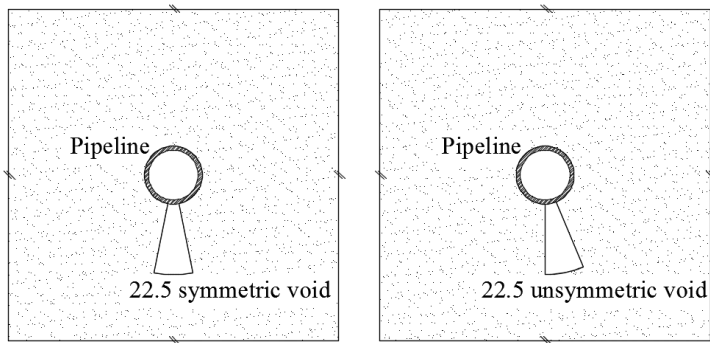


(a)

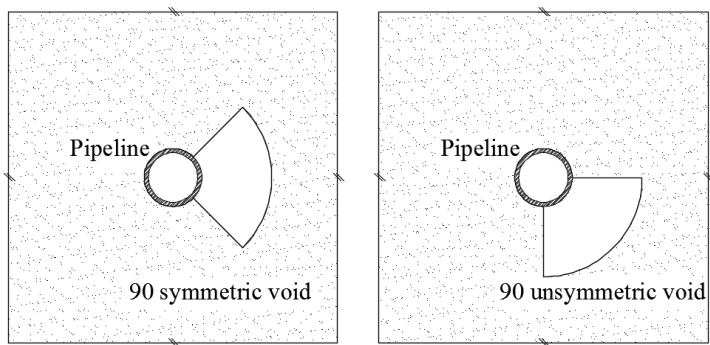


(b)

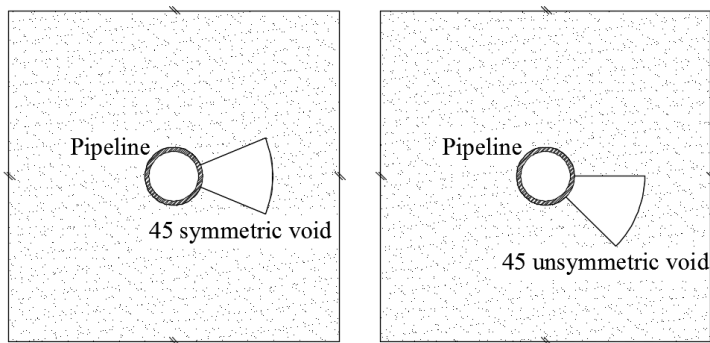
Figure 3-5: Cross sectional schematic of symmetric and un-symmetric void angles of (a) 90° (b) 45° and (c) 22.5° at the invert, and (d) 90° (e) 45° and (f) 22.5° at the springline
(cont.)



(c)

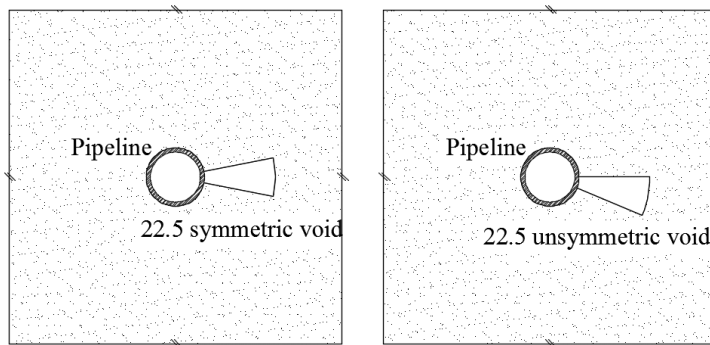


(d)



(e)

Figure 3-5: Cross sectional schematic of symmetric and un-symmetric void angles of (a) 90° (b) 45° and (c) 22.5° at the invert, and (d) 90° (e) 45° and (f) 22.5° at the springline
(cont.)



(f)

Figure 3-5: Cross sectional schematic of symmetric and un-symmetric void angles of (a) 90° (b) 45° and (c) 22.5° at the invert, and (d) 90° (e) 45° and (f) 22.5° at the springline

The voids at the invert and the springline are considered separately. Voids symmetric and un-symmetric about the springline and invert were applied (Figure 3-5). The void angle and its geometric shape are varied according to Table 1. Vertical localized support at the void is also applied at the middle of the voids to simulate localized soil support over an area of pipe perimeter, producing an angle of 22.5° at the centre of the pipe (Figure 3-5).

The pipe is considered in medium sand with 2 m soil cover above the crown and 2 m below the invert. The width of soil beside the pipe springline is selected as 4 m in order to avoid any boundary effects. A surcharge of 30 kPa is applied at the ground surface to simulate the effects of vehicles and other live loads. An internal pressure of 400 kPa is applied in the pipeline. Preliminary analysis of a pipe was carried out with and without internal pressure. Stresses in longitudinal and circumferential directions were higher by 7% and 19%, respectively, for the pipe with the internal pressure than the pipe without an internal

pressure. Since water mains in service are always subjected to an internal pressure, a pipe with an internal pressure was considered in this study.

Table 3-1: Parametric study

	Symmetric			Unsymmetric		
Invert*	90	45	22.5	90	45	22.5
Springline*	90	45	22.5	90	45	22.5

* Definitions are provided in Figure 3-5

3.4 Numerical Modeling

Numerical modelling is performed using the finite element package ANSYS, version 15.0. A nonlinear 3D coupled soil-pipeline structural simulation has been performed with static loads. A simple Drucker Prager model is used to simulate the elasto-plastic material property of soil. Also, geometric nonlinearity is taken into account by allowing large displacements.

3.4.1 Model Description

The finite element model consists of SOLID186 3D solid elements for the pipeline and SOLID65 solid elements for the soil. The interface between pipe and soil is modelled using CONTA174 and TARGE170 contact elements. The maximum size of the element along the length of the pipeline is kept at 50 mm in order to compensate the accuracy of the results with the computational time. A typical view of the FE model is given in Figure 3-6.

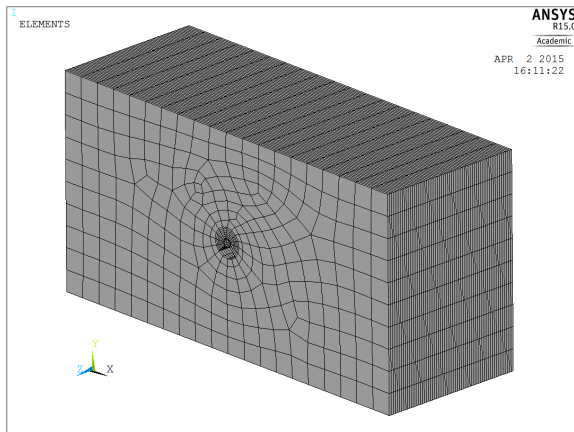


Figure 3-6: Typical finite element mesh used to model the pipe-soil structure

SOLID186 is a higher order 3-D 20-node solid element that exhibits quadratic displacement behavior. The element is defined by 20 nodes having three degrees of freedom per node: translations in the nodal x, y, and z directions. Since it also supports stress stiffening, large deflection, and large strain capabilities, this element is selected to model the isotropic linear elastic behaviour of the CI water main. Soil is modelled using SOLID65 elements, which is the Legacy element of SOLID186 and supports simple Drucker Prager failure criterion. Similar to SOLID186, SOLID65 is defined by eight nodes having three degrees of freedom at each node: translations in the nodal x, y, and z directions. This element also supports stress stiffening, large deflection, and large strain capabilities (ANSYS). CONTA174 is defined as an 8-node surface-to-surface element, which represents the contact and sliding between the two surfaces. The element has the same geometric characteristics as the solid or shell element face with which it is connected. Since the cast iron pipe is stiffer than the soil, TARGE170 are overlaid on pipe elements while CONTA174 elements are overlaid on soil elements.

3.4.2 Materials

In the finite element analysis, the CI pipe is modeled as an isotropic linear elastic material, since the linear elastic limit of CI material is above 150 MPa (Seica and Packer 2004). The elastic modulus, Poisson's ratio and density of the pipe are 206 GPa, 0.26 and 7850 kg/m³, respectively.

The Elastic modulus, Poisson's ratio and density of the soil are 100 MPa, 0.3 and 2344 kg/m³, respectively (based on Rajani and Tesfamariam, 2004). Furthermore, the soil is modeled as an isotropic elastoplastic material based on Drucker-Prager criteria. The friction angle, dilatancy angle and cohesion are 32°, 25° and 0.5 kPa, respectively. The material parameters are selected to perform preliminary analysis presented in this paper. The effect of different material parameters are considered further in the Chapter 4 and Chapter 5.

3.4.3 Boundary Conditions

Boundary conditions (BCs) are simulated in the finite element model using displacement constraints as discussed below:

- The longitudinal displacements of soil and pipe are restrained at the end plane of the pipe by applying $U_z=0$. Displacements in x and y directions are set free.
- Since the pipe and soil are symmetric about the pipe mid plane, longitudinal displacements of soil and pipe are set symmetric, while displacements are allowed in horizontal and vertical directions.

- The bottom plane of the soil is fixed in all directions by applying $U_x=0$, $U_y=0$ and $U_z=0$.
- Vertical localized support at the void is applied at points over a perimeter, producing 22.5^0 at the pipe centre (Figure 3-5a).

Self-weight of the system due to gravity is applied first in a single step initially. External loading including surcharge and internal pressure is applied using a number of sub steps. The final pipe stresses are examined. Time difference between each sub step was kept low for the convergence of the solution.

3.4.4 Model Validation

To validate the FE model used in this study, an analytical model developed by Rajani and Tesfamariam (2004), modified by Shao and Zhang (2008), is used. The geometry and material properties for both the FE model and analytical model used in the study are selected to align with the current structural model being used. Since the study is based on fully the three dimensional FE analysis, the FE method uses a continuum model to simulate the behaviour of soil, whereas the analytical method used the Winkler model.

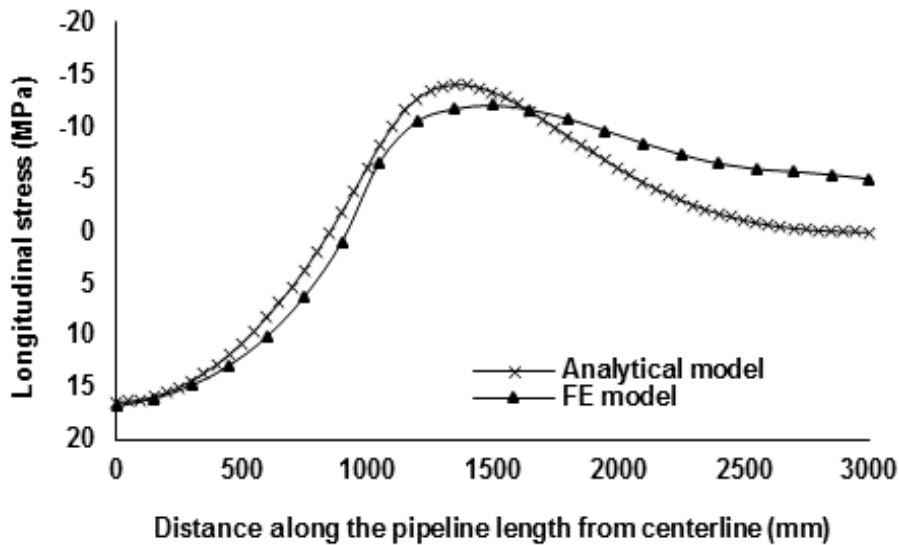


Figure 3-7: Comparison of results from analytical model and finite element analysis

Figure 3-7 shows a comparison of longitudinal stress along the length of the pipe, calculated using FE analysis and Winkler based model. The overall calculated results using the FE model (ANSYS) agrees, to some extent, with those calculated using the analytical model, as can be seen in Figure 3-7. On the far side of the pipeline (to the right in Figure 3-7), FE results show non-zero longitudinal stress since the pipe was restrained in the longitudinal direction. However, the current paper focuses on the stresses around the unsupported zone of the pipeline. The FE model is therefore considered reasonable for the current purpose.

3.5 Results

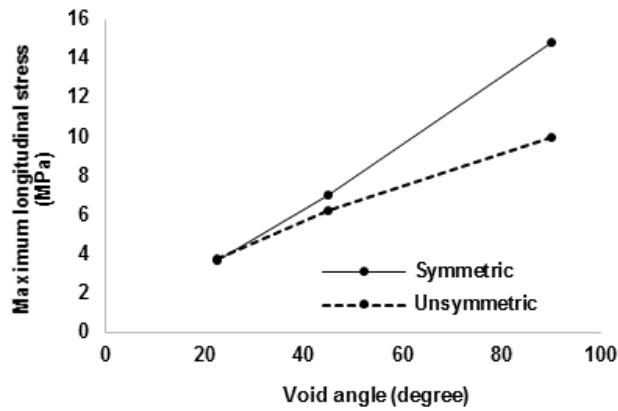
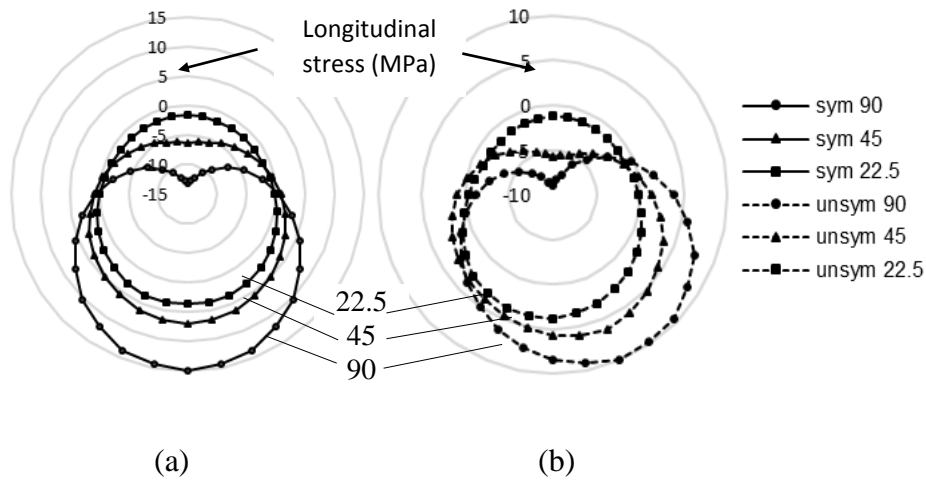
Separate numerical analyses have been carried out for voids without localized point supports and with localized point supports to examine the effects of local stress concentrations due to point supports on the pipeline with erosion voids. In both analyses,

the effect of void size is investigated by changing the pipe's circumferential extent of the voids, defined by an angle produced by the part of the circumference at the pipe center (void angle). Void angles of 90^0 , 45^0 and 22.5^0 are considered. The location of the void is another factor of influence to the stress distribution in the pipe. Voids that are symmetric and unsymmetric about the invert and springline of the pipe were considered (Figure 3-5). Only tensile stresses in the pipeline have been investigated in this study, because tension is the most critical in regards to the failure by hoop fracture or longitudinal fracture.

3.5.1 Effect of Void Geometry without Point Supports

Figures 3-8 and Figure 3- 9 plot longitudinal stresses around the pipe outer circumference for the void spaces located near the invert and springline of the pipe, respectively. The maximum longitudinal stresses occurred at the location of the void.

For the symmetric voids, the maximum longitudinal tension is at the invert when the void is at the invert (Figure 3-8a) and is at the springline when the void is at the springline (Figure 3-9a). For the springline void angles of 45^0 and 22.5^0 , the maximum tensile stress occurred on the side opposite to the void location, whereas for the symmetric 90^0 void angle, the maximum tension occurred on the same side of the void location (Figure 3-9a). This phenomenon can be further explained by the fact that the longitudinal stress is mainly affected by the bending stress. For the symmetric 90^0 void angle, the pipe laterally bends towards the void location, creating the maximum tension on the same side as the void location. However, for symmetric void angles of 45^0 and 22.5^0 , the pipe laterally bends in the opposite direction, creating the maximum tension in the opposite side of the void.



(c)

Figure 3-8: Variation in longitudinal stresses around the pipe circumference at mid-length of the void (a) for the symmetric case, (b) for the unsymmetric case and (c) Maximum longitudinal stresses, for voids at the invert

Figure 3-8(c) and Figure 3-9(c) reveal that the highest longitudinal stresses for symmetric voids are 14.8 MPa and 4.4 MPa, for voids at the invert and springline, respectively. The longitudinal stresses are calculated to be higher when the void is at the invert than those at the springline. This is in general agreement with those reported in the literature. Meguid

and Kamel (2014) reported that the percentage increase in longitudinal stresses due to erosion voids is about 80% at the springline and is about 225% at the invert for concrete pipes.

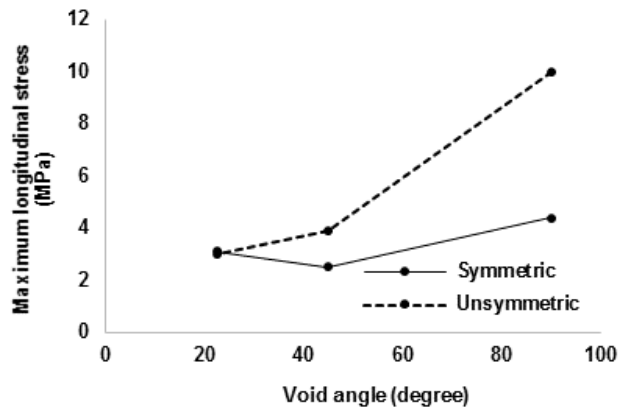
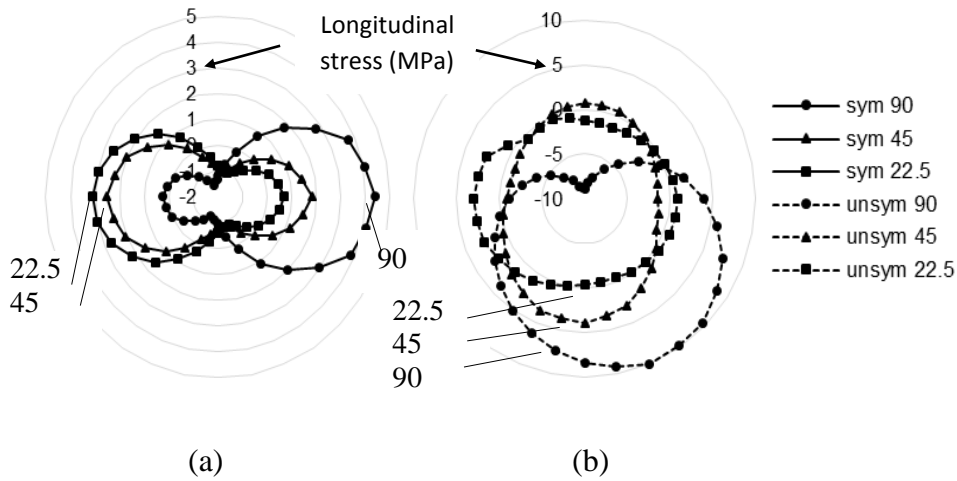


Figure 3-9: Variation in longitudinal stresses around the pipe circumference (a) for the symmetric case, (b) for the unsymmetric case and (c) Maximum longitudinal stresses, for voids at the springline

The longitudinal stresses are higher for symmetric invert voids than unsymmetric invert voids (Figure 3-8c), whereas the longitudinal stresses are higher for unsymmetric voids located at the springline (Figure 3-9c). The effects of unsymmetry were higher for the springline voids.

Hoop stresses around the inner circumference of the pipes are plotted in Figure 3-10 and Figure 3-11, respectively, for voids located near the invert and the springline. The maximum tension in hoop direction is observed at the invert and the crown, when the symmetric void is present at invert (Figure 3-10a). Similarly, in the case of the void being located at the springline, maximum hoop tension occurred at the invert and the crown (Figure 3-11a). In addition, irrespective to the location of the void, the effect of unsymmetry produced the higher tensile stresses adjacent to the pipe invert and crown.

Figure 3-10(b) and Figure 3-11(b) reveal that the hoop stress is higher for voids located at the springline (i.e. 10.2 MPa) than that for voids located at the invert (i.e. 7.9 MPa). This phenomenon is in agreement with the results reported by Tan and Moore (2007). Hoop stress in the pipeline is the combination of stress due to internal pressure, thrust force and bending moment at the pipe wall resulting from external soil pressure. Tan and Moore (2007) concluded that the bending moments developed in the pipe wall are higher for voids at the springline than those for voids at the invert.

However, the shape of void geometry (i.e. symmetric or un-symmetric) has relatively less influence on the maximum hoop stress compared to the influence on the maximum longitudinal stress as seen in Figures 3-8(c), 3-9(c), 3-10(c) and 3-11 (c).

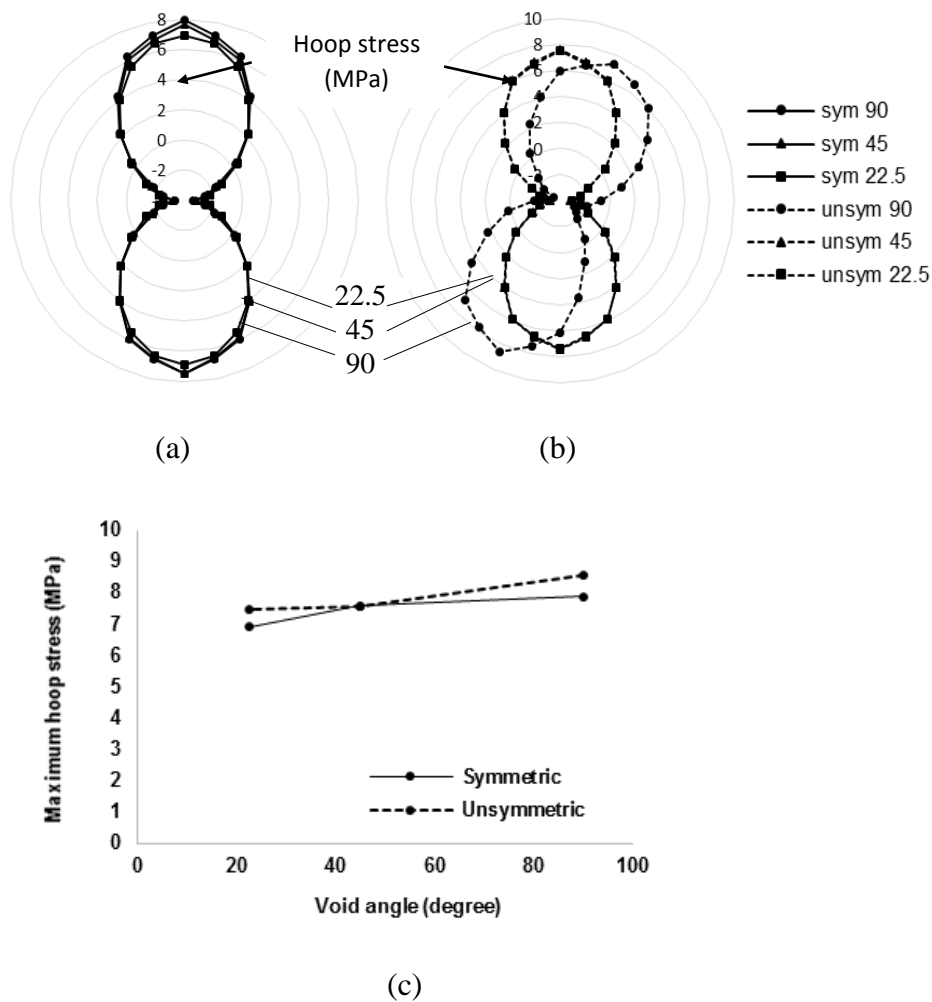
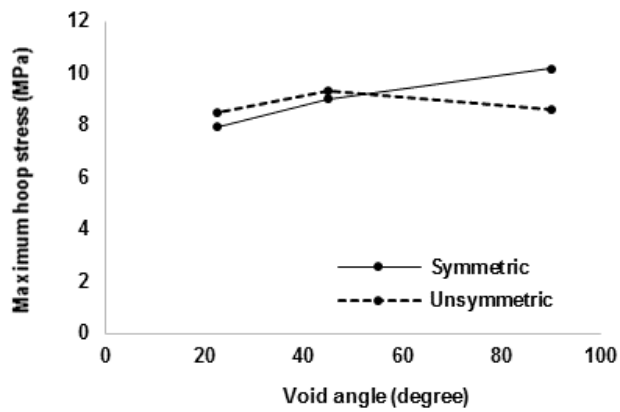
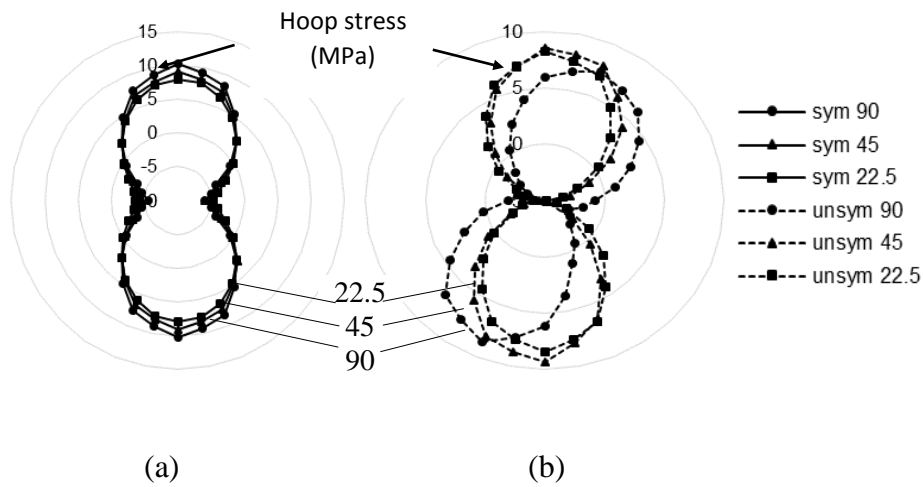


Figure 3-10: Variation in hoop stresses around the pipe circumference (a) symmetric voids, (b) unsymmetric voids and (c) Maximum hoop stresses, for voids at the invert

It is also evident from Figures 3-8(c) and 3-10(c) or Figures 3-9(c) and 3-11(c) that hoop stress is greater than the longitudinal stress, as observed in Balkaya et al. (2014), for smaller void sizes. However, for larger void sizes, the longitudinal stress is greater than the hoop stress. This is because of the pipe bending towards the void creating higher flexural stresses in longitudinal direction. This may explain the circumferential crack observed in water mains due to the development of longitudinal stresses.



(c)

Figure 3-11: Variation in hoop stresses around the pipe circumference (a) symmetric voids, (b) unsymmetric voids and (c) Maximum longitudinal stresses, for voids at the springline

3.5.2 Effect of Void Geometry with Point Supports

The presence of localized point supports increases the pipe wall stresses significantly. Longitudinal stresses and hoop stresses around the pipe circumference are plotted in Figure 3-12 and Figure 3-13 respectively, for the void with point supports located near the pipe

invert. For the cases considered, the maximum longitudinal stresses range from 200 MPa to 400 MPa and the maximum hoop stresses range from 100 MPa to 600 MPa in Figure 3-12 and Figure 3-13. As discussed above, these maximum longitudinal and hoop stresses ranged between 3 MPa and 14 MPa for the partially supported pipes without point supports. The high pipe stresses for the pipes with point support thus exceed the tensile strength of the material (i.e. 150 MPa to 400 MPa for cast iron) that may lead to the pipe failure. Pipe stresses were also significantly higher for the springline voids with point support but are not included in this paper; these stresses were however less than the stresses for the voids located at the pipe invert.

It is also revealed that unsymmetric void, despite its location, always leads to higher stresses in both longitudinal and hoop directions, when subjected to the point supports.

It should be noted that rigid point supports are considered for the analysis of stress presented in this paper. However, the localized supports to the real pipes may be flexible. Research is currently underway to investigate the effects of flexible point supports on the stress development in buried water mains.

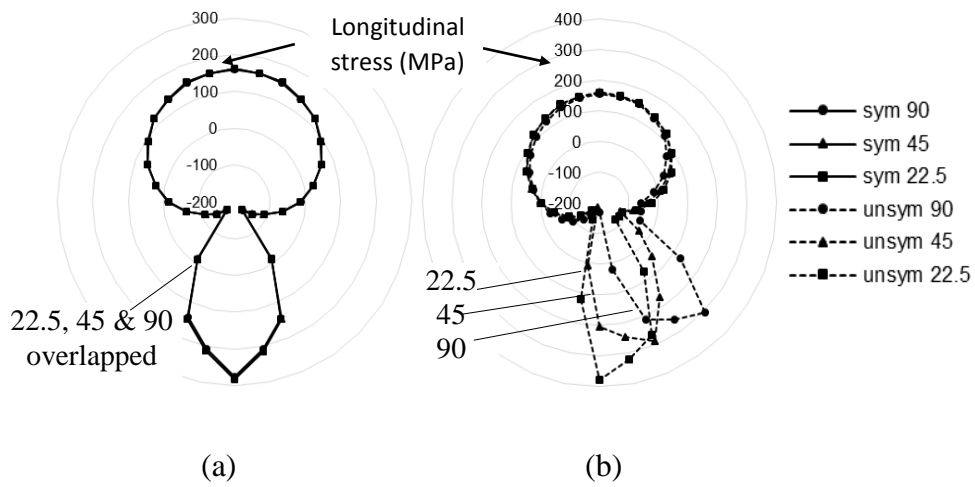


Figure 3-12: Variation in longitudinal stresses around the pipe circumference (a) for symmetric, (b) for unsymmetric, voids at invert

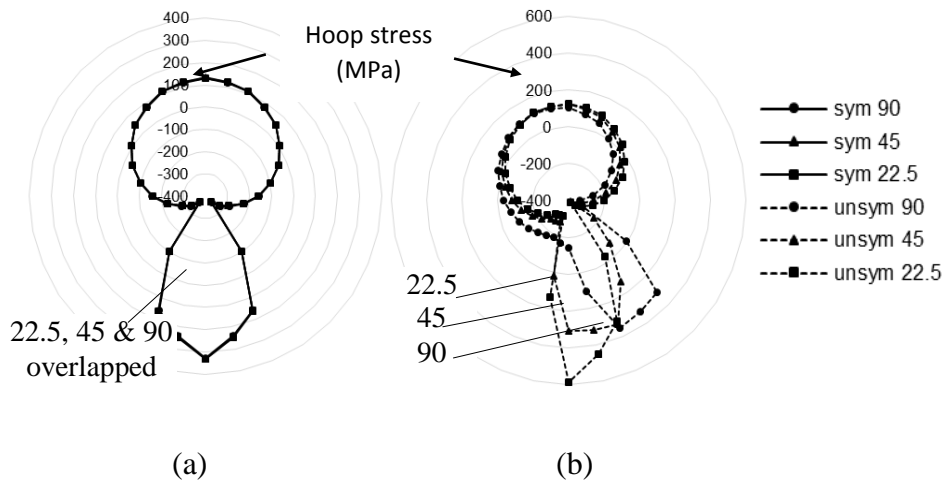


Figure 3-13: Variation in hoop stresses around the pipe circumference (a) for symmetric, (b) for unsymmetric, voids at invert

3.6 Conclusions

The results of three dimensional FE analyses of buried partially supported water mains are presented in this paper. Development of pipe wall stresses under different locations and sizes of erosion voids with and without point supports are investigated. The results of analyses reveal that the longitudinal and hoop stresses in the pipe are influenced by the erosion voids with and without point supports. For the erosion voids without point supports, the hoop stress is greater than the longitudinal stress for smaller void sizes and the longitudinal stress is greater than the hoop stress for larger void sizes, particularly when the void is located near the invert of the pipe. The maximum longitudinal and hoop stresses generally occur at the locations of voids. The hoop stress is found to be higher for the springline voids than for the invert voids.

The longitudinal stresses are calculated to be higher for the symmetric invert voids than the unsymmetric invert voids, whereas the stresses are higher for unsymmetric voids for the springline voids. The effect of unsymmetry of voids is higher for the springline voids. The symmetry has relatively less influence on the maximum hoop stress compared to the maximum longitudinal stress.

The presence of localized point supports appears to increase the pipe wall stresses significantly. The maximum longitudinal and hoop stresses were significantly higher (about 100 times) for the pipes with points supports than the pipes without point supports. Rigid point supports were considered in this research for investigation of influence on the

pipe stresses. Further research in investigating the effects of flexible point supports on the stress development in buried water mains is proposed.

Acknowledgements

The financial support for this research is provided by Research and Development Corporation of Newfoundland and Labrador, which is gratefully acknowledged.

3.7 References

Arsenault, E. (2015) Work Superintendent, Infrastructure and Public Works Department, The City of Mount Pearl, Personal Communication.

ANSYS (2015). ANSYS® Academic Research, Release 16.2. ANSYS, Inc.

Balkaya, M., Moore, I. D., and Sağlam, A. (2012). “Study of Nonuniform Bedding Support Because of Erosion under Cast Iron Water Distribution Pipes.” *Journal of Geotechnical and Geoenvironmental Engineering* 138 (10): 1247–56. doi:10.1061/(ASCE)GT.1943-5606.0000689.

Makar, J. M., Desnoyers, R., and McDonald, S. E. (2001). “Failure Modes and Mechanisms in Gray Cast Iron Pipe.” In *Underground Infrastructure Research Conference*, 1–10. Kitchener, Ontario.

Meguid, M. A., and Kamel, S. (2014). “A Three-Dimensional Analysis of the Effects of Erosion Voids on Rigid Pipes.” *Tunnelling and Underground Space Technology* 43 (July): 276–89. doi:10.1016/j.tust.2014.05.019.

- Rajani, B., and Tesfamariam, S. (2004). "Uncoupled Axial, Flexural, and Circumferential Pipe–soil Interaction Analyses of Partially Supported Jointed Water Mains." *Canadian Geotechnical Journal* 41 (6): 997–1010. doi:10.1139/t04-048.
- Rajeev, P., Kodikara, J., Robert, D., Zeman, P., and Rajani, B. (2013). "Factors Contributing to Large Diameter Water Pipe Failure as Evident from Failure Inspection." <http://researchbank.swinburne.edu.au/>.
- Seica, M. V., and Packer, J. A. (2004). "Mechanical Properties and Strength of Aged Cast Iron Water Pipes." *Journal of Materials in Civil Engineering* 16 (1): 69–77. doi:10.1061/(ASCE)0899-1561(2004)16:1(69).
- Shao, Y., and Zhang, T. (2008). "Elastoplastic Pipe-Soil Interaction Analyses of Partially-Supported Jointed Water Mains." *Journal of Zhejiang University SCIENCE A* 9 (11): 1497–1506. doi:10.1631/jzus.A071327.
- Tan, Z., and Moore, I. D. (2007). "Effect of Backfill Erosion on Moments in Buried Rigid Pipes." In *Transportation Research Board 86th Annual Meeting*. <http://trid.trb.org/view.aspx?id=802342>.
- Water main Break Clock (2015) "Why So Many Water Main Breaks?", <http://www.watermainbreakclock.com/>, accessed on April 15, 2015.

Chapter 4. Stresses in Cast Iron Water Mains Subjected to Non-Uniform Bedding and Localized Concentrated Forces

Kasuni H. Liyanage, Ashutosh Sutra Dhar

Department of Civil Engineering, Faculty of Engineering and Applied Science, Memorial

University of Newfoundland, St. John's, NL, Canada

Abstract

A number of water main breaks occur every year in municipalities due to aging, aggressive environmental conditions and undesirable soil conditions. However, the failure mechanism observed in cast iron water mains is often obscure. Non-uniform soil support conditions resulting from the erosion of the surrounding soil by the water escaping from leaks may induce excessive stresses on the pipe wall. Due to partial erosion of backfill soil or the presence of large rock pieces, the localized point supports on the pipe accentuate the pipe wall stresses further. This research employs three-dimensional finite element analysis to investigate the effects of non-uniform soil support and the localized point support on the pipe wall stress. This study results in the development of a better understanding of the mechanism of cast iron water main failure. It is shown that a localized support with a spring constant (stiffness) of 1500 N/mm may result in the failure of cast iron water mains. An existing analytical solution for calculating pipe wall stress is also evaluated using the finite element analysis.

Keywords: Pipe – soil interaction, cast-iron pipe, water main, longitudinal stress, circumferential stress, circumferential cracking

Nomenclature

D = pipe outer diameter

E_p = Young's modulus of pipe

E_s = Young's modulus of soil

F_z = maximum spring load

I_{zz} = moment of inertia

k'_s = elastic foundation modulus

M_{xx} = bending moment

q = line load

R = pipe radius

v = vertical deflection

v_b = vertical deflection in unsupported zone

v_c = vertical deflection in plastic zone

v_e = vertical deflection in the elastic zone

α = factor used to replace 0.65 in elastic foundation modulus

λ = reciprocal of the flexural characteristic length

ν_s = Poisson's ratio

σ_x = flexural stress

ϕ' = peak angle of internal friction

ψ = dilation angle

4.1 Introduction

Pipelines used in water transportation systems, known as water mains, are important infrastructure used to carry potable water to city dwellers. The breakage of pipelines may result in disruption of water service, loss of water, and damage to other infrastructure (e.g. roads and building foundations) by the escaping water. A number of water main breakages are reported every year across municipalities. According to the Watermain Break Clock (2015), about 850 water main failures occur in North America per day. The city of Mount Pearl in the Province of Newfoundland and Labrador in Canada reported more than 50% of water loss through their deficient water infrastructure (Frick and Manuel 2005). Municipalities are facing challenges with maintaining the structural integrity of the water pipelines.

Pipes with different materials are being used for the transportation of potable water. These include cast iron (CI), ductile iron (DI), steel, polyvinyl chloride (PVC) and asbestos cement. Cast iron and ductile iron pipes constitute the highest volume of the existing municipal water mains in North America (Folkman 2012). Cast iron is one of the oldest pipe materials used in the potable water system, which was phased out after the introduction of ductile iron pipes in the 1950s (AWWSC 2002). However, since most of

the earlier water distribution pipelines were cast iron, a large volume of cast iron water mains exist in municipal water distribution systems to date.

Among the materials used for municipal water mains, those constructed with cast iron have been reported to experience the most of the water main failures (Folkman 2012). Pipe material deterioration due to corrosion is considered to be the major cause of the failure. Folkman (2012) reported based on a study of water main breaks in USA and Canada that one in four water breaks is caused by corrosion. The excessive wall stress development due to mechanical loading under the influence of wall thinning by the corrosion may cause pipeline failures.

Several failure modes such as circumferential cracking, longitudinal cracking, joint failure, blowouts have been identified for cast iron water mains (Rajani et al. 1996). Among these, circumferential cracking or ring bending is the most commonly encountered mode of failure for cast iron pipes (Liyanage and Dhar 2015, Makar et al. 2005, Folkman 2012). The circumferential cracking results from longitudinal stresses caused by thermal contraction and/or by longitudinal bending of the pipe (Rajani et al. 1996, Seica and Packer 2006, Trickey et al. 2016). Trickey et al. (2016) demonstrated that longitudinal bending may be the dominant cause of circumferential cracking in water mains. The longitudinal bending in buried water mains may occur due to non-uniform bedding support and/or frost actions above the pipe. The non-uniform bedding support results from the erosion of the bedding and/or backfill materials by the water escaping from pipe leaks or other sources that may leave a portion of the pipe unsupported. The lack of support on the pipe may cause additional stresses on the pipe wall in the vicinity of the unsupported zone (Balkaya et al.

2012). Dhar et al. (2004) demonstrated that the lack of soil support within a localized zone around flexible pipes can lead to stress/strain concentration around that zone. They conducted finite element analysis, evaluated using the test results on full-scale pipes buried in a laboratory facility (Dhar 2002), to investigate the stress/strain concentration in pipes around a soft zone of soil using cross-sections to evaluate different stiffnesses. The study revealed that the relative stiffness of the pipe (with respect to the stiffness of the surrounding soil) influences the stress/strain concentration around the soft zone. The stress concentration was higher for pipes with higher relative stiffness (Dhar et al. 2004). However, the stress concentration around the soft zone for cast-iron pipes has not been well-investigated. The modulus of elasticity of cast-iron material varies over a wider range that may lead to different relative stiffness, which requires further investigation.

Differential ground movement resulting from frost action is considered as another cause of longitudinal bending in buried pipes, when soils with varying frost susceptible properties (frost susceptibilities) exist along the length of the pipe (Trickey et al. 2016). The soils with varying frost susceptibilities are expected particularly near the intersection of major arterial roads with residential streets, where the major arterial road is constructed of high grade pavement materials and the residential street is constructed of low grade pavement materials (Trickey et al. 2016). Trickey et al. (2016) showed that if the same granular backfill material is used for the major arterial road and the local road, the frost-induced differential ground movement and the resulting longitudinal bending can be avoided. This implies that the ring fracture observed in the water main below the major arterial road, where the same backfill material is used, is not associated with the frost-induced

differential ground movement. The non-uniform bedding support is likely the major cause of the circumferential cracking for the pipes under major arterial roads. The failure mechanism resulting from non-uniform bedding support is of particular interest for current research.

Some studies are available in the literature on the investigation of the longitudinal stresses and the circumferential cracking in water mains. Rajani and Tesfamariam (2004) developed a Winkler pipe – soil interaction model and derived analytical solutions for the calculation of the longitudinal stresses in buried water mains having a localized unsupported zone (void) at the pipe invert. Seica and Packer (2006) proposed a method to incorporate non-symmetrical geometric properties of the pipe cross section and the non-linearity of the stress-strain relation for estimating the bending stiffness of un-corroded and uniformly corroded cast iron pipes by considering the pipe as a beam. Balkaya et al. (2012) employed three-dimensional finite element analysis to calculate the wall stresses in a thin-wall and a thick-wall cast-iron water main considering localized voids around the pipes. Balkaya et al. (2012) found peak pipe wall stress in the circumferential direction and concluded that longitudinal fracture is likely to occur in the pipes. However, as mentioned above, the majority of cast iron water main failure was due to circumferential cracking.

Makar et al. (2005) indicated that the circumferential cracking in small diameter grey cast iron pipes is associated with corrosion pitting. The presence of a corrosion pit in the pipe undergoing bending is expected to cause a triaxial state of stress on the pipe wall, resulting in a failure mechanism that is different from the one predicted using conventional analysis.

Longitudinal stress may also be caused by localized concentrated support near the erosion voids around the pipeline. Water escaping through leaks may wash away fine to medium soil particles leaving relatively coarse particles (such as rock pieces or stones) at void spaces that may exert concentrated forces on the pipe wall. It was recognized that a sharp object with high stiffness, like a rock or stone, may accentuate fluctuating stresses on the pipe wall (Rajani and Kleiner 2010). However, no study on the effects of such localized forces on pipeline damage is available in the literature. Liyanage and Dhar, (2015) conducted a preliminary study on the effects of rigid concentrated support on the localized pipe wall stresses. The presence of rigid localized supports was found to increase the pipe wall stresses very significantly. However, the study had not investigated effect of flexible localized supports on pipe wall stresses.

In this investigation, three-dimensional finite element analysis is employed to investigate the wall stresses in cast iron water mains due to non-uniform bedding conditions including localized concentrated forces. An analytical model (Rajani and Tasfamariam 2004) for calculating longitudinal bending stress in pipes is also evaluated using the three-dimensional finite element (FE) analysis. An analytical model is desired for practical design that provides a simpler tool for pipe stress analysis. However, the applicability of the simplifying assumptions employed in the development of the analytical model requires evaluation.

4.2 FE Modelling

Three-dimensional coupled pipe – soil interaction analyses are performed using a general purpose finite element package ANSYS, version 15.0 (ANSYS 2015). Buried cast iron pipelines under surface surcharge load and internal water pressure are considered. Lack of ground support is applied to a particular region along the length of the pipeline as shown in Figure 4-1.

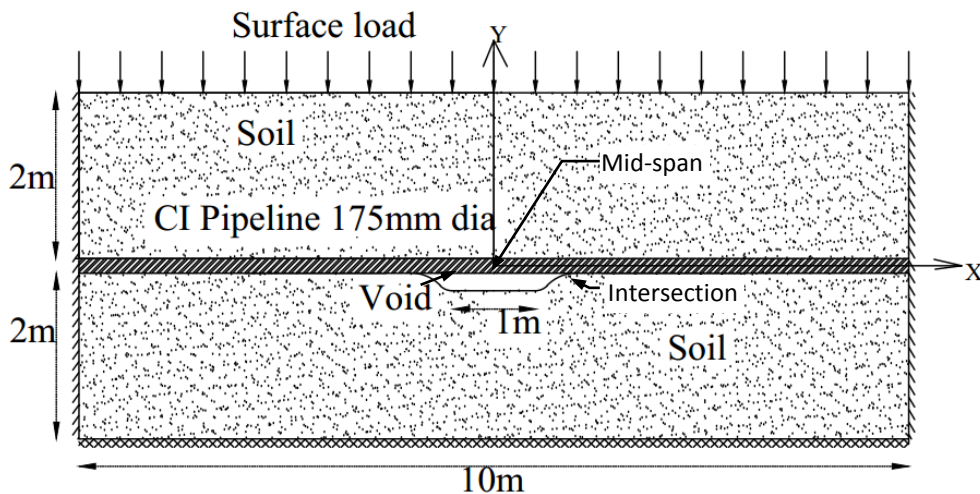


Figure 4-1: Schematic of a longitudinal section of the pipe-soil system

A 10 m long and 175 mm diameter (outer) cast iron pipe with 10 mm and 5 mm of wall thicknesses, termed as thick and thin pipes, respectively, is considered. The pipe has 2.0 m of soil cover above its crown and 2.0 m of depth below the pipe invert. The width of soil on each side of the pipe springline is selected to be 2.0 m in order to minimize any boundary effects. Analysis was performed with the width of the soil as 4 m. The difference in maximum pipe stresses with 2 m and 4 m of soil width was about 3%). An unsupported length of 1.0 m at mid-length of the pipe is modelled. The pipe is loaded with an internal

pressure of 400 kPa, a pressure within the range of typical operating pressures of water mains. The normal operating pressure in water pipelines typically ranges from 350 kPa to 550 kPa (Water Security Agency 2004). A surface surcharge of 25 kPa is considered to account for surface live load. This load is equivalent to an additional layer of 1.2 m of overburden soil or the effects of snow and frost loads. Rajani et al. (2000) and Rajani and Tesfamariam (2004) estimated the frost load on buried water mains to be as high as 50% of the earth load (which is around 25 kPa for the analysis presented here).

4.3 Model Description

Only half of the soil and pipe, including the unsupported zone, is modeled to take advantage of the symmetry of the system. The pipe and the soil are modelled using SOLID186 and SOLID65 elements, respectively. SOLID186 is a high order 3-D 20-node solid element that exhibits quadratic displacement behavior. SOLID65 element is a legacy element of SOLID186 that supports the Drucker Prager failure criterion. This is an 8-node element with three translational degrees of freedom at each node (ANSYS 2015).

The interaction between pipe and soil is modelled using contact surface element (CONTA174) and target segment element (TARGE170). These elements overlie solid elements and describe the boundaries of the deformable bodies. Use of the contact and target elements allows for the modelling and meshing of two separate bodies (i.e., pipe and soil) that can interact together without having common nodal points. Since the cast iron pipe is stiffer than the soil, TARGE170 elements are positioned over the pipe elements where CONTA174 elements are located over the soil elements. Material properties for the

contact and target elements are chosen to provide fully bonded interaction between the pipe and the soil. Fully bonded interaction was found to calculate successfully the pipe stresses in pipe – soil interaction, particularly when the elastic-plastic soil model is used for the soil (Balkaya et al. 2012). When an elastic-plastic soil model is used, the maximum shear angle of friction at the interface is limited by the shear strength of the soil (governed by angle of internal friction and cohesion of the soil). The difference of the stresses calculated using a typical value of interface friction and a value corresponding to the soil shear strength is not significant for pipes in granular soil (Balkaya et al. 2012). Analysis has been however carried out with an interface friction coefficient of 0.5 and with a fully bonded interface, where the difference between the pipe stresses is found less than 2%, which is negligible.

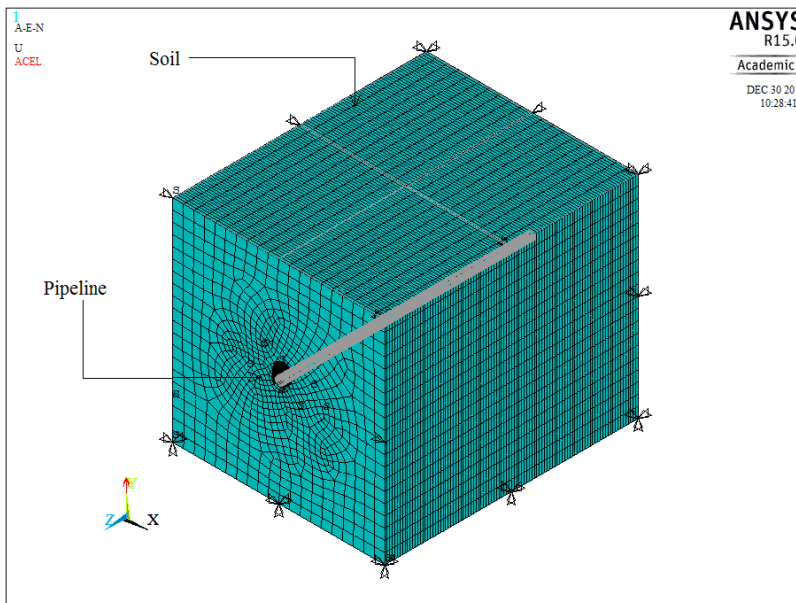


Figure 4-2: Typical finite element mesh used to model the pipe-soil structure

A typical view of the FE model is shown in Figure 4-2. Since the pipe and soil are symmetric about the pipe mid plane, longitudinal displacement of soil and pipe is restrained

on both sides of the mesh (i.e., $U_z = 0$), while displacements are allowed in horizontal (x) and vertical (y) direction. The bottom plane of the soil is fixed in all directions (i.e., $U_x = 0$, $U_y = 0$, $U_z = 0$).

4.4 Material Parameters

Material parameters play an important role in the simulation using FE analysis. Researchers use different typical values of material parameters in the analysis of pipe – soil interaction depending on the conditions of the pipe and the surrounding soil. Balkaya et al. (2012) investigated two 300 mm diameter cast iron pipelines with 12 mm and 4 mm wall thicknesses using Young's modulus for the cast iron as 70 GPa and Young's modulus for the soil as 40 MPa. The Young's modulus of cast iron can, however, vary from less than 70 GPa to as high as 138 GPa (ASM International 1990). A value of Young's modulus higher than 200 GPa for cast iron is also reported in the literature (Cooper et al. 1999). Rajani and Tesfamariam (2004) employed 206 GPa of Young's modulus for analysis of cast iron pipes.

Soil modulus can also vary along the length of the pipeline and can be low when the soil becomes loose. A higher pipe material modulus with lower soil modulus would result in a higher relative stiffness of the pipe that may cause higher bending stresses in the pipe (Liyanaage and Dhar 2015, Dhar et al. 2004). The material parameters are chosen here to provide a higher value of the relative stiffness to represent a worst case scenario.

The Young's modulus for cast iron material of 138 GPa is taken based on the upper bound value for ASTM A48 Class 40 (ASM International 1990). The Young's modulus of 206

GPa, a value used by Rajani and Tesfamariam (2004), is also considered for evaluation of the analytical model of Rajani and Tesfamariam (2004) using FE analysis.

Table 4-1: Material Parameters

Item	Cast iron	Medium Sand
Unit weight	77 kN/m ³	23 kN/m ³
Modulus of elasticity	206 GPa/138GPa	24 MPa
Poisson's ratio	0.26	0.25
Friction angle	-	38°
Cohesion	-	0.5 kPa
Dilatancy angle	-	15°

Estimation of the soil parameters is a challenging task in modelling for soil-structure interaction analysis. Soil parameters are chosen based on the typical values for pipe backfill (i.e. crushed rock). The Young's modulus for the backfill is taken as 25 MPa. This modulus is consistent with the recommended value of pipe backfill consisting of AASHTO soil type A-1-a (Crushed rock, clean gravels) recommended in Webb (2015). The elasto-plastic behaviour of soil is modelled using the Drucker-Prager material model. A very low value of cohesion (i.e. 0.5 kPa) is allocated to the backfill material in order to avoid numerical instability. Angle of internal friction is chosen as the typical value for the backfill soil ($\phi' = 38^\circ$). Analysis is carried out with different values of dilation angles (i.e., $\psi = 15^\circ, 20^\circ$ and 25°). The effects of the dilation angle within this range on the pipe wall stress are found to

be less than 5%. The dilation angle of 15° is then used for the rest of the analysis. The material parameters used in the analysis are summarised in Table 4-1.

4.5 Analytical Solution (Rajani and Tasmariam 2004)

Rajani and Tasmariam (2004) developed a pipe-soil interaction model and derived analytical solutions for the longitudinal stresses in the pipeline. In the development of the model, the authors considered a pipe under a uniformly distributed line load. The pipe was modelled as an elastic beam. The supporting soil was modeled using Winkler springs. The soil bedding was divided into three different regions: unsupported region, plastic region, and elastic region (Figure 4-3). The following general solutions for vertical deflections were obtained for the three separate regions (Rajani and Tasmariam 2004).

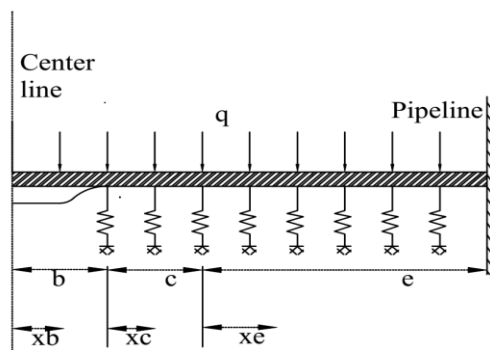


Figure 4-3: Winkler pipe-soil model (After Rajani and Tasmariam, 2004)

Unsupported region:

$$v_b = \frac{qx_b^4}{24E_p I_{ZZ}} + \frac{B_1 x_b^3}{6} + \frac{B_2 x_b^2}{2} + B_3 x_b + B_4 \quad [1]$$

Plastic region:

$$v_c = \frac{-F_z x_c^4}{24E_p I_{zz}} + \frac{C_1 x_c^3}{6} + \frac{C_2 x_c^2}{2} + C_3 x_c + C_4 \quad [2]$$

Elastic region:

$$v_e = \exp(\lambda x_e)(E_1 \cos \lambda x_e + E_2 \sin \lambda x_e) + \exp(-\lambda x_e)(E_3 \cos \lambda x_e + E_4 \sin \lambda x_e) \quad [3]$$

The solutions include 12 constants such as: B₁, B₂, B₃, B₄, C₁, C₂, C₃, C₄, E₁, E₂, E₃ and E₄.

The constants can be determined using the continuity and compatibility boundary conditions. Further detail on the analytical method is available at Rajani and Tesfamariam (2004). The other parameter in the solution is, λ , which is the reciprocal of the flexural characteristic length and is defined as,

$$\lambda = \sqrt[4]{\frac{k'_s}{4E_p I_{zz}}} \quad [4]$$

where k'_s is the elastic foundation modulus. For the elastic foundation modulus, Rajani and Tesfamariam (2004) adopted Eq. (5) from (Vesic, 1961).

$$k'_s = \frac{0.65 E_s}{1-\nu_s^2} \sqrt[12]{\frac{E_s D^4}{E_p I_{zz}}} \quad [5]$$

In the above equations, D is the pipe diameter, I_{zz} is the moment of inertia of the pipe cross-section, E_p is the Young's modulus of pipe material, E_s is the Young's modulus of soil, ν_s is the Poisson's ratio of soil, q is the line load, F_z is the maximum spring load, and v corresponds to the vertical deflections (v_b in unsupported zone, v_c in plastic zone and v_e in the elastic zone).

The deflection solutions (Eq. 1 to 3) are used to calculate the bending moments through applying Euler-Bernoulli beam theory as follows.

$$M_x = -E_p I_{zz} v'' \quad [9]$$

The maximum flexural stresses (in the longitudinal direction) at the pipe cross-sections are then calculated using the beam bending theory (Eq. 10):

$$\sigma_x = M_x R / I_{zz} \quad [10]$$

where R is the radius of the pipe.

4.6 Comparison of Models

For comparison of the analytical solution with the results from finite element analysis, longitudinal stress in the pipe is calculated using the solution of Rajani and Tesfamariam (2004), discussed above. For this purpose, a MATLAB code is developed to determine the constants in the equations (Eqs. 1 – 3) and calculate the longitudinal stresses.

Since the analytical model uses a line load to represent the surcharge and earth load, a line load corresponding to the load used in the finite element model is calculated. The earth load is calculated as the prism load (the weight of soil directly above the pipe width and length) above the pipe. The surcharge effect is calculated as qD , where ‘ q ’ is the surcharge pressure and ‘ D ’ is the pipe diameter. Surcharge load is chosen to provide a line load closer to the one used in Rajani and Tesfamariam (2004). The resulting line load is calculated to be 21.2 N/mm.

The elastic spring constant for the analytical model is obtained using Eq. (5). However, the factor '0.65' (called herein as ' α ') in the equation is varied to provide a better match of the results with those obtained using finite element analysis. As discussed below, the analytical solution with the spring constant calculated using $\alpha = 0.65$ provided overly conservative longitudinal stresses. Vesic (1961) also overestimated the bending moment using the spring constant for an infinitely long elastic beam. The current study utilizes a range of magnitudes of the α factor to identify a value suitable for application to the partially supported buried pipeline.

The analytical model is first compared with two-dimensional finite element analysis performed through modelling the pipe as beam elements (BEAM188 in ANSYS) and idealizing the soil as elastic spring (COMBIN14 in ANSYS). The same spring constant and loading are used for both FE and analytical models. Figure 4-4 compares the longitudinal stress (flexural stress) at the pipe invert from the analytical and the FE solutions. As seen in Figure 4-4, the analytical solution matches with the results of 2D finite element analysis, which is expected since the idealizations in both of the models are the same.

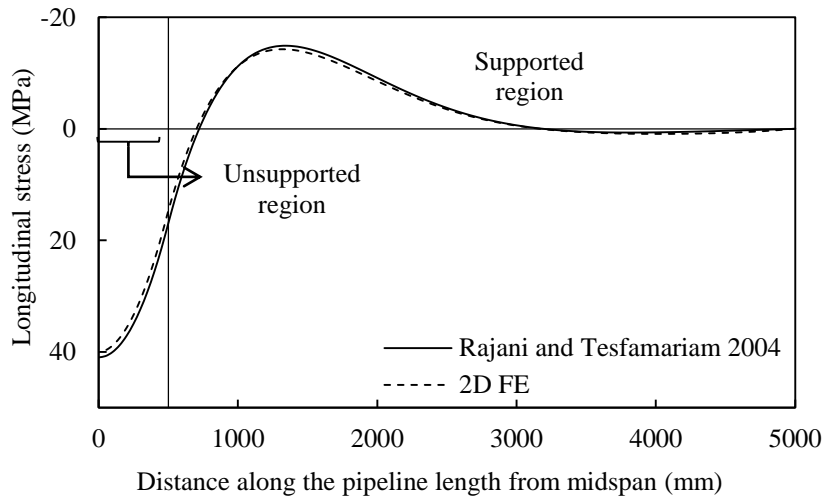


Figure 4-4: Comparison of flexural stresses from analytical model and 2D FE analysis

The analytical solution is then evaluated with three-dimensional finite element analysis. In the 3D FE model, a void over the full width of the pipe (180° void angle as shown in Figure 4-5) is employed to simulate the 2D idealization of the pipe-soil system used in Rajani and Tesfamariam (2004). Despite that the 2D idealization does not require the void thickness, two void thicknesses (200 mm and 50 mm) are considered in the FE analysis to investigate the effects.

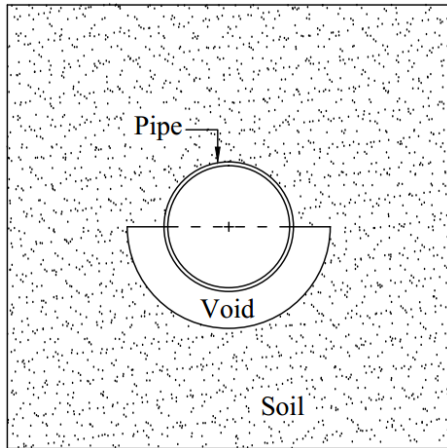
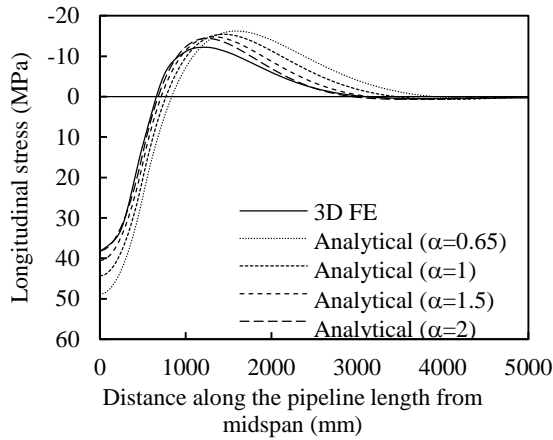
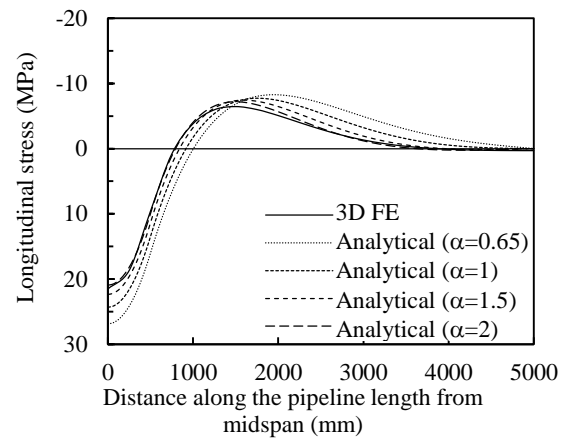


Figure 4-5: Cross-section of pipe-soil system with 180° void at the invert

The results of the analytical solution and 3D finite element analysis are compared in Figure 4-6 and Figure 4-7. The figures compare the invert longitudinal stresses for the void thicknesses of 200 mm and 50 mm, respectively. It should be noted that the bending stress is only considered in the calculation of the longitudinal stress using the analytical solution. However, the finite element analysis includes the contribution of both axial force and bending moment in the longitudinal stress calculations. The contribution of axial force (axial stress) from FE analysis is calculated from the algebraic sum of the longitudinal forces (combined effect) at each cross section of the pipeline. The axial stress is then subtracted from the combined longitudinal stresses to obtain the flexural stresses. The flexural stresses are compared in Figure 4-6 and Figure 4-7. The results of analytical solutions with different values of ' α ' are included in the figures.

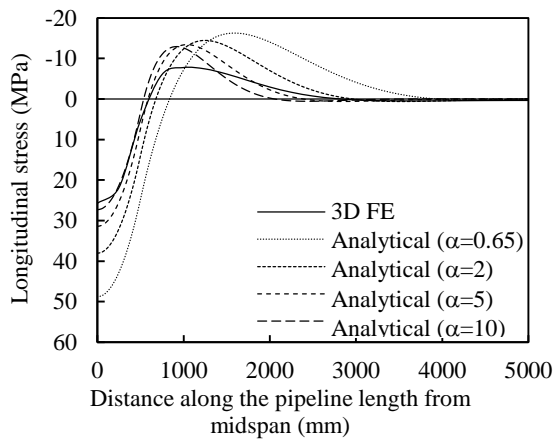


(a) Thin wall pipe

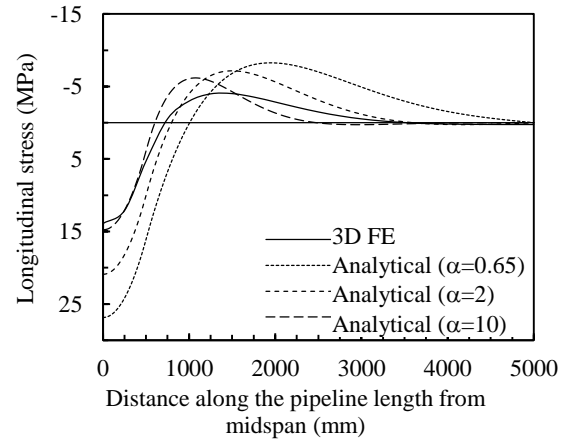


(b) Thick wall pipe

Figure 4-6: Comparison of flexural stresses for a void thickness of 200 mm



(a) Thin wall pipe



(b) Thick wall pipe

Figure 4-7: Comparison of flexural stresses for a void thickness of 50 mm

The comparison shows that the analytical solution with $\alpha = 0.65$ overestimates the longitudinal stress near the unsupported zone with respect to the 3D finite element calculations. With a higher value of α , the analytical solution approaches similar results to

that of the 3D FE solution for both thick and thin wall pipes. A higher value of α corresponds to a higher value of spring constant. This implies that the soil stiffness is underestimated in the equation (Eq. 5) of Vesic (1961) for the partially supported pipe problem. Vesic's equation was also reported to provide underestimation of the spring stiffness for beam-on-spring modeling of jointed pipe culverts (Sheldon et al. 2015).

The thickness of void appears to contribute significantly to the soil bedding stiffness. The analytical solution approaches similar results to that of the 3D FE solution for $\alpha = 2$ for the void thickness of 200 mm. However, for the void thickness of 50 mm, a much higher value of the factor ($\alpha = 10$) is required for the results of the analytical solution to be close to the results of FE analysis. This implies that the soil support (reaction) is higher for a smaller void thickness.

In the comparisons presented above, elastic ground support is only considered that evaluates the elastic component of the analytical solution. Rajani and Tafamariam (2004) indicated that the contribution of soil plasticity is not significant with an unsupported length of up to 2 m. An unsupported length of 1 m is considered in the analysis presented here.

To investigate the effect of soil elasto-plasticity, FE analysis is then performed using both elastic and elasto-plastic soil models. Figure 4-8 shows a comparison of longitudinal stresses for the thick and thin wall pipes with elastic and elasto-plastic soil models.

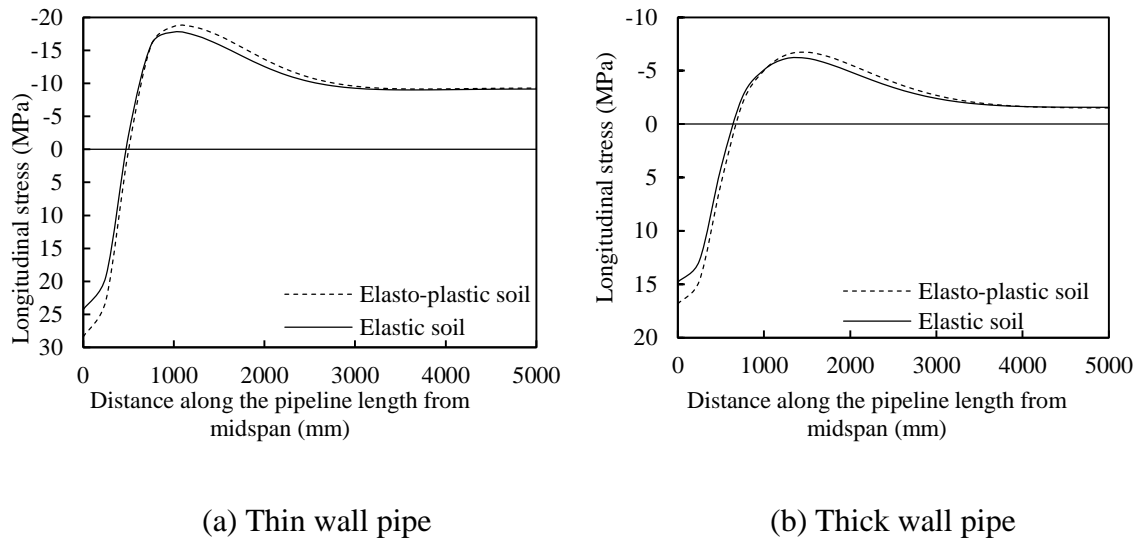


Figure 4-8: Flexural stresses with elastic and elasto-plastic soil models

In Figure 4-8, the analysis with elasto-plastic soil model provided 10 to 20% higher stress than the elastic model. This result is consistent with the findings from Rajani and Tasfamariam (2004), where higher longitudinal stresses were calculated for the pipe with an elasto-plastic soil model. The higher bending stress in the pipeline is the result of lower resistance to bending deformation offered by the elasto-plastic soil. The study indicates that the effect of soil plasticity is not negligible for the unsupported length of 1 m.

4.7 Effect of Voids

The FE modelling is used to investigate the effects of void sizes and void locations on the wall stresses in a pipeline with a localized void in the bedding/backfill. Thin and thick wall pipes with two different void thicknesses (50 mm and 200 mm, respectively) are investigated for different pipe material moduli. Three different void configurations at the invert of the pipe, as shown in Figure 4-9, are considered.

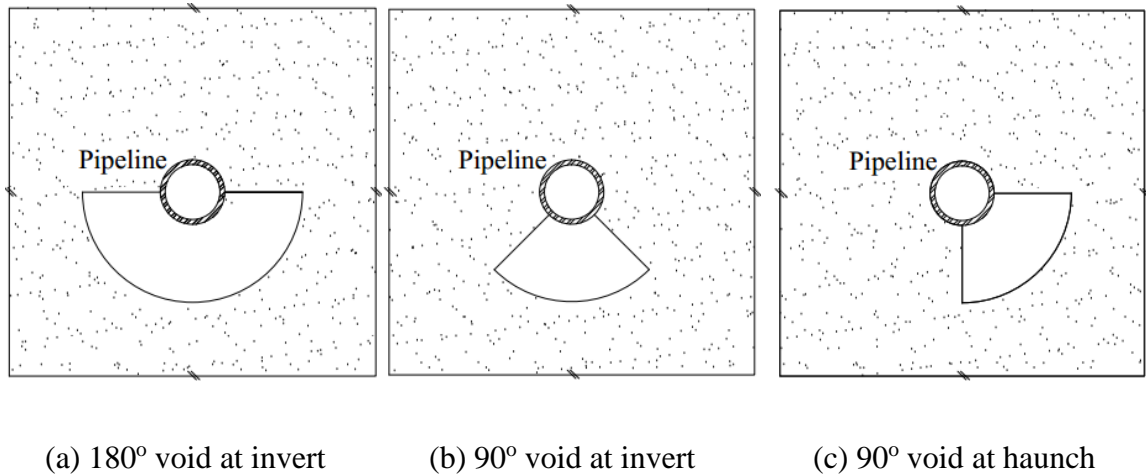


Figure 4-9: Void sizes and locations

Liyanage and Dhar (2015) showed that longitudinal stress in a cast iron water main is higher for an invert void. Meguid and Kamel (2014) reported similar observations for concrete pipes, where the invert void was found to provide significantly higher longitudinal stress in the pipeline compared to the voids at other locations.

The calculated maximum stresses in the longitudinal and circumferential directions for different cases of analysis are summarized in Table 4-2. In Table 4-2, the negative sign (-) corresponds to compression and the positive (+) sign corresponds to tension. The maximum stresses at the mid-length (mid-span) of the unsupported zone are included in the table. The longitudinal stresses are calculated to be the maximum at the mid-span. The maximum circumferential stresses are also at the mid-span for the void located between the invert and the springline. For this location of the void, soil support is available to the pipe at the invert. However, when the unsupported zone is at the invert, the maximum circumferential stresses were calculated near the intersection between the supported and

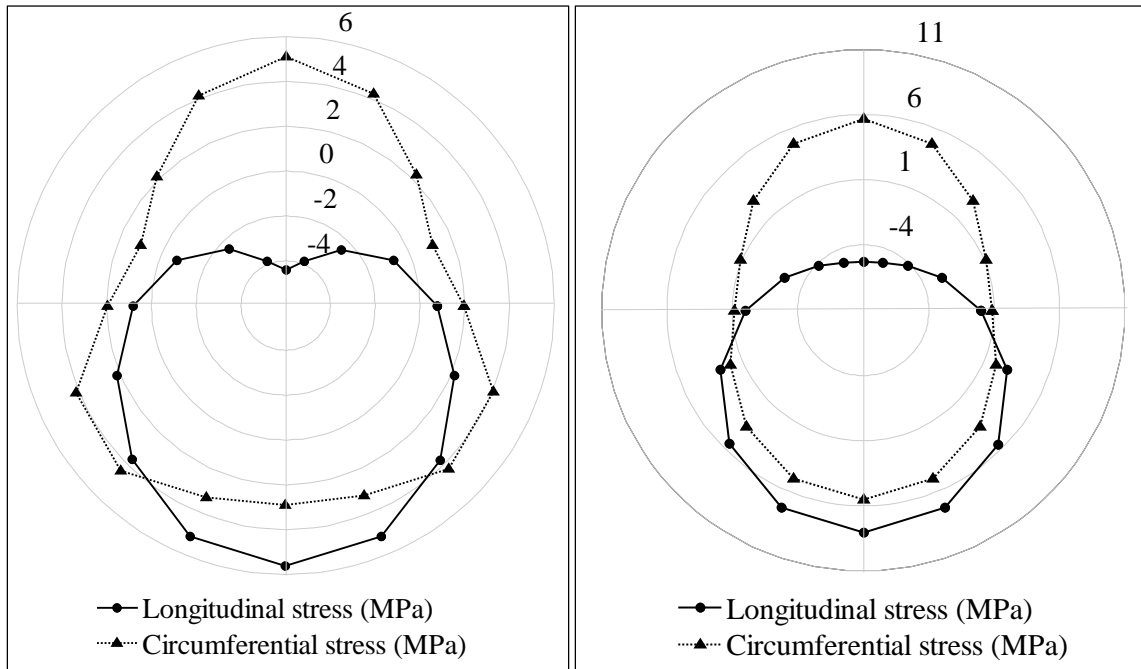
unsupported zones (see Figure 4-1), where soil support is available to the pipe at the invert. The high stress at the intersection is the result of abrupt changes in the invert soil support. The effect of the abrupt changes in the soil support is a subject of further investigation and is not within the scope of this paper.

Table 4-2: Maximum stresses in pipe wall at mid-span of the unsupported zone

Wall thickness	Elastic modulus of pipe	Void angle	Void location	Void thickness (mm)	Maximum circumferential stress (MPa)		Maximum longitudinal stress (MPa)	
10 mm	206 GPa	180°	Invert	200	6.4	-0.1	13.2	-13.1
10 mm	206 GPa	180°	Invert	50	5.8	0.7	9.3	-8.8
10 mm	138 GPa	180°	Invert	200	6.2	0.1	11.4	-11.2
10 mm	138 GPa	180°	Invert	50	5.7	0.9	8.1	-7.5
10 mm	138 GPa	90°	Invert	50	5.1	1.0	5.6	-4.4
10 mm	138 GPa	90°	Haunch	50	12.0	-5.4	4.6	-3.3
5 mm	206 GPa	180°	Invert	200	17.0	-4.6	22.3	-19.6
5 mm	206 GPa	180°	Invert	50	15.3	-1.9	16.4	-12.1
5 mm	138 GPa	180°	Invert	200	15.9	-3.4	19.3	-16.3
5 mm	138 GPa	180°	Invert	50	14.2	-0.9	14.4	-10.1

As seen in Table 4-2, the maximum longitudinal stresses are generally higher than the maximum circumferential stresses, except for in the case where the void is located between

the invert and the springline. For void location between the invert and the springline, the circumferential stresses are higher than the longitudinal stresses. The stresses around the pipe circumference for the thick wall pipes with different void angles are plotted in Figure 4-10.



(a) Void angle 90°

(b) Void angle 180°

Figure 4-10: Stress distribution along the circumference of thick wall pipes (void thickness = 50 mm, pipe modulus = 138 GPa)

The longitudinal stresses on the outer surface of the pipe and the circumferential stresses on the inner surface of the pipe are plotted in the Figure 4-10, where the stresses are the maximum. Figure 4-10 shows that the maximum longitudinal stresses are located at the invert, where the void is located. However, the maximum circumferential stress is located

at the crown (where soil support exists), particularly for 90° void. In Figure 4-10, the maximum longitudinal stress is higher than the maximum circumferential stress at the invert of the pipe. The circumferential stress is about 55% and 75% of the longitudinal stress for 90° and 180° voids, respectively. The higher longitudinal tension (relative to the circumferential stress) extends toward the pipe haunch (below pipe springline). Due to the high longitudinal stresses, circumferential cracking is expected near the invert, which is often observed in the field. Figure 4-11 shows a circumferential crack near the pipe invert observed in the City of Mount Pearl in the province of Newfoundland and Labrador in Canada.



Figure 4-11: A circumferential crack near the pipe invert in the City of Mount Pearl, adapted from Liyanage and Dhar, (2015)

The magnitude of the maximum longitudinal or circumferential stresses (i.e. 8.1 MPa or 5.7 MPa) for the cases presented in Figure 4-10 are however much less than the tensile

strength of the pipe material. The tensile strength of cast-iron can be as high as 290 MPa (ASM International 1990). This implies that additional mechanisms are involved in the failure of the water main, as discussed further in the following section.

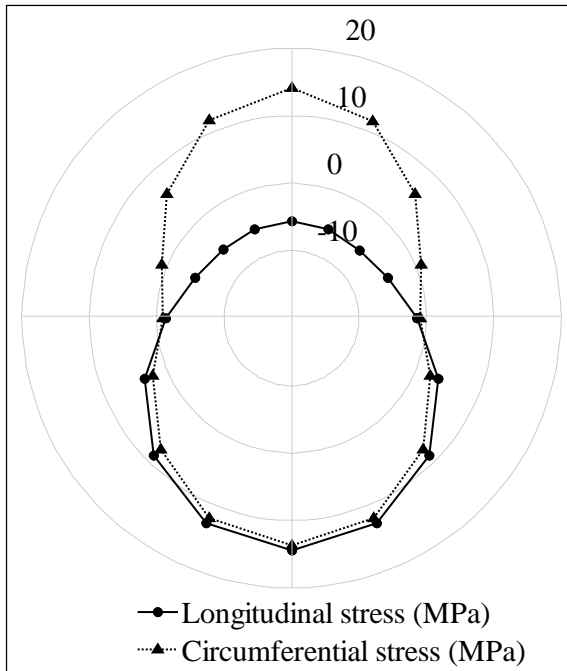


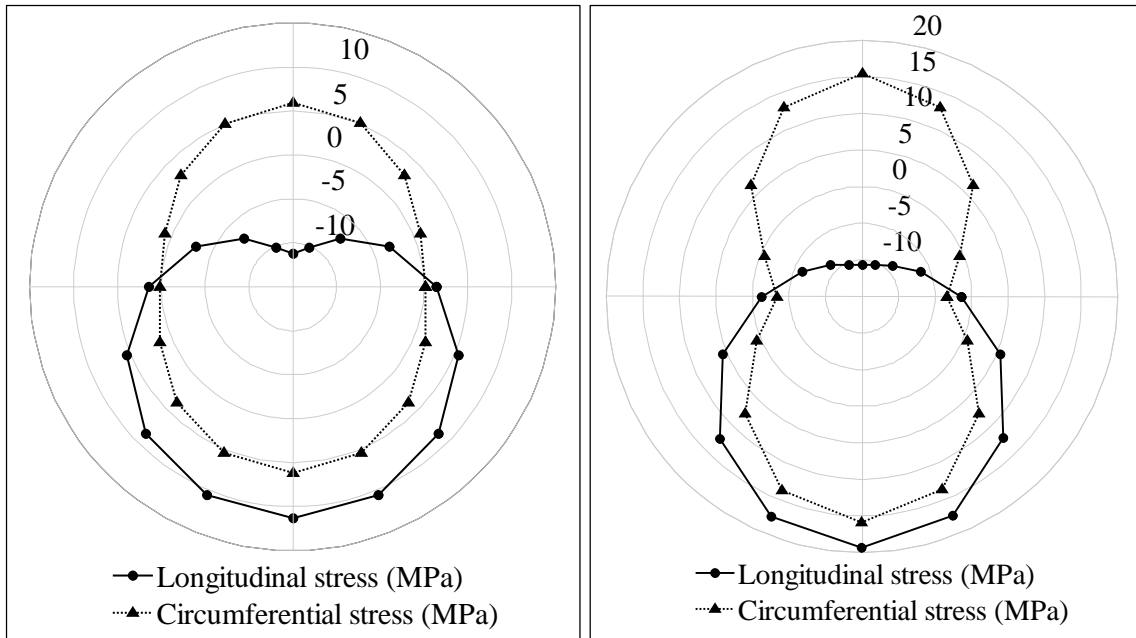
Figure 4-12: Stress distribution around thin wall pipes (void thickness=50 mm, void angle=180°, $E_p=138$ MPa)

The longitudinal stresses are also higher than the circumferential stresses at the invert for the thin wall pipe (Figure 4-12). Figure 4-12 compares the stresses for a thin wall pipe with a void angle of 180°. The maximum circumferential stress (at the invert) is almost the same as the maximum longitudinal stress in the figure. The circumferential stress is thus relatively higher for the thin wall pipe with respect to the thick wall pipe. The thin wall pipe has less flexural stiffness than the thick wall pipe. The longitudinal stress is higher for the pipe with a higher flexural stiffness (i.e., thick wall pipe). The magnitudes of stresses

in the thin wall pipe are however higher than the stresses in the thick wall pipe due to the lower flexural stiffness.

Relatively high longitudinal stress is also calculated for pipes with higher modulus of elasticity. For the thick wall pipes with $E_p = 206$ GPa and $E_p = 138$ GPa, the calculated longitudinal stresses are 9.3 MPa and 8.1 MPa, respectively. The corresponding stresses for the thin wall pipe are 16.4 MPa and 14.4 MPa, respectively (Table 4-2). A higher E_p indicates a higher flexural stiffness of the pipe cross-section. This confirms again that the longitudinal stress is higher in the pipe having higher flexural stiffness of the cross-section.

As observed earlier, a thicker void was found to cause higher stresses in the pipe wall. The pipe stresses for a 200 mm thick void with a void angle of 180° are plotted in Figure 4-13. The stresses for a 50 mm thick void are discussed in Figure 4-10 and Figure 4-12. The maximum longitudinal tension in the thick wall pipe increases from 8.1 MPa to 11.4 MPa for a void thickness increase from 50 mm to 200 mm. For the thin wall pipe, the stress increases from 14.4 MPa to 19.3 MPa. The circumferential tension increases from 5.7 MPa to 6.2 MPa in the thick-wall pipe and from 14.2 MPa to 15.9 MPa in the thin-wall pipe.



(a) Thick wall pipe

(b) Thin wall pipe

Figure 4-13: Pipe stresses for a void thickness of 200 mm ($E_p = 138$ MPa, void angle = 180°)

Figure 4-14 plots the longitudinal and circumferential stresses for a void located between the invert and the springline (void unsymmetric about vertical or horizontal axis). The stresses at the mid-span of the void are plotted in the figure, since the maximum stresses are calculated at this location. In Figure 4-14, the longitudinal stresses are higher between the invert and the springline, where the void is located. Liyanage and Dhar (2015) demonstrated that the maximum longitudinal stress occurs at the location of the void around the pipe circumference. However, the circumferential stresses are higher at a different location around the pipe circumference. The circumferential stress is higher where soil support is available to the pipe near the invert (on the other side of the void).

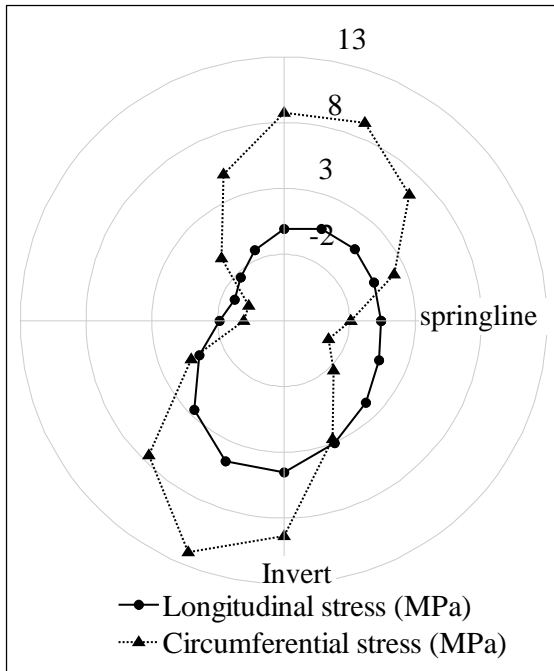


Figure 4-14: Pipe stresses for the void between the invert and springline

4.8 Effects of Localized Supports

Localized soil reactions are sometime expected on the buried pipe. The localized support may result from the erosion of small soil particles which leaves coarse particles around the pipe within a localized zone. In addition, pipe backfill may contain large pieces of rock that may exert concentrated force when in contact with the pipe. Figure 4-15 shows the presence of rock pieces in a pipe backfill exhumed in Newfoundland and Labrador, Canada. Farshad (2006) revealed that the concentrated force from pieces of stone, wood pieces and local damage can lead to fracture in plastic pipes. The effect of the concentrated force on the metal pipe is not investigated. Liyanage and Dhar (2015) conducted a preliminary study on the effects of rigid localized support. The presence of rigid localized supports was found to increase the pipe wall stresses significantly.



Figure 4-15: Pipe backfill containing rock pieces

In this section, a study on the effect of a more practical and flexible localized support conditions on pipe wall stress is presented. The localized support was modelled as elastic springs (connected to the nodes on the pipe) to account for the flexibility of the support. Figure 4-16 shows idealization of the localized reaction forces considered in this investigation.

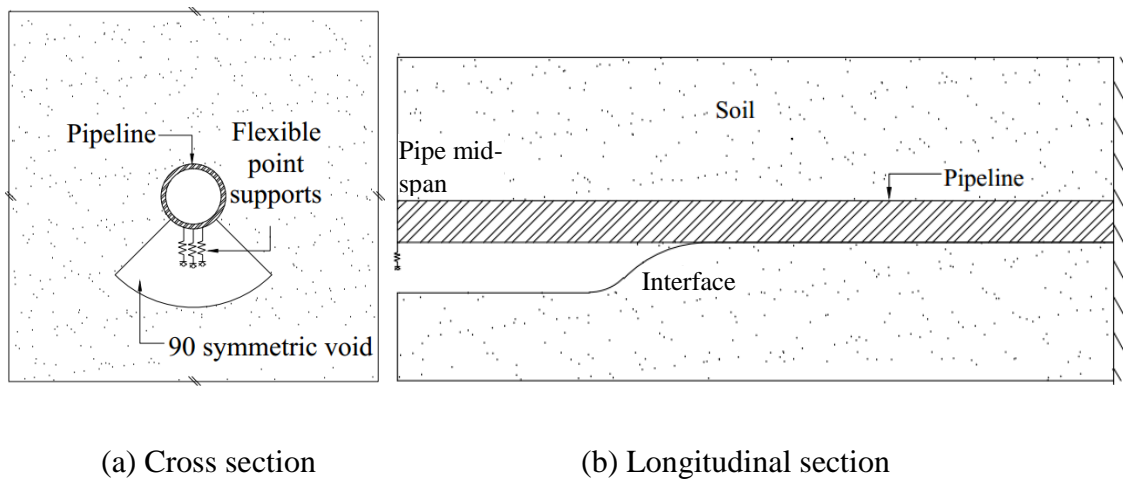
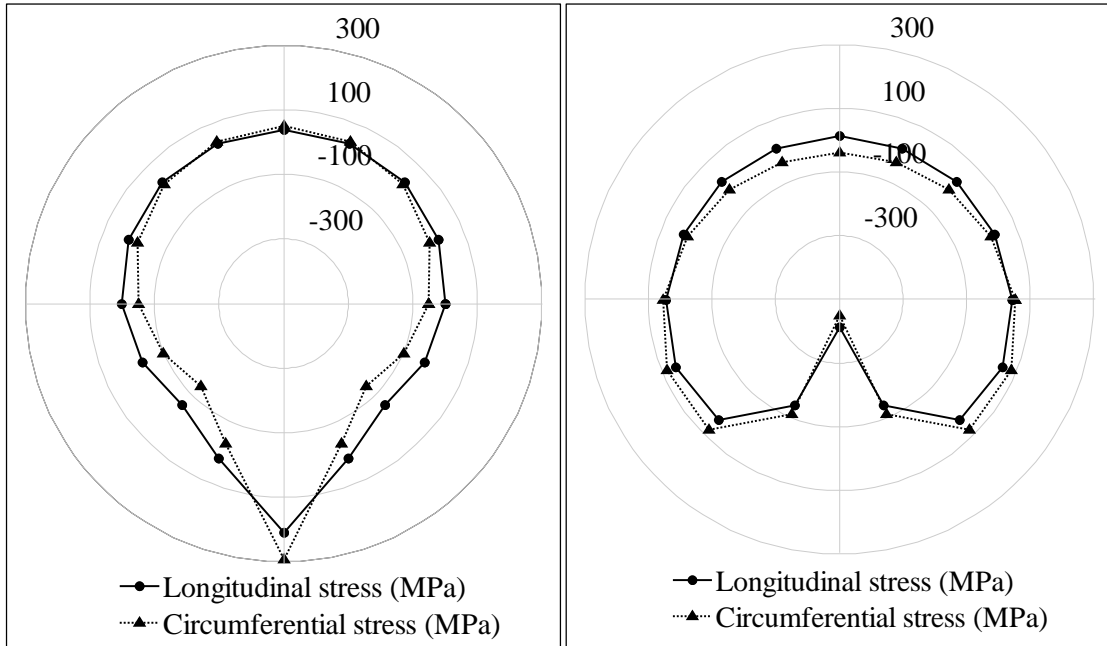


Figure 4-16: Modeling point support

Spring element, COMBIN14, is used to model a flexible support condition. The spring constant is varied to investigate the effects of support stiffness on the pipe wall stress. A 90° void with a void thickness of 50 mm at the invert of the pipe is considered. Elastic moduli of both the pipe and soil are taken as 138 GPa and 24 MPa, respectively.



(a) Inner wall

(b) Outer wall

Figure 4-17: Stresses on a partially supported pipe with localized soil reactions

Figure 4-17 plots the circumferential and longitudinal stresses around the partially supported pipes with localized soil reactions. The stresses in Figure 4-17 are for the thick wall pipe with a spring constant of 1500 N/mm. High longitudinal and circumferential stresses are observed at the pipe invert in Figure 4-17. In Figure 4-17 (a), the maximum longitudinal tension is 208.8 MPa and the maximum circumferential tension is 292.4 MPa (on the inner wall of the pipe). However, the maximum longitudinal and circumferential

tensions for the same pipe without point supports are 5.6 MPa and 10 MPa, respectively (Figure 4-10). The localized support has thus caused an increase in stress of about 30 to 40 times.

For a spring stiffness of 1500 N/mm, the maximum tensile stress reaches the stress level (292.4 MPa), which is close to the tensile strength of the cast iron material (293 MPa, ASM International 1990). The high tension thus may lead to pipe failure. Much higher compressive stresses (negative stress) are also calculated on the outer surface of the pipe (Figure 4-17b). However, the compressive stresses do not exceed the compressive strength of cast iron. Cast iron material has higher compressive strength (as high as 1000 MPa, ASM International 1990) than the tensile strength. The failure of the pipe is thus expected to initiate at the inner surface where the tensile strength limit is reached.

The study reveals that a point support with a spring constant of 1500 N/mm may lead to the failure of the pipe. The spring stiffness 1500 N/mm can be provided by a rock piece or hard objects in the bedding. It is therefore important to consider this effect in the selection of backfill material during pipeline installation.

4.9 Conclusions

This paper presents an investigation of the stresses in pipelines with an erosion void near the invert of the pipe using FE analysis. The effects of localized support resulting from non-uniform erosion or the presence of large soil particles (rock pieces) are investigated. An analytical solution for the calculation of longitudinal stress in partially supported pipes is evaluated using FE analysis. The conclusions from the study are provided below.

- The analytical solution of Rajani and Tesfamariam (2004) supports the results of the current two-dimensional finite element analysis using Winkler spring. However, the method overestimates the longitudinal stresses in the pipe with respect to the results from three-dimensional finite element analysis. The overestimation of the stress is due to underestimation of the soil support (soil stiffness) using the equation of Vesic (1961). The thickness of the void appears to contribute to the stiffness of the supporting soil. The soil stiffness is higher for thinner voids. Modification of a factor (α) in the Vesic's equation was found to provide a reasonable estimate of the spring constant for the analytical solution.
- The three-dimensional finite element analysis shows that the longitudinal and circumferential stresses in the pipeline are influenced by the erosion voids. The longitudinal tension is higher than the circumferential tension at the invert of the pipe, which may extend to the haunch.
- The longitudinal stress is higher for the pipes with higher flexural stiffness. The maximum longitudinal stress occurs at the location of the void.
- The presence of localized point supports appears to increase the pipe wall stresses significantly. Stiffness of the point support influences the pipe stress. A point support with a stiffness value of 1500 N/mm may result in the failure of a cast iron pipe. Therefore, the pipe backfill material should be carefully selected to avoid any point support to the pipeline.

Acknowledgements

The financial support for this research is provided by Research and Development Corporation of Newfoundland and Labrador, which is gratefully acknowledged. The picture in Figure 4-11 was provided by Mr. Eric Arsenault at the City of Mount Pearl.

4.10 References

ANSYS (2015). ANSYS® Academic Research, Release 16.2. ANSYS, Inc.

ASM International (1990). ASM Handbook, Volume 01 - Properties and Selection: Irons, Steels, and High-Performance Alloys. ASM International Handbook Committee.

Online version retrieved from:

<http://app.knovel.com/hotlink/toc/id:kpASMHVPS1/asm-handbook-volume-01/asm-handbook-volume-01>.

AWWSC (2002). "Deteriorating Buried Infrastructure: Management Challenges and Strategies.", Office of Ground Water and Drinking Water, US Environmental Protection Agency, Washington.

Balkaya, M., Moore, I. D., and Sağlam, A. (2012). "Study of Nonuniform Bedding Support Because of Erosion under Cast Iron Water Distribution Pipes." *Journal of Geotechnical and Geoenvironmental Engineering*, 138(10), 1247–1256.

Cooper, C.A., Young, R.J. and Elliott, R., (1999). "Cast Iron: A Natural Metal Matrix Composite", ICCM-12 Conference, Paris, July 1999, paper 1053, ISBN 2-9514526-2-4.

- Dhar, A.S. (2002). "Limit States of Profiled Thermoplastic Pipes under Deep Burial" Ph.D. Thesis, Department of Civil and Environmental Engineering. University of Western Ontario. London. Canada. 285 p.
- Dhar, A. S., Moore, I. D., & McGrath, T. J. (2004). "Two-dimensional analyses of thermoplastic culvert deformations and strains." *Journal of geotechnical and geoenvironmental engineering*, ASCE, 130(2), 199-208.
- Farshad, M. (2006). "Chapter 3 - Fracture of plastic pipes." *Plastic Pipe Systems*, M. Farshad, ed., Elsevier Science, Oxford, 53–100.
- Folkman S. (2012). "Water Main Break Rates in the USA and Canada: A Comprehensive Study." Research Report, Utah State University Buried Structures Laboratory, Logan, UT, USA.
- Frick, G.R. and Manuel, J. (2005). "Leak Detection Program: The City of Mount Pearl", *Proc. Leakage 2005*, 12-14 September 2005, Halifax, NS, Canada, 7 p.
- Liyanage, K., and Dhar, A. S. (2015). "Three dimensional finite element analyses of partially supported water mains." *GeoQuebec 2015*, 68th Canadian Geotechnical Conference, Quebec City, QC, September 21-23, 2015.
- Makar, J. M., Rogge, R., McDonald, S., and Tesfamariam, S. (2005). "The effect of corrosion pitting on circumferential failures in grey iron pipes." Research Report, American Water Works Association, Denver, CO, USA, 115p.

- Meguid, M. A., and Kamel, S. (2014). "A Three-Dimensional Analysis of the Effects of Erosion Voids on Rigid Pipes." *Tunnelling and Underground Space Technology* 43 (July): 276–89. doi:10.1016/j.tust.2014.05.019.
- Rajani, B. and Kleiner, Y. (2010). "Fatigue Failure of Large-Diameter Cast Iron Mains", *Water Distribution System Analysis 2010 (WDSA 2010)*, Tucson, AZ, USA, Sept. 12-15.
- Rajani, B., Makar, J., McDonald, S., Jen, C., and Viens, M. (2000). "Investigation of Grey Cast Iron Water Mains to Develop a Methodology for Estimating Service Life", *Research Report*, ISBN1-58321-063-6, AWWA Research Foundation and American Water Works Association, USA.
- Rajani, B., and Tesfamariam, S. (2004). "Uncoupled axial, flexural, and circumferential pipe–soil interaction analyses of partially supported jointed water mains." *Canadian Geotechnical Journal*, 41(6), 997-1010.
- Rajani, B., Zhan, C. and Kuraoka, S. (1996). "Pipe-soil interaction analysis of jointed water mains", *Canadian Geotechnical Journal*, 33, pp. 393-404.
- Seica, M. V., and Packer, J. A. (2006). "Simplified Numerical Method to Evaluate the Mechanical Strength of Cast Iron Water Pipes." *Journal of Infrastructure Systems*, 12(1), 60-67.

- Sheldon, T, Sezen, H, and Moore, I. (2015). "Beam-on-Springs Modeling of Jointed Pipe Culverts." *J. Perform. Constr. Facil.* , 10.1061/(ASCE)CF.1943-5509.0000729, 04015002.
- Trickey, S. A., Moore, I.D. and Balkaya, M. (2016). "Parametric study of frost-induced bending moments in buried cast iron water pipes", *Tunnelling and Underground Space Technology* 51, pp. 291-300.
- Vesic, A. B. (1961). "Bending of Beams Resting on Isotropic Elastic Solid." *Journal of the Engineering Mechanics Division*, 87(2), 35–54.
- Watermain Break Clock (2015). "Why So Many Water Main Breaks?" <<http://www.watermainbreakclock.com/>> (accessed on December 20, 2015)
- Water Security Agency (2004). "Water Pipeline Design Guidelines", EPB 276, Environmental and Municipal Management Services Division, Water Security Agency, Regina, Saskatchewan, downloaded from <http://www.saskh2o.ca/DWBinder/epb276.pdf> (accessed on March 8, 2016).
- Webb, M. C. (2015). "Development of Constrained Soil Modulus Values for Buried Pipe Design." *Proc. ASCE Pipelines 2015 conference*, Baltimore, MD, USA, Aug. 23-26, pp. 1695-1710.

Chapter 5. Numerical Modelling of Buried Cast Iron Water Mains Subjected to Pitting Corrosion

Kasuni H. Liyanage, Ashutosh Sutra Dhar

Department of Civil Engineering, Faculty of Engineering and Applied Science, Memorial

University of Newfoundland, St. John's, NL, Canada

Abstract

Circumferential cracking has been identified as the most common type of failure mode for cast iron water mains. However, the mechanism of the circumferential cracking in the water mains is not well understood. Some researchers postulated that the circumferential cracking is due to pitting corrosion on pipe wall that causes stress concentration, resulting in the higher longitudinal stress. This paper presents a detailed numerical study based on finite element analysis to investigate the effect of pitting corrosion on the failure mechanism of cast iron water mains. The study shows that corrosion pits as well as the relative stiffness of the pipe, with respect to the surrounding soil, play important roles for the longitudinal stress increase on the pipe wall. Longitudinal stress is generally higher than the circumferential stress for the pipes with higher relative stiffness. For a particular pipe, longitudinal stress is higher for smaller corrosion pits. Localized forces on the pipe wall from surrounding ground can increase the longitudinal stress. A localized support with a spring constant (stiffness) of 400 N/mm can result in the circumferential cracking of cast iron water mains.

5.1 Introduction

Cast iron is one of the oldest pipe materials used in potable water systems. Although cast-iron was phased out from water main application in the 1950s (AWWSC 2002), a large volume of cast iron water mains still exist in the municipal water distribution system. Folkman (2012) reported based on a study of water main breaks in USA and Canada that about 28% of water mains currently consist of cast iron. The other materials for water mains include ductile iron (DI), steel, polyvinyl chloride (PVC) and asbestos cement. As well-documented in the literature over the last few decades, Folkman (2012) also indicated that cast iron has been the most failing pipe material. However, the failure mechanisms of the cast iron pipe are not well-understood to date. Rajani et al. (1996) identified several failure modes such as circumferential cracking, longitudinal cracking, joint failure, and blowouts for cast iron water mains. Among these, circumferential cracking or ring bending is the most commonly encountered mode of failure, particularly for small-diameter cast iron pipe (Liyanage and Dhar 2015, Makar et al. 2005, Folkman 2012). Trickey et al. (2016) demonstrated that the dominant cause of the circumferential cracking in water mains may be the longitudinal bending that results from non-uniform bedding support and/or frost actions in the soil above the pipe. The erosion of the bedding and/or backfill materials by the water escaping from pipe leaks or other sources may be the cause of non-uniform bedding support. The lack of ground support causes additional stresses on the pipe wall near the unsupported zone (Balkaya et al. 2012). Dhar et al. (2004) revealed that the lack of soil support within a localized zone can lead to stress/strain concentration in flexible pipes. The stress/strain concentration was higher for pipes with higher stiffness relative to

the soil (Dhar et al. 2004). Study on the stress concentration for cast-iron pipes has been limited.

Balkaya et al. (2012) investigated a 450 mm diameter cast iron water pipe with a modulus of elasticity of 75 GPa that was buried in a granular fill with a modulus of elasticity of 20 MPa. They calculated higher circumferential stress in the pipe wall and concluded that longitudinal fracture was likely to occur in the pipes. However, a majority of cast iron water main failures occurred due to longitudinal stress, resulting in circumferential cracking. Liyanage and Dhar (2016) indicated however that for pipes with a higher material modulus of elasticity, the longitudinal stress could be higher than the circumferential stress. The modulus of elasticity of cast iron pipe materials varies widely and can be higher than 200 GPa (Liyanage and Dhar 2016, Makar et al. 2005), which is much higher than the modulus of elasticity considered in Balkaya et al. (2012).

Makar et al. (2005) conducted a study on cast iron water mains paying particular attention to circumferential cracking, the most common mode of failure for water distribution networks. They reported that the circumferential cracking occurs in small diameter (100 to 250 mm diameter) pipes that are typically used for water distribution systems. The corrosion pits of varying sizes are identified as the cause for the circumferential failures. Makar et al. (2005) tested four pipe samples in bending, each having an artificial pit hole in the pipe wall. Pipe wall strains were measured using the neutron diffraction method. The test arrangement was similar to the four-point bending test with the central loads (two central contact points) closer than the distance used in standard test methods. Based on the study, it was postulated that circumference cracking in small diameter pipes is associated

with corrosion pitting. The presence of a corrosion pit in the pipe undergoing bending is expected to cause a triaxial state of stress on the pipe wall, resulting in a failure mechanism that is different from the one predicted using conventional analysis. Makar et al. (2005) completed a FE based parametric study for pipes with different sizes of corrosion pits to study the size of a pit that may cause circumferential cracking. The pipe was investigated under a line load representing the ground load including frost effects. The supporting soil was represented using one-dimensional springs. It was concluded that corrosion pit diameters ranging from 10 mm to 40 mm can cause circumferential cracking to the pipe under soil covers of 3 m to 6 m. However, the effects of the corrosion pit on the behaviour of the buried pipe were not investigated considering the three-dimensional complex ground conditions that are expected in the field.

This paper presents a three-dimensional finite element (FE) investigation of a buried small diameter cast iron pipe with corrosion pits. A pipe with a corrosion pit on the wall is investigated considering uniform and non-uniform bedding conditions with or without localized point loads. Localized concentrated support (or force) is sometimes expected on buried pipes near the corrosion pit where water leaking through the hole (pit) may wash away fine to medium soil particles, leaving behind coarser particles (such as rock pieces or stones). Rajani and Kleiner (2010) recognized that sharp object with high stiffness, like a rock or stone, may accentuate fluctuating stresses on the pipe wall. Liyanage and Dhar (2015, 2016) demonstrated that the localized point support causes stress concentration, leading to pipeline failure. The effects of non-uniform bedding and localized point support on pipes subjected to a corrosion pit have not been investigated to date.

5.2 FE Model

Cast iron pipes with a diameter of 175 mm (outer), length of 10 m and wall thicknesses of either 10 mm or 5 mm are considered for the investigation. The pipes with 10 mm or 5 mm thicknesses are called herein as thick-wall or thin-wall pipes, respectively. The pipe is considered to be buried in medium dense granular fill with 2 m of soil cover above the pipe crown. The pipe is loaded with an internal pressure of 400 kPa and a surface surcharge of 25 kPa (after Liyanage and Dhar, 2016). The surface load is equivalent to an additional layer of 1.2 m of overburden soil or the effects of snow and frost loads (Rajani et al. 2000).

A corrosion pit hole of different diameters is included on the pipe wall. The corrosion pit is located at the mid-length of the pipe at the invert. Several cases of buried pipes with a corrosion pit are considered for the analysis. These include:

- 1) a pipe buried in a uniform soil mass;
- 2) a pipe having a lack of support (a void) within the bedding at the invert (Figure 5-1); and
- 3) a pipe with a void at the invert and a localized concentrated force near the void.

A general purpose FE package, ANSYS (ANSYS 2015), is used for the analysis of the pipe-soil system. Considering the symmetry of the system about a vertical plane passing through the mid-span, only half of the pipe-soil system is modelled. Figure 5-1 shows a schematic of the idealized problem. To study the lack of soil support, an unsupported zone (void) of 1 m length is considered at the mid-length of the pipe (Figure 5-1). The void is

symmetric about the pipe invert. The width and the thickness of the unsupported zone are varied.

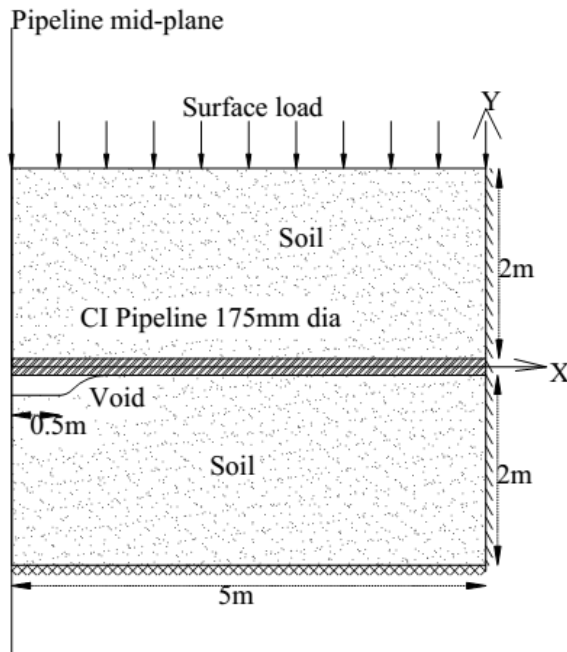


Figure 5-1: Schematic of a longitudinal section of buried pipe

Figure 5-2 shows the idealization of the pipe with localized concentrated force. Flexible concentrated support (or force) is modelled using elastic springs. The springs are placed at the mid-length of the pipe (and void), near the corrosion pit.

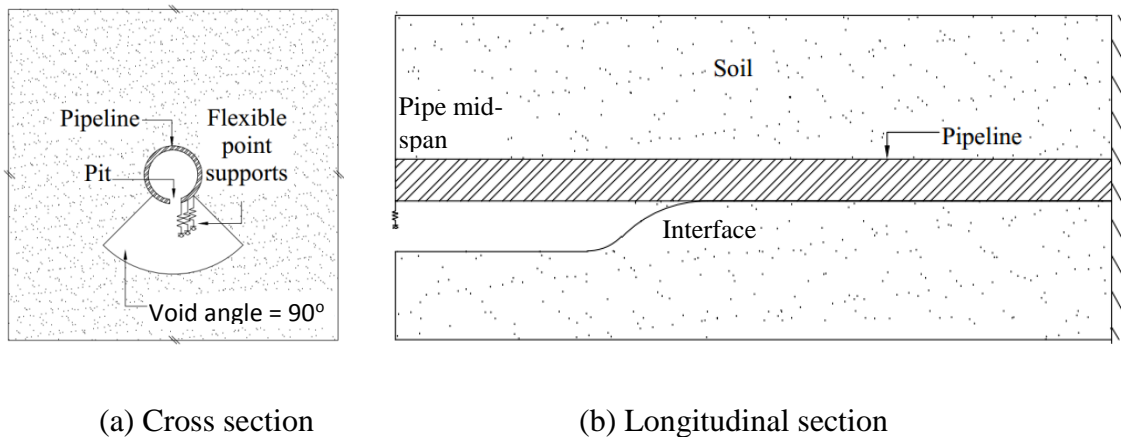
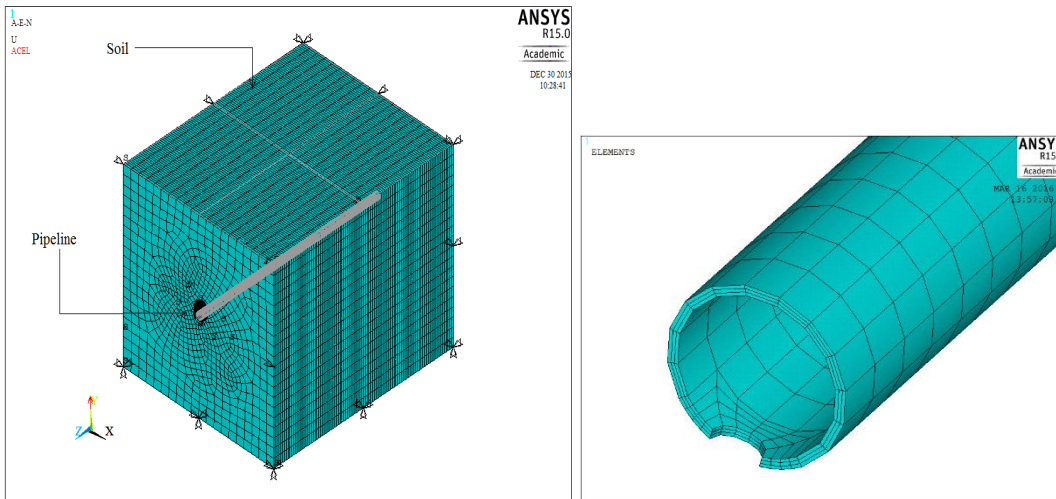


Figure 5-2: Idealization of pipe with concentrated support near the void

The cast iron pipeline is modelled using SOLID186 elements and the soil is modelled using SOLID65 elements. The interface between pipe and soil is modelled using the contact surface element (CONTA174) and the target segment element (TARGE170). This approach allows us modelling of two separate solid bodies (e.g. pipe and soil) that can interact together without having common nodal points (Liyanage and Dhar 2016). Material properties for the contact and target elements are chosen to provide fully bonded interaction between the pipe and the soil. Balkaya et al. (2012) demonstrated that fully bonded interface can be used for modelling pipe – soil interaction, when elastic-plastic soil model is used for the soil. For elastic-plastic soil, the maximum interface friction is limited by the shear strength of the soil rather than the shear strength of the interface. Interface shear strength is usually somewhat less than the soil shear strength (around two third of the shear strength of soil). However, pipe stresses calculated based on the soil shear strength or interface shear strength are very similar (Balkaya et al. 2012).

A symmetric boundary condition is applied at the plane of symmetry. Longitudinal movement of the pipe at the far-end is restrained, where Horizontal and vertical movements are allowed. Figure 5-3 shows a typical FE model used. The bottom plane of the soil is fixed in all directions (i.e., $U_x = 0$, $U_y = 0$, $U_z = 0$).

The FE mesh includes 100 elements along the length of the pipeline (element size of 50mm), 16 elements around the circumference of the pipe and 3 elements through the thickness of the pipe as shown in Figure 5-3. The corrosion pit (50 mm diameter) is modelled as a circular hole penetrating the whole wall thickness. The FE mesh is refined around the corrosion hole (Figure 5-3). Analysis have been carried out with two different mesh densities (i.e., 2812 elements per area and 72 elements per area) around the corrosion pit. However, the differences in stresses are found to be less than 1%. A mesh density of 72 elements per area is therefore used to save the computational time (Figure 5-3b).



(a) Overall mesh

(b) Pipe mesh

Figure 5-3: A typical FE model

A parametric study was performed to determine the optimum width and depth of the problem through minimizing the boundary effects with a minimum computational time. Based on the study, the width of soil beside the springline of the pipe and the depth of soil below the invert of the pipe is selected to be 2 m each.

In order to simulate the localized concentrated supports, elastic spring elements COMBIN14, are used in the finite element model. The spring constant value is used to adopt the rigidity condition of the idealized concentrated support.

5.3 Material Parameters

Upper bound and lower bound values of Young's modulus for cast iron material are considered to investigate the effect of pipe material modulus. Cast iron has an upper bound value of Young's modulus of 138 GPa and a lower bound value of 70 GPa, according to ASTM A48 Class 40 (ASM International 1990).

Soil parameters are chosen based on the typical values for pipe backfill (i.e. granular fill), after Liyanage and Dhar (2016). The Young's modulus for the backfill is taken as 25 MPa. The elasto-plastic behaviour of soil is modelled using the Drucker-Prager material model. A very low value of cohesion (i.e. 0.5 kPa) is allocated to the backfill material in order to avoid numerical instability. The angle of internal friction is chosen as the typical value for the backfill soil ($\phi' = 38^\circ$). Analysis is carried out with different values of dilation angles (i.e., $\psi = 15^\circ, 20^\circ$ and 25°), where no significant difference in the pipe stresses were calculated. A dilation angle of 15° is then chosen for the analysis. The material parameters used in the analysis are summarised in Table 5-1.

Table 5-1: Properties of materials and other parameters

Pipe material (cast iron) properties		Soil Properties	
Density	7850 kg/m ³	Density	2344 kg/m ³
Elastic modulus	206GPa, 138GPa, 70GPa	Young's modulus	24MPa
Poisson's ratio	0.26	Poisson's ratio	0.25
		Friction angle	38°
		Dilatancy angle	15°
		Cohesion	0.5kPa

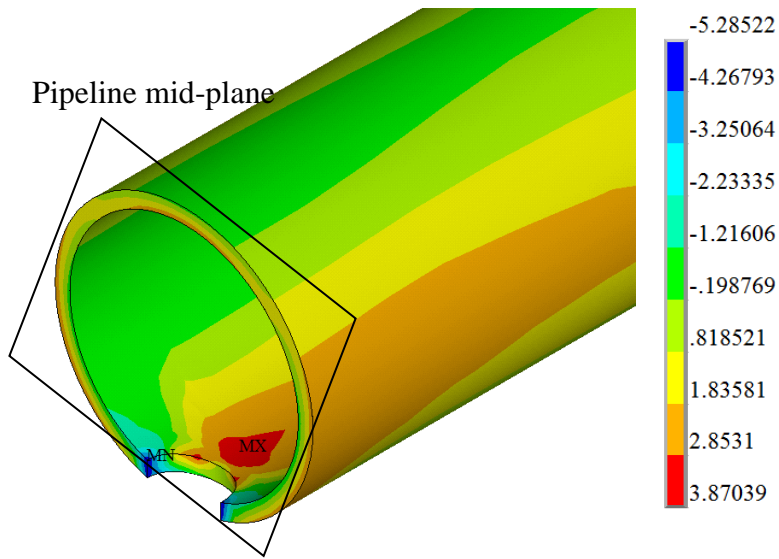
5.4 Effects of Bedding Support

FE analysis is used to investigate the effects of soil bedding on the pipe with a corrosion pit. The corrosion pit is idealized as a 50mm diameter circular hole on the pipe wall located at the invert of the pipe. Pipe wall thickness is 10mm. The following bedding conditions are considered.

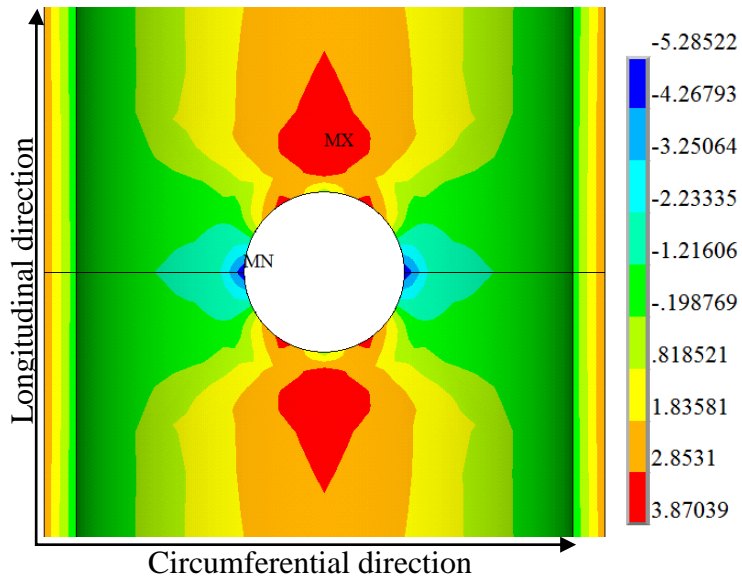
1. Uniform pipe bedding.
2. The bedding includes a 1 m long and 50 mm thick void at the invert of the pipe. The void is symmetric about the pit hole both in circumferential and longitudinal direction. The void extends 90° and 180° around the pipe circumference symmetrically about the pipe invert (see Figure 5-2a for void angle).

For the pipe in uniform soil bedding, concentration of longitudinal and circumferential stresses is observed around the pit. Figure 5-4 and Figure 5-5 plot the contour of longitudinal and circumferential stresses, respectively, near a 50 mm diameter corrosion pit. These stresses are for the moduli of elasticity of 138 GPa and 24 MPa for the pipe material and the soil, respectively.

The maximum longitudinal tensile stress in Figure 5-4 (i.e. 4 MPa) is much less than the maximum circumferential tensile stress in Figure 5-5 (i.e. 25 MPa). The longitudinal tensile stresses are located on two sides of the pit along the pipe axis. The longitudinal compressive stresses, which are higher than the longitudinal tensile stresses, are located along the pipe circumference (Figure 5-4). The circumferential tensile stresses are also located along the pipe axis near the pit. The circumferential compressive stresses are along the pipe circumference (Figure 5-4). The type of stresses encountered for the pipe in the uniform soil bedding thus suggests longitudinal splitting of the pipe when the stress exceeds the strength of the material.

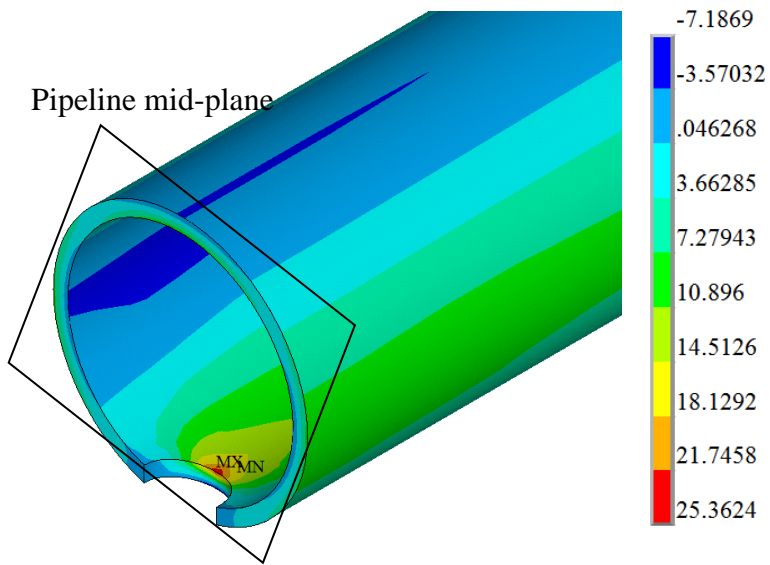


(a) Overall stresses near the pit (MPa)

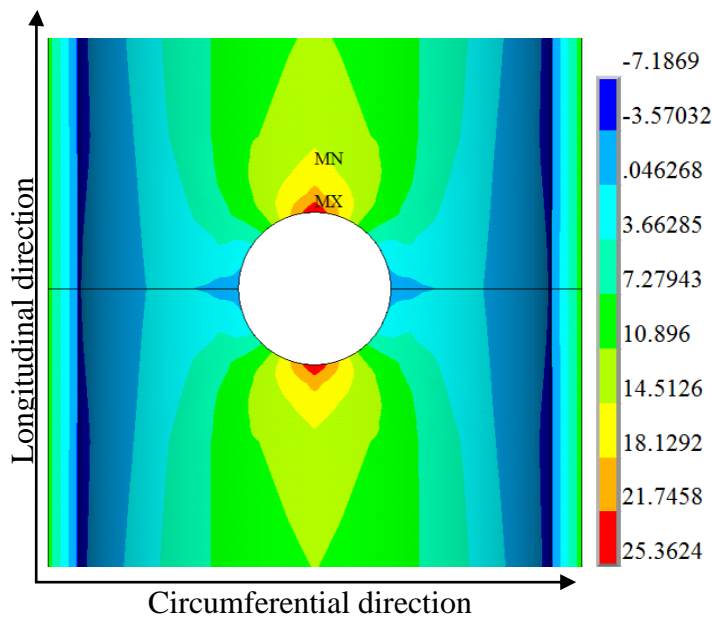


(b) Stresses around the pit (MPa)

Figure 5-4: Longitudinal stresses for the pipe in uniform bedding



(a) Overall stresses near the pit (MPa)



(b) Stresses around the pit (MPa)

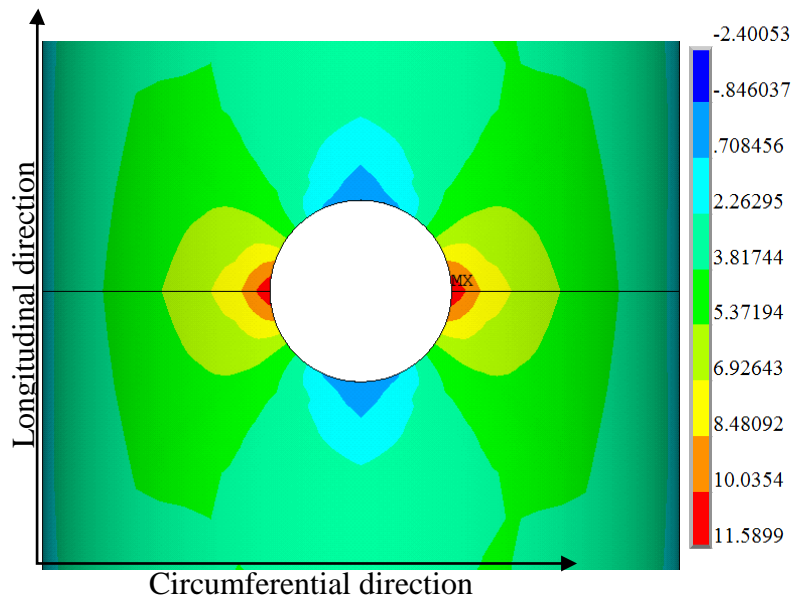
Figure 5-5: Circumferential stresses for the pipe in uniform bedding

The void at the pipe invert is found to cause redistribution of pipe wall stresses. For a 1 m long and 50 mm thick void, the maximum longitudinal tension is higher than the maximum

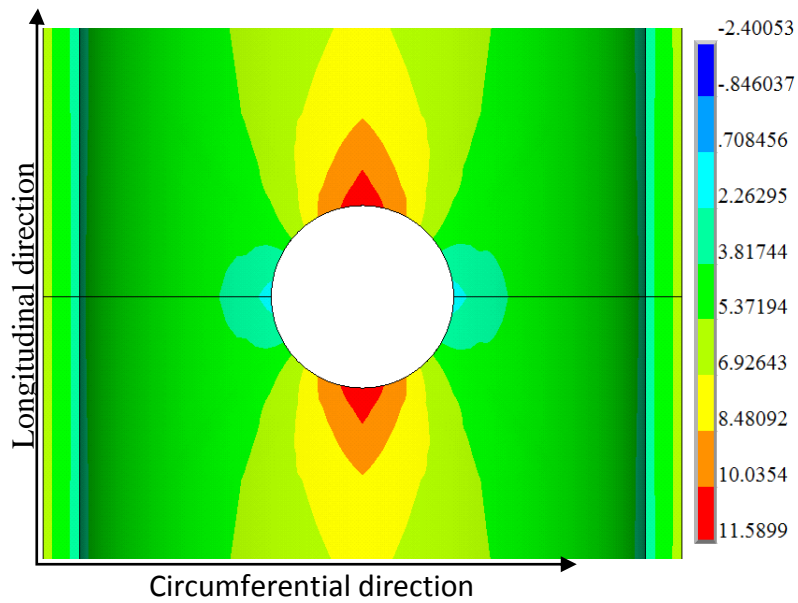
circumferential tension (Figure 5-6). The moduli of elasticity of the materials for these calculations are the same as those used for the analysis with uniform soil (i.e. 138 GPa for cast iron and 24 MPa for soil).

Figure 5-6 plots the stresses for a 90° wide void at the pipe invert. The magnitude of the maximum longitudinal stress is 11.6 MPa in Figure 5-6, where the maximum circumferential stress is 9.7 MPa. The maximum longitudinal stress is higher than the stress for the pipe with uniform soil bedding (Figure 5-4). However, the circumferential stress is decreased due to the lack of support at the pipe foundation (Figure 5-6).

Pipe stresses for a 180° wide void are also calculated where the maximum longitudinal and the maximum circumferential stresses are calculated to be 20.2 MPa and 10.4 MPa, respectively. The maximum longitudinal tensions align along the circumferential direction of the pipeline on the two sides of the pit. Similar patterns of longitudinal strain contours were observed by Makar et al. (2005) experimentally using the neutron diffraction method in their testing of pipes with an artificially milled pit at the invert that was subjected to bending. Although the intensity of the maximum longitudinal stress is less than the strength of the material, the alignment of the maximum stresses suggests a possibility of circumferential cracking if the other factors, including stress corrosion cracking (SCC), contribute.



(a) Longitudinal stress (MPa)



(b) Circumferential stress (MPa)

Figure 5-6: Stresses in the pipe wall for 1 m long void in the soil bedding (void extends 90°)

Circumferential tensile stresses are calculated to be higher near the intersection between the unsupported and supported pipe zones at the invert and near the pit. Near the intersection, the pipe stress is influenced by the abrupt change in the soil support. The effect of the abrupt changes in the soil support is a subject of further investigation and is not within the scope of this paper. Only the circumferential stresses near the pit are investigated.

The contour plots discussed above also reveal that the longitudinal stress is the maximum at the mid-length of the pipe on two opposite sides of the pit along the pipe circumference. However, the circumferential stress is not at its maximum at the mid-length, but located near the edge of the pit along the pipe length. Figure 5-7 shows stress distribution around the pipe circumference in polar plots in which radial coordinates indicate the intensity of the stresses in longitudinal and circumferential directions and angular coordinates indicate the angles along the pipe circumference. Longitudinal stresses at the mid-length of the pipe (where the stress magnitude is the highest) are plotted in the figure. Therefore, the curve discontinues at the invert where the pit is located. The circumferential stresses around the pipe circumference at the location of the maximum circumferential stress are included in the figure (Figure 5-7). The figure reveals that the highest tension around the pipe circumference is in the longitudinal direction near the invert at the location of the pit.

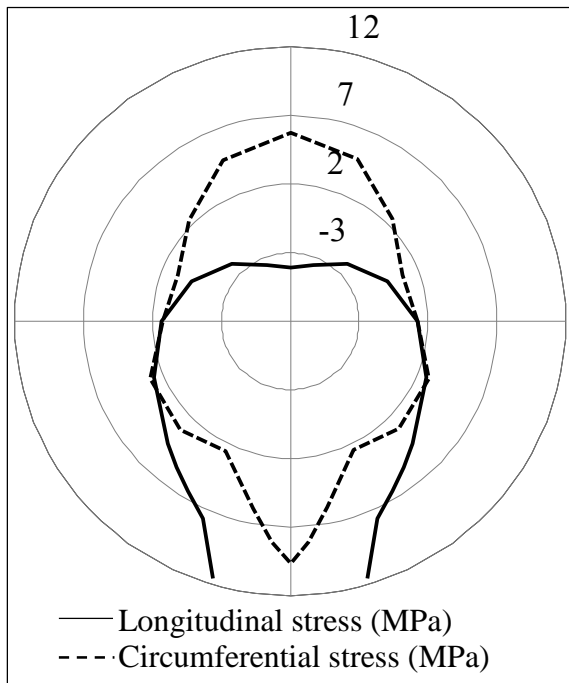


Figure 5-7: Stresses around pipe circumference

To illustrate the effect of the size of the void in the bedding, unsupported zones with 90° and 180° void angles are investigated for void thicknesses of 50mm and 200 mm with a thick wall pipe (10mm thickness). The moduli of elasticity of the pipe material and the soil are 138GPa and 24 MPa, respectively. Figure 5-8 plots the distribution of longitudinal and circumferential stresses for different void angles. It shows that when the void angle increases (wider void), both the maximum longitudinal stress and the maximum circumferential stress increase for the thick wall pipe. However, the effect is more on the longitudinal stress.

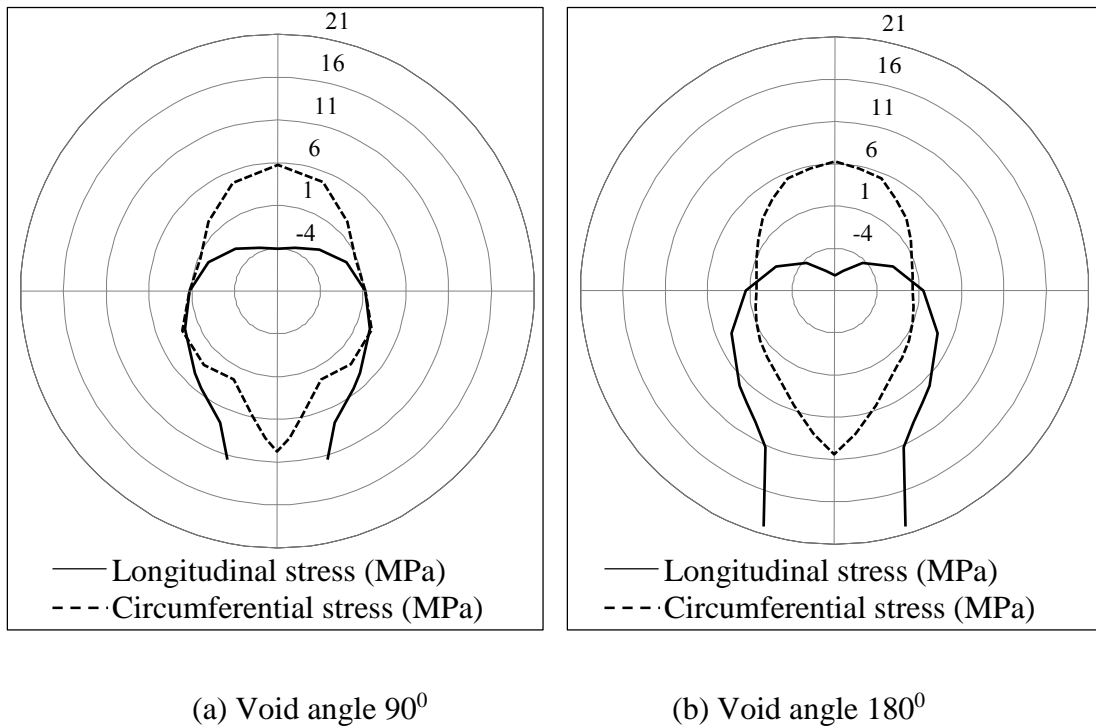


Figure 5-8: Stresses at pipe mid-length in a thick-wall pipe with a void depth of 50mm

Pipe stresses are also examined for two different void depths (i.e., 50mm and 200mm). The results are shown in Figure 5-9. As observed in Figure 5-9, the longitudinal stresses are significantly increased and circumferential stresses are somewhat reduced with the increase of void depth. For the increase of the void depth from 50 mm to 200 mm, the maximum longitudinal stress increased by 50% and the maximum circumferential stress reduced by 1% to 13%. Increases in void depth thus contribute to the increase of the maximum longitudinal tension.

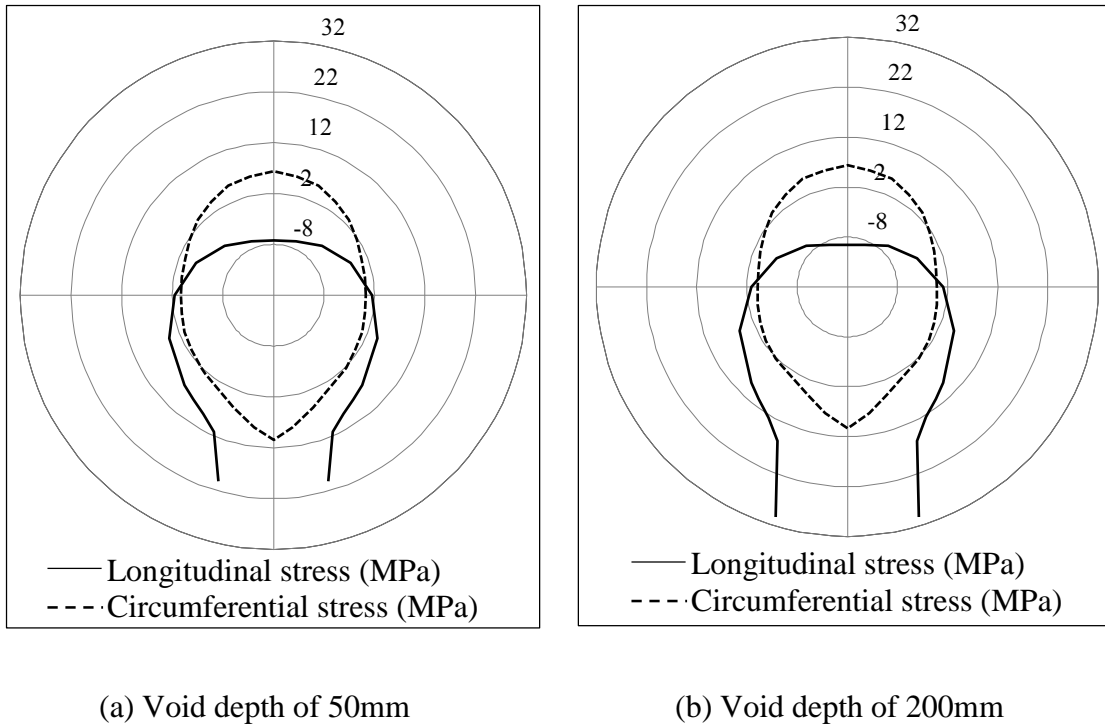
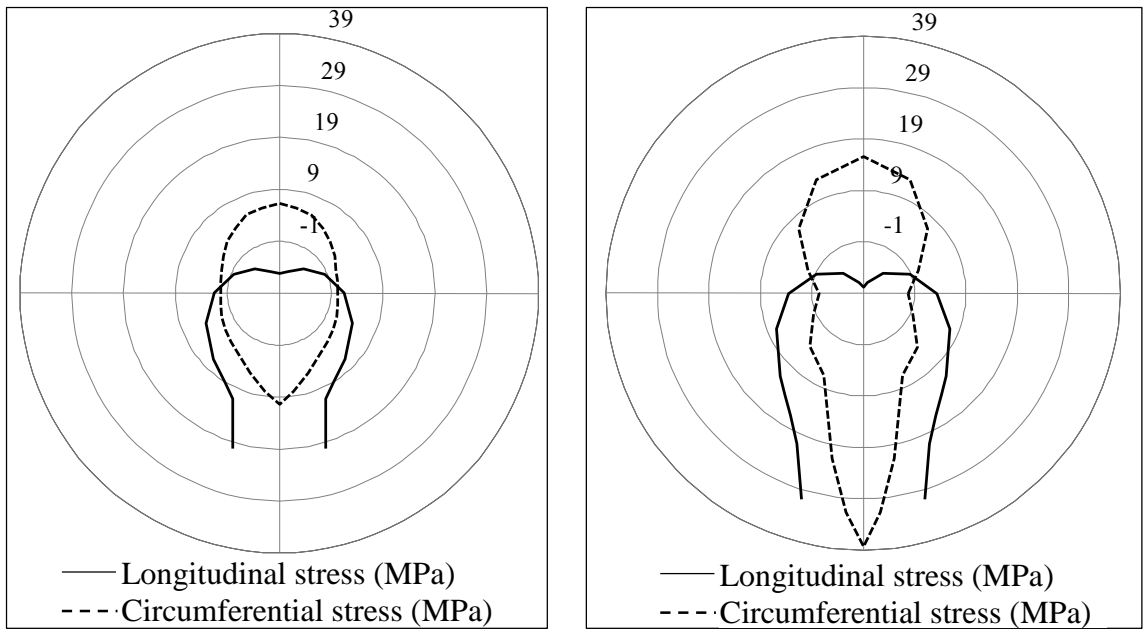


Figure 5-9: Stresses in a thick pipe for a void angle of 180°

5.5 Effect of Material Stiffness

The moduli of elasticity of the pipe material and the surrounding soil often control the stress distribution on the wall of buried pipes. To investigate this effect, finite element analyses have been conducted for a thick wall (10mm in thickness) and a thin wall (5mm in thickness) pipes with different moduli of elasticity of the pipe material. The results are plotted in Figure 5-10. In Figure 5-10, pipe stresses are higher for the thin-wall pipe than those in the thick wall pipe. However, the thick wall pipes exhibit higher longitudinal stresses than circumferential stresses. The maximum longitudinal stress is almost double the maximum circumferential stress (Figure 5-10a).



(a) Thick wall pipe

(b) Thin wall pipe

Figure 5-10: Pipe stresses for a void angle and thickness of 180° and 50mm, respectively (Pipe modulus = 138GPa)

Table 5-2 shows the pipe wall stresses under different conditions where the stresses are expressed in term of a parameter called “Factor of Safety (FOS)”. The “Factor of safety” is defined as the ratio of the strength of the material to the maximum stress in the pipe component. The strength of cast iron material is taken as 293MPa (ASM International 1990).

Table 5-2: Factor of safety in longitudinal and circumferential directions of the pipe for different conditions

Wall thickness (mm)	Pipe Modulus (GPa)	Void angle	Void depth (mm)	FOS in Longitudinal direction	FOS in circumferential direction
10	138	180	200	9.70	28.53
10	138	180	50	14.53	28.17
10	138	90	200	15.84	36.86
10	138	90	50	25.28	30.21
10	70	90	50	34.27	26.54
5	138	180	50	9.50	7.65
5	138	90	200	9.44	10.39
5	138	90	50	14.17	9.04

Table 5-2 reveals that the factor of safety reduces in longitudinal direction when the pipe modulus increases, the void angle increases or the void depth increases. The factor of safety is generally lower in the longitudinal direction than in the circumferential direction except for the case with the modulus of elasticity of 70 GPa for the pipe material. Circumferential cracking is thus anticipated for pipes with a higher modulus of elasticity. This is also consistent with the authors' findings for pipes without corrosion pits (Liyanage and Dhar, 2016).

Table 5-3: Maximum pipe stresses for varying pit sizes and relative stiffness

Pit size (mm)	Relative stiffness	Maximum longitudinal stress (MLS)		Maximum circumferential stress (MCS)		Ratio of MLS/MCS
		Tension (MPa)	Compression (MPa)	Tension (MPa)	Compression (MPa)	
40	9.64	8.88	-3.08	9.56	-3.70	0.93
40	19.00	11.84	-4.21	7.98	0.85	1.48
40	28.36	13.91	-4.98	10.15	-4.28	1.37
50	9.64	8.55	-3.02	11.04	0.94	0.77
50	19.00	11.59	-4.10	9.70	0.78	1.19
50	28.36	13.74	-4.84	10.13	-4.26	1.36
60	9.64	7.90	-2.94	13.00	-3.69	0.61
60	19.00	10.99	-3.96	11.58	0.69	0.95
60	28.36	12.87	-4.56	10.69	-4.11	1.20

In order to identify the pipe stiffness for which longitudinal stresses are higher, the pipe wall stresses are investigated against a relative bending stiffness of the pipe-soil system.

The relative bending stiffness is defined as:

$$R = \frac{E_p I_{zz}}{E_s D^4},$$

where R is the relative stiffness, E_p is the modulus of elasticity of the pipe material, I_{zz} is the moment of inertia of pipe cross-section, E_s is the modulus of elasticity of soil and D is the outer diameter of the pipe.

Analyses are carried out with different parameters for a 50 mm thick void extended over 90° at the pipe invert. The results are summarized in Table 5-3. In Table 5-3, the ratio of the longitudinal and the circumferential stress varies from 0.61 to 1.48 for the cases considered. The maximum circumferential and longitudinal stresses are plotted against the relative stiffness for different sizes of the corrosion pit in Figure 5-11.

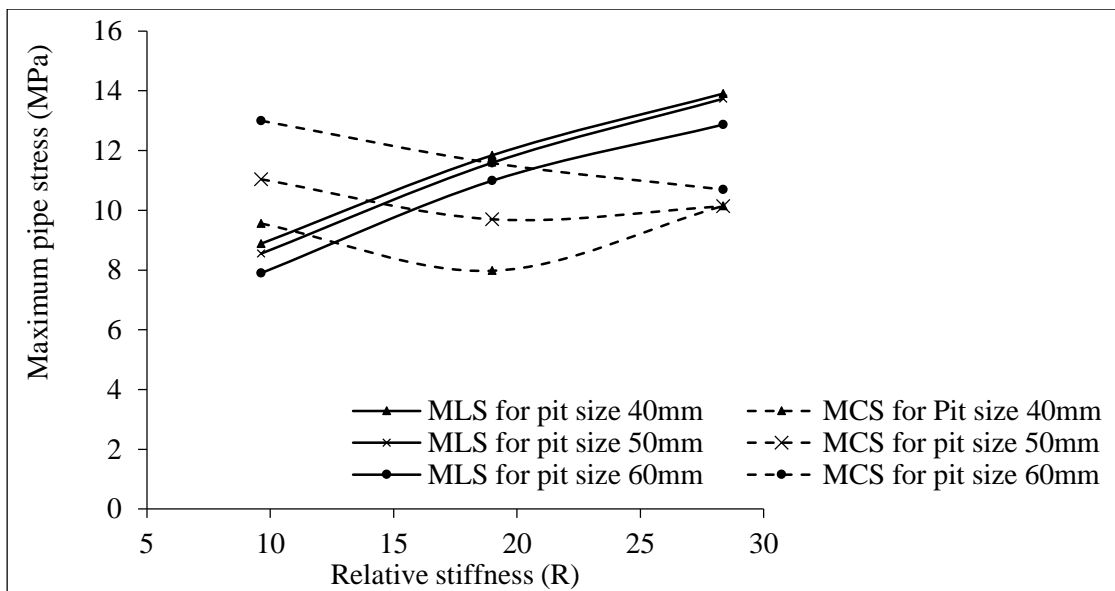


Figure 5-11: Maximum longitudinal and circumferential stresses with relative stiffness

In Figure 5-11, the longitudinal stresses are lower and the circumferential stresses are higher for larger pit sizes. Makar et al. (2005) also measured higher elastic strains for larger pit sizes. Figure 5-11 shows that the longitudinal stress increases and the circumferential

stress decreases with the increase of the relative stiffness. It thus reveals that for higher relative stiffness, longitudinal stress governs the pipe's structural condition where circumferential cracks are expected.

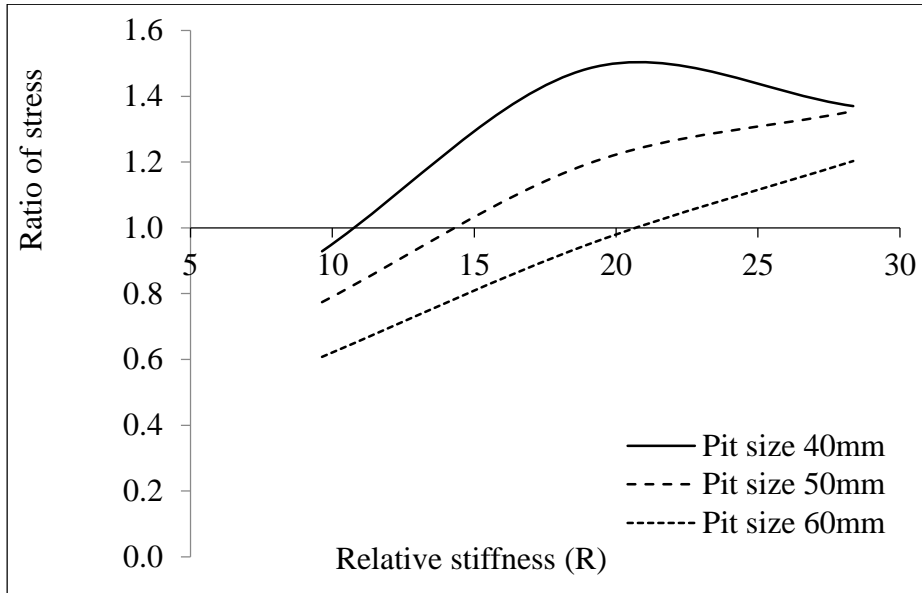


Figure 5-12: Maximum stresses in longitudinal and circumferential directions as a function of relative stiffness between pipe and soil for different pit sizes

The ratios of the maximum longitudinal stress to the maximum circumferential stress are plotted against the relative stiffness in Figure 1-12. The figure shows that the longitudinal stress becomes higher than the circumferential stress (the ratio is greater than one) for a higher relative stiffness value, for each case. The longitudinal stresses become higher at lower relative stiffness values for smaller pits than for larger pits. For the pipeline investigated, the ratio is greater than one for a relative stiffness of 10.5, 14 and 20.5 for pit sizes of 40mm, 50mm and 60mm, respectively.

5.6 Effect of Localized Point Forces

As discussed earlier, pipes are often subjected to localized forces from the surrounding ground. Particularly, when soil surrounding the pipe is eroded due to leakage of water, fine soil particles may be washed away in the earlier stages, leaving coarse soil particles in the vicinity of the pipe wall. This may result in a localized hard spot around the pipe that may provide concentrated support/force to the pipe wall.

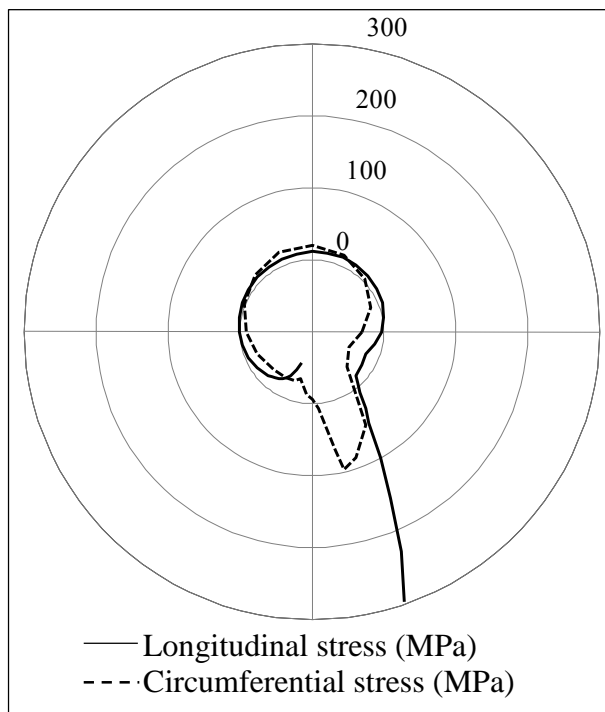


Figure 5-13: Stresses on a partially supported pipe with localized soil reactions

To illustrate the adverse effect of the localized force, analysis has been carried out on a thick cast iron pipeline with pipe modulus, void angle and void depth of 138GPa, 90° and 50m, respectively. The rigidity of the supports is simulated using the spring constant of the spring elements. Using a trial and error method it was found that a spring constant of

400N/mm can produce the peak stress of 296MPa in the longitudinal direction, which is higher than the tensile strength of class 40 cast iron material, 293MPa (ASM International 1990). However, the maximum circumferential stress is only 96MPa (Figure 5-13). Hence, the effect of concentrated supports increased the maximum longitudinal stress by 25 times. The spring constant of 400N/mm could be caused due to the conglomeration of rock particles in the bedding support.

Table 5-4: Maximum stresses for voids with localized supports

Wall thickness (mm)	Pipe Modulus (GPa)	Void angle	Void depth (mm)	Maximum longitudinal stress (MPa)		Maximum circumferential stress (MPa)		Ratio of MLS/MCS
				Tension (MPa)	Compression (MPa)	Tension (MPa)	Compression (MPa)	
10	138	180	200	317.23	-584.37	99.85	-182.92	3.18
10	138	180	50	306.13	-580.71	98.62	-180.31	3.10
10	138	90	200	298.81	-578.39	96.22	-179.00	3.11
10	138	90	50	296.35	-578.78	96.14	-178.51	3.08
10	70	90	50	294.67	-552.97	92.12	-171.44	3.20
5	138	180	50	1068.00	-1431.71	271.21	-435.73	3.94
5	138	90	200	1054.51	-1426.33	264.48	-427.51	3.99
5	138	90	50	1052.38	-1421.39	262.22	-422.51	4.01

A sensitivity analysis is performed to investigate the effect of pipe properties, such as wall thickness and modulus, and erosion void conditions such as void angle and depth, when the pipe approaches the failure stage caused by localized supports. The spring constant of 400N/mm is used in these analyses to observe how these different cases lead to failure. The results are summarized as follows in Table 5-4.

Comparison of Table 5-2 and Table 5-4 reveals that the ratio of maximum longitudinal stress to maximum circumferential stress is in the range of 3 to 4 for all the cases analysed with localized support, while the same ratio is in the range of 0.65 to 3 for the cases analyzed without localized support. Therefore, circumferential cracking will occur before the longitudinal cracking for pipes with localized support. Stresses in the thin wall pipes are very high compared to the stresses in the thick wall pipes. Thus the thin wall pipes may approach the failure stage with less rigidity of the localized support. When the pipe thickness is reduced by half, the maximum longitudinal stress increases 3.5 times, while the maximum circumferential stress increases 2.7 times.

The results are presented in terms of the factor of safety in Table 5-5. The table presents the factor of safety in the longitudinal direction for different pipe moduli and void conditions in a thick pipe and a thin pipe. A similar observation to the cases analysed without localized support (Table 5-2) can be found in the cases analysed with the localized support. As the pipe modulus increases, void angle increases or void depth increases, the factor of safety decreases. Then the pipe may fail with less rigidity of the localized support. For thin pipes, the factor of safety in the longitudinal direction and in the circumferential direction varies very slightly as the void angle and depth increases.

Table 5-5: Factor of safety in longitudinal and circumferential directions of the pipe with localized supports for different conditions

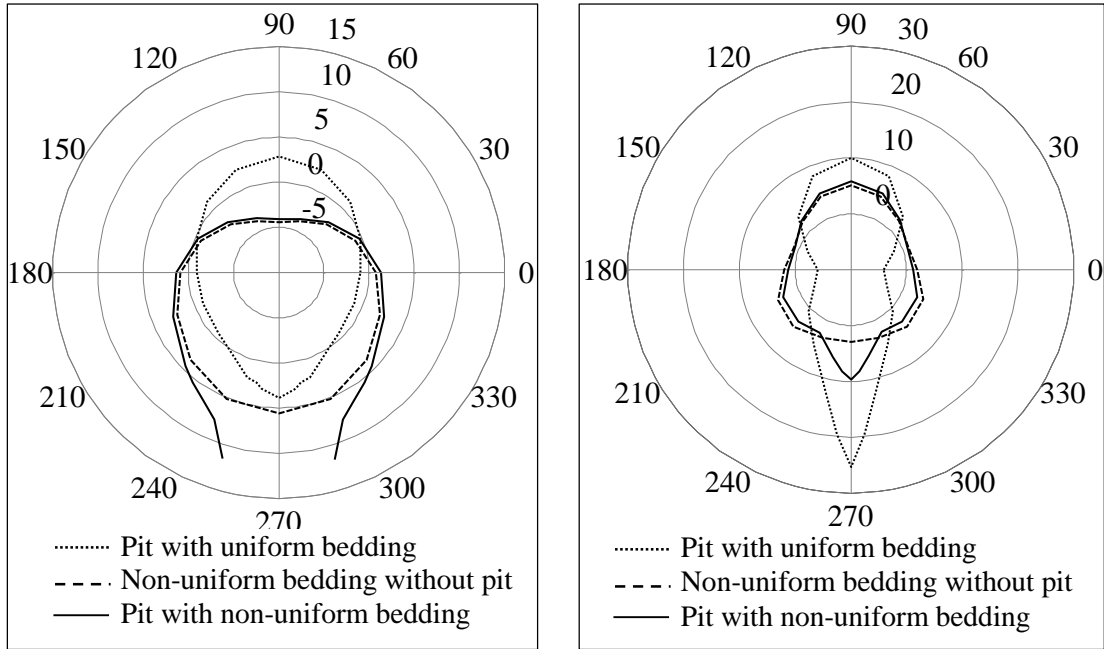
Wall thickness (mm)	Pipe Modulus (GPa)	Void angle	Void depth (mm)	FOS in Longitudinal direction	FOS in circumferential direction
10	138	180	200	0.924	2.934
10	138	180	50	0.957	2.971
10	138	90	200	0.981	3.045
10	138	90	50	0.989	3.048
10	70	90	50	0.994	3.181
5	138	180	50	0.274	1.080
5	138	90	200	0.278	1.108
5	138	90	50	0.278	1.117

A comparison between the cases, analysed with and without the localized supports, shows that the factor of safety in the circumferential direction for thick pipes and thin pipes is always in a decreasing trend for the cases analysed with localized supports.

5.7 Comparison of Pipe with and without Pit

Figure 5-14 presents a comparison of pipe stresses for pipes with and without corrosion pit. The figure includes pipe stresses for pipes with corrosion pit having uniform and partially supported bedding, and for a pipe without corrosion pit having partially

supported bedding. In the Figure 5-14, stresses are low for the pipe in uniform bedding even with a corrosion pit. Non-uniform bedding appears to contribute to the increase of pipe wall stresses. Presence of corrosion pit causes further increase of the stresses more significantly.



(a) Longitudinal stress

(b) Circumferential stress

Figure 5-14: Comparison of stresses for the pipe with and without pit.

Similar effects are observed for the pipe with localized bedding force (Figure 5-15). Corrosion pit is found to increase the longitudinal stress more significantly, leading to circumferential failure of the pipe.

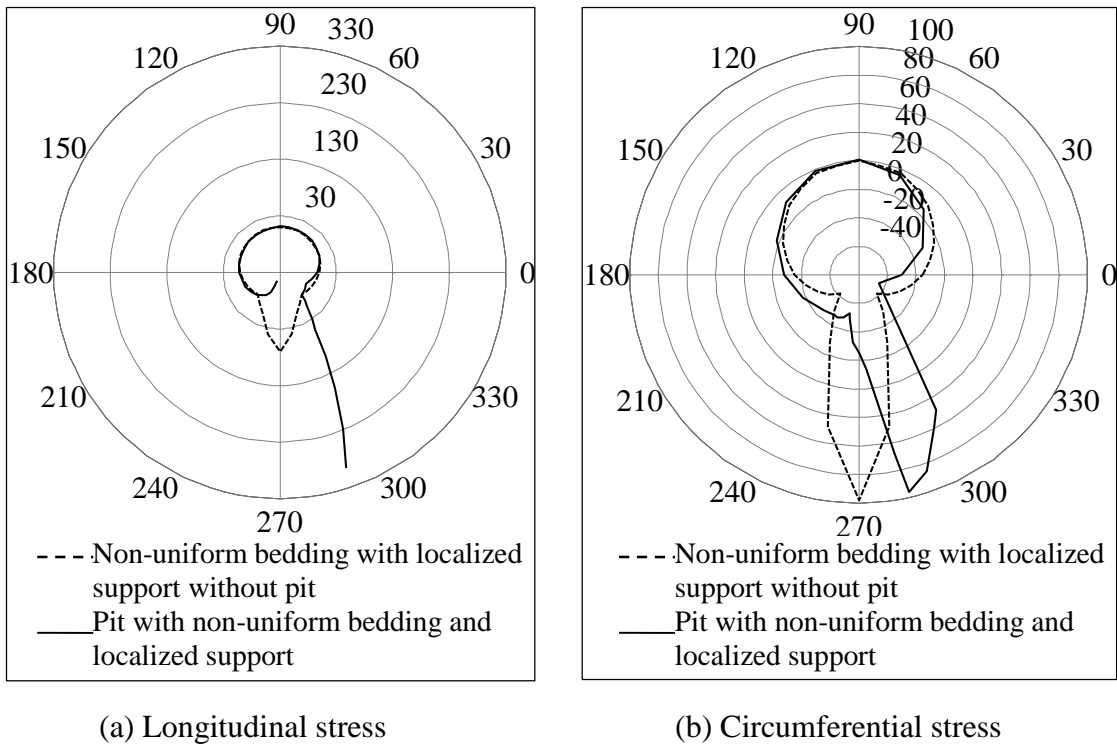


Figure 5-15: Comparison of stresses for the pipe with and without pit with localized support.

5.8 Conclusions

The study investigates the effect of pitting corrosion on the failure mechanisms of cast iron water mains through a detailed numerical study based on finite element analyses. The results reveal that the corrosion pits as well as the relative stiffness of the pipe contribute to the longitudinal stress development on the pipe wall. The effect of localized forces on the pipe wall found to be a critical factor for the failure of cast iron water mains. The following conclusions are derived from this study.

- For a pipe with a corrosion hole, the maximum longitudinal tension is much less than the maximum circumferential tension when the pipe is on uniform soil bedding. Therefore, the failure mode of the pipe in uniform bedding would be longitudinal splitting. Lack of bedding support (e.g., void), at the pipe invert, causes redistribution of pipe wall stresses, decreasing the maximum circumferential stress while increasing the maximum longitudinal stress. The pattern of the longitudinal stress contours, aligned along the circumferential direction of the pipeline, suggests a possible circumferential cracking, if the other factors cause the stresses to exceed the strength of the material. The factor of safety of pipe is reduced in the longitudinal direction when the void is wider and the depth of the void increases.
- The longitudinal stress is higher than the circumferential stress for higher relative stiffness of the pipe with respect to soil. The longitudinal stresses become higher at lower relative stiffness values for smaller pits than for larger pits. The pipe stresses are higher for the thin-wall pipe than those in the thick-wall pipe.
- For the cases analysed with localized support with a spring constant of 400N/mm, the maximum longitudinal stress is about 3 to 4 times the maximum circumferential stress, while it is about 0.65 to 3 times for the cases analyzed without localized support. As the pipe modulus increases, void width increases or void depth increases, the factor of safety of the pipe decreases. Thus, the pipe may fail at a lower rigidity of the localized support ($<400\text{N/mm}$).

- The study reveals that corrosion pit significantly contribute to the circumferential cracking of the pipe, which is usually observed in the field.

5.9 References

ANSYS (2015) ANSYS® Academic Research, Release 16.2. ANSYS, Inc.

ASM International. (1990). Properties and Selection: Irons, Steels, and High-Performance Alloys. ASM International. http://www.asminternational.org/online-catalog/handbooks/-/journal_content/56/10192/06181G/PUBLICATION.

American Water Works Service Co., Inc. (AWWSC). (2002). “Deteriorating buried infrastructure management challenges and strategies”. Available on-line at <http://www.epa.gov/safewater/tcr/pdf/infrastructure.pdf>. Accessed May 16, 2016.

Balkaya, M., Moore, I. D., and Sağlamer, A. (2012). “Study of Nonuniform Bedding Support Because of Erosion under Cast Iron Water Distribution Pipes.” *Journal of Geotechnical and Geoenvironmental Engineering* 138 (10): 1247–56. doi:10.1061/(ASCE)GT.1943-5606.0000689.

Dhar, A. S., Moore, I. D., and McGrath, T. J. (2004). “Two-dimensional analyses of thermoplastic culvert deformations and strains.” *Journal of geotechnical and geoenvironmental engineering*, ASCE, 130(2), 199-208.

Farshad, M. (2006). “3 - Fracture of Plastic Pipes.” In *Plastic Pipe Systems*, edited by Mehdi Farshad, 53–100. Oxford: Elsevier Science. <http://www.sciencedirect.com/science/article/pii/B9781856174961500045>.

- Liyanage, K., and Dhar, A. S. (2015). “Three Dimensional Finite Element Analyses of Partially Supported Water Mains.” In 68th Canadian Geotechnical Conference. Quebec City.
- Liyanage, K., and Dhar, A. S. (2016). “Stresses in Cast Iron Water Mains Subjected to Non-Uniform Bedding and Localized Concentrated Forces.” *Soils and Foundations Journal* (under review).
- Makar, J.M., Rogge, R., McDonald, S., and Tesfamariam, S. (2005). “The Effect of Corrosion Pitting on Circumferential Failures in Grey Iron Pipes.” Denver: American Water Works Association.
- Meguid, M. A., and Kamel, S. (2014). “A Three-Dimensional Analysis of the Effects of Erosion Voids on Rigid Pipes.” *Tunnelling and Underground Space Technology* 43 (July): 276–89. doi:10.1016/j.tust.2014.05.019.
- Rajani, B., Makar, J., McDonald, S., Jen, C., and Viens, M. (2000). “Investigation of Grey Cast Iron Water Mains to Develop a Methodology for Estimating Service Life”, Research Report, ISBN1-58321-063-6, AWWA Research Foundation and American Water Works Association, USA.
- Rajani, B., and Kleiner, Y. (2001). “Comprehensive Review of Structural Deterioration of Water Mains: Physically Based Models.” *Urban Water, Ground Water in the Environment*, 3 (3): 151–64. doi:10.1016/S1462-0758(01)00032-2.

- Rajani, B., and Kleiner, Y. (2010). "Dynamic Influences on Deterioration Rates of Individual Water Mains (I-WARP)." Denver: Water Research Foundation and the Institute for Research in Construction, National Research Council Canada.
- Rajani, B., and Kleiner, Y. (2013). "External and Internal Corrosion of Large-Diameter Cast Iron Mains." *Journal of Infrastructure Systems* 19 (4): 486–95. doi:10.1061/(ASCE)IS.1943-555X.0000135.
- Rajani, B., and Tesfamariam, S. (2004). "Uncoupled Axial, Flexural, and Circumferential Pipe–soil Interaction Analyses of Partially Supported Jointed Water Mains." *Canadian Geotechnical Journal* 41 (6): 997–1010. doi:10.1139/t04-048.
- Rajani, B.B., Robertson, P. K., and Morgenstern, N. R. (1995). "Simplified Design Methods for Pipelines Subject to Transverse and Longitudinal Soil Movements." *Canadian Geotechnical Journal* 32 (2): 309–23. doi:10.1139/t95-032.
- Folkman, S. (2012). "Water Main Break Rates in the USA and Canada: A Comprehensive Study." Utah State University Buried Structures Laboratory.
- Trickey, S. A., and Moore, I. D. (2005). "Numerical Study of Frost-Induced Ring Fractures in Cast Iron Water Pipes." In *Canadian Geotechnical Conference*. Saskatoon.
- Trickey, S. A., Moore, I. D., and Balkaya, M. (2016). "Parametric study of frost-induced bending moments in buried cast iron water pipes", *Tunnelling and Underground Space Technology* 51, pp. 291-300.

Chapter 6. Summary

6.1 Introduction

Municipal water distribution systems include a large volume of cast iron pipes. Cast iron water mains are failing at a growing rate over the last several decades. A number of failure modes of the pipe are identified. These include circumferential cracking, longitudinal splitting, blowout holes, spiral cracking and bell shearing. Among these, the circumferential cracking is identified as the predominant mode of failure experienced in the field. However, the mechanism of the circumferential cracking of the pipe is not well understood to date. Conventional analysis predicts pipe wall cracking in longitudinal direction resulting from excessive circumferential stresses. Research attention is required to identify the causes for the circumferential cracking that results from excessive longitudinal stresses. Several factors, such as corrosion pits on the pipe wall, non-uniform bedding support and localized concentrated forces are considered as the contributors for the longitudinal stresses on the pipe wall.

This research investigates the pipe wall stresses considering the factors contributing to the longitudinal stresses on the pipe wall (i.e. corrosion pit, non-uniform bedding and localized forces). Three dimensional finite element analysis is employed for the study using a general purpose finite element software, ANSYS. The findings of this research and recommendations for future research in this area are outlined below.

6.2 Conclusions

6.2.1 Erosion Voids with Rigid Localized Support

A study with different locations, sizes and geometric shapes of erosion voids in pipe backfill, revealed that the circumferential stress in the pipe wall is greater than the longitudinal stress for smaller void sizes. The longitudinal stress is, however, greater than the circumferential stress for larger void sizes, particularly when the void is located near the invert of the pipe. The maximum longitudinal and maximum circumferential stresses generally occur at the locations of voids. The circumferential stress is found to be higher for the springline voids than for the invert voids. Localized rigid concentrated supports are found to increase pipe wall stresses significantly.

6.2.2 Partially Supported Bedding with Flexible Localized Supports

In partially supported pipes, the lack of support at the pipe invert can cause higher longitudinal tension than the circumferential tension at the invert of the pipe, which may extend to the haunch. The longitudinal tension is higher for pipes with higher flexural stiffness. Flexible point supports with a spring stiffness value of 1500 N/mm may result in the failure of a cast iron pipe. An analytical solution proposed by Rajani and Tesfamariam (2004) for calculation of longitudinal stresses in partially supported water mains is found to overestimate the longitudinal stresses with respect to the results of the three dimensional finite element analysis. A modification factor (α) is proposed in calculating the coefficient of subgrade reaction to account for the overestimation.

6.2.3 Effect of a Corrosion Pit

A corrosion pit on the pipe wall causes redistribution of stresses around the pit. In a pipe with a corrosion pit on uniform bedding, the circumferential stress is higher than the longitudinal stress. Lack of bedding support at the pipe invert causes to decrease the maximum circumferential stress and to increase the maximum longitudinal stress. The factor of safety reduced in the longitudinal direction when relative stiffness of the pipe with respect to soil is increased, and for wider and thicker voids. Pit size also contributed to stress redistribution significantly. For smaller pit size, the longitudinal stresses exceed the circumferential stresses for a lower value of relative stiffness than for a larger pit. The presence of the localized support resulted in an increase in the maximum longitudinal stress which is about 3 to 4 times the maximum circumferential stress for a spring constant of 400N/mm. A localized support with a spring constant of 400N/mm or less may cause circumferential cracking on the pipe wall.

6.3 Recommendations for Future Study

Recommendations for relevant future research are suggested as follows.

- Investigate the three dimensional stresses of large diameter cast iron water mains.
- Conduct field monitoring to obtain more information of failure mechanisms and causes.
- Integrate experimental investigation of failure of cast iron water mains with different flexural stiffnesses of the pipe.

- Incorporate the effect of seasonal fluctuations as a temperature induced force.
- Account for long term material behaviour of bedding soil and asses the influence of concentrated forces on the pipe wall stresses.
- Investigate the effect of using Drucker-Prager and Mohr Coulomb type material models in the simulation of pipe behaviour. As discussed earlier, the Drucker-Prager model accounts for the effect of intermediate stress, while the Mohr Coulomb model neglects the intermediate stress.
- Consider the effect of nonlinear relationship of the pipe material in the pipe-soil interaction modelling for cast iron water mains.